PHOTOELECTRIC INVESTIGATIONS OF AA CETI AND UZ PUPPIS

By

RAYMOND H. BLOOMER, JR.

A DISSERTATION PRESENTED TO THE GRADUATE COUNCIL
OF THE UNIVERSITY OF FLORIDA IN PARTIAL FULFILLMENT OF THE REQUIREMENTS
FOR THE DEGREE OF DOCTOR OF PHILOSOPHY

UNIVERSITY OF FLORIDA
1973

ACKNOWLEDGEMENTS

In the years spent in the preparation of this dissertation many persons unselfishly gave their time and talents to support the effort. Perhaps most critical, however, were the encouragement, patience, and opportunities offered to the author which resulted in the determination necessary to carry on through many nights of observing, through hours of reducing data, and during the time spent in analyzing the data and writing the manuscript.

First among these persons was Dr. K. Y. Chen who chaired the Supervisory Committee, made innumerable suggestions about the work, gave up nights of use on the telescope, and encouraged the author at every stage. Perhaps more important were the love of astronomy, the self-reliance, and the discipline which resulted directly from his leadership and example.

Dr. F. B. Wood served on the Supervisory Committee and was responsible for the author's work at the Dr. Remeis Sternwarte, Bamberg, West Germany, through a National Science Foundation grant. He was the first to instruct this author on the proper use of the telescope and continued to offer help by giving up time on the telescope which he could have used for his work and by giving advice based upon his many years of experience with photometric observations. It was an honor to have had the opportunity to participate with him in several research efforts not associated with this dissertation

which resulted in contributions which he and this author published together.

Other members of the Supervisory Committee were Dr. A. G. Smith, Dr. F. E. Dunnam, and Dr. H. A. Van Rinsvelt. The author wishes to thank them for reading the manuscript and making suggestions which resulted in improvements upon it.

Dr. J. E. Merrill offered advice, as only he could, on the Russell-Merrill model. Of particular value were discussions concerning the application of the model to W UMa systems.

The author would like to thank Mr. W. W. Richardson for doing many of the final inked drawings. He also did many drawings which do not appear here which were used in various presentations and papers. Mr. H. Schrader also worked in these efforts, competently handling the photographic problems of making slides and pictures.

The cooperation from several persons at the Air Force Weapons Laboratory, Kirtland Air Force Base, where the entire text was written, was essential in the completion of this work. The author wishes to thank Lt. Col. M. Bacon, Major R. Prater, and Dr. A. Callender for their understanding and support during the final stages.

An extraordinary exercise in patience was accomplished by the author's wife during the five years of graduate study. She typed all the drafts and the final copy of the manuscript.

The work is dedicated to the author's father who taught him the most important lessons of all.

TABLE OF CONTENTS

Page

ACKNOWLEDGEMENTS ii

LIST OF TABLES vi

LIST OF FIGURES ix

ABSTRACT xii

CHAPTER

I INTRODUCTION 1

II INSTRUMENTATION AND OBSERVATIONS 5

- Dr. Remeis Sternwarte 5
- Rosemary Hill Observatory 8
- Differential Photoelectric Photometry 17
- General Observational Procedures 18

III REDUCTIONS OF THE DATA 20

- Preliminary Steps 20
- Differential Magnitudes 21
- Light Time Correction 22
- The Period 23
- Light and Color Curves 23

IV AA CETI 25

- History 25
- Photoelectric Observations 29
- Light Elements 37
- Color Curves 44
- Light Curves 49
- The Model 56
- The Rectification of the Light Curves of AA Ceti . 62
- Solutions of the Light Curves of AA Ceti 65
- Summary of Results and Suggestions for Further Work 90

TABLE OF CONTENTS (continued)

CHAPTER Page

V UZ PUPPIS 92

History 92
Photoelectric Observations 98
Light Elements 103
Color Curves 107
Light Curves 107
Rectification of the Light Curves 118
Solutions of the light Curves of UZ Puppis 120
Summary of Results and Suggestions for Further Work 148

APPENDIX 149

LIST OF REFERENCES 170

BIOGRAPHICAL SKETCH 172

LIST OF TABLES

Table		Page
1	The equatorial coordinates, spectral types, and catalogue designations for AA Ceti, its companion star, and the comparison and check stars used in this investigation	27
2	Some early observations of the double star ADS 1581	28
3	First order extinction coefficients and their probable errors used in the reduction of data pertaining to AA Ceti	32
4	The differential magnitudes between the comparison and check stars used during the photometric investigation of AA Ceti	34
5	The differential magnitudes between the companion and comparison stars and the weights used for each measurement to calculate the average and probable error	35
6	Times of minimum light of AA Ceti and the weights used to calculate the light elements	38
7	Coefficients used in the rectification of the light curves of AA Ceti	64
8	Elements of the system AA Ceti	66
9	Results of analysis of the yellow light curves of AA Ceti and RR Centauri	81
10	Average differences of the observed data and the theoretical shapes over the yellow light curve of AA Ceti	84
11	Average differences of the observed data and the theoretical shapes over the blue light curve of AA Ceti	86
12	Average differences of the observed data and the theoretical shapes over the ultraviolet light curve of AA Ceti	88

13 Spectroscopic orbital elements of UZ Puppis from Struve (1945) 95

14 The coordinates and Bonner Durchmusterung numbers of stars related to the investigation of UZ Puppis 98

15 The differential magnitudes between the comparison and check stars used during the photometric investigation of UZ Puppis 99

16 First order extinction coefficients and their probable errors used in the reduction of data pertaining to UZ Puppis 102

17 Times of minimum light of UZ Puppis and the weights used to calculate the light elements 104

18 Coefficients used in the rectification of the light curves of UZ Puppis 119

19 Elements of the system UZ Puppis assuming $L_3 \neq 0$ 133

20 Elements of the system UZ Puppis assuming $L_3 = 0$ 134

21 Average differences of the observed data and the theoretical shapes over the yellow ($L_3 \neq 0$) light curve of UZ Puppis 136

22 Average differences of the observed data and the theoretical shapes over the yellow ($L_3 = 0$) light curve of UZ Puppis 138

23 Average differences of the observed data and the theoretical shapes over the blue ($L_3 \neq 0$) light curve of UZ Puppis 140

24 Average differences of the observed data and the theoretical shapes over the blue ($L_3 = 0$) light curve of UZ Puppis 142

25 Average differences of the observed data and the theoretical shapes over the ultraviolet ($L_3 \neq 0$) light curve of UZ Puppis 144

26 Average differences of the observed data and the theoretical shapes over the ultraviolet ($L_3 = 0$) light curve of UZ Puppis 146

27 AA Ceti observations in yellow 150

28 AA Ceti observations in blue 153

29 AA Ceti observations in ultraviolet 156

30 Statistical study of the solutions to the light variations of AA Ceti 159

31 UZ Puppis observations in yellow 160

32 UZ Puppis observations in blue 163

33 UZ Puppis observations in ultraviolet 166

34 Statistical study of the solutions to the light variations of UZ Puppis 169

LIST OF FIGURES

Figure	Page

1 A blink microscope used for the routine search of sky patrol plates at the Dr. Remeis Sternwarte, Bamberg, West Germany 7

2 The dome of the thirty-inch reflecting telescope at the Rosemary Hill Observatory 11

3 The photometer base and amplifiers attached to the Cassegrain focus of the thirty-inch telescope 13

4 A chart recorded tracing of photometric measurements on AA Ceti and its comparison star taken on the night of 10/29-30/72 16

5 A finding chart for AA Ceti, or BV 1481, and the comparison and check stars used in this investigation 31

6 The observed minus the calculated times of minimum light of AA Ceti used in the calculation of the light elements 41

7 The observed minus the calculated times of minimum light of AA Ceti derived from the photoelectric data only 43

8 The b-v curve for AA Ceti after subtraction of the third light of the companion star 46

9 The u-b curve for AA Ceti after subtraction of the third light of the companion star 48

10 The v light curve of AA Ceti after subtraction of the third light of the companion star and adjustment of the magnitude scale to 0.0 magnitude at maximum light 51

11 The b light curve of AA Ceti after subtraction of the third light of the companion star and adjustment of the magnitude scale to 0.0 magnitude at maximum light 53

12 The u light curve of AA Ceti after subtraction of the third light of the companion star and adjustment of the magnitude scale to 0.0 magnitude at maximum light 55

13 The theoretical solution of the yellow light curve plotted with the rectified data of the primary eclipse of AA Ceti 68

14 The theoretical solution of the yellow light curve plotted with the rectified data of the secondary eclipse of AA Ceti 70

15 The theoretical solution of the blue light curve plotted with the rectified data of the primary eclipse of AA Ceti 72

16 The theoretical solution of the blue light curve plotted with the rectified data of the secondary eclipse of AA Ceti 74

17 The theoretical solution of the ultraviolet light curve plotted with the rectified data of the primary eclipse of AA Ceti 76

18 The theoretical solution of the ultraviolet light curve plotted with the rectified data of the secondary eclipse of AA Ceti 78

19 An early light curve of UZ Puppis by Florja (1937) . . . 94

20 Radial velocity curves of UZ Puppis by Struve (1945) . . 97

21 A finding chart for UZ Puppis and the comparison star used in this investigation 101

22 The observed minus the calculated times of minimum light of UZ Puppis which were found in this investigation 106

23 The b-v color curve for UZ Puppis 109

24 The u-b color curve for UZ Puppis 111

25 The yellow light curve of UZ Puppis adjusted to 0.0 magnitude at maximum light 113

26 The blue light curve of UZ Puppis adjusted to 0.0 magnitude at maximum light 115

27 The ultraviolet light curve of UZ Puppis adjusted to 0.0 magnitude at maximum light 117

28 The theoretical solution of the yellow light curve plotted with the rectified data of the primary eclipse of UZ Puppis 122

29 The theoretical solution of the yellow light curve plotted with the rectified data of the secondary eclipse of UZ Puppis 124

30 The theoretical solution of the blue light curve plotted with the rectified data of the primary eclipse of UZ Puppis 126

31 The theoretical solution of the blue light curve plotted with the rectified data of the secondary eclipse of UZ Puppis 128

32 The theoretical solution of the ultraviolet light curve plotted with the rectified data of the primary eclipse of UZ Puppis 130

33 The theoretical solution of the ultraviolet light curve plotted with the rectified data of the secondary eclipse of UZ Puppis 132

Abstract of Dissertation Presented to the
Graduate Council of the University of Florida in Partial
Fulfillment of the Requirements for the Degree of Doctor of Philosophy

PHOTOELECTRIC INVESTIGATIONS OF AA CETI AND UZ PUPPIS

By

Raymond H. Bloomer, Jr.

June, 1973

Chairman: Dr. Kwan-Yu Chen
Major Department: Physics and Astronomy

Two eclipsing binary stars were observed photoelectrically using the thirty-inch reflecting telescope of the University of Florida at the Rosemary Hill Observatory. The entire light variation of each star was measured in three colors, and a total of over 1,400 useful observations were made. A period study was undertaken for each star, and solutions of the light curves were found based upon the Russell-Merrill model.

The star, AA Ceti, was found to be a variable by the author in a routine search of sky patrol plates at the Dr. Remeis Sternwarte, Bamberg, West Germany. It is the brighter component of the visual binary Aitken 1581. Photometric measurements during the winters of 1971 and 1972, combined with times of faint light from the Bamberg plates, showed the orbital period of the system to be $0^{d}.53617353 \pm 0^{d}.00000050$ p.e. The light curves which were constructed displayed W UMa-type variations. The total secondary eclipse was flat at yellow and blue wavelengths, but the system became significantly fainter in ultraviolet light as the total phase progressed. The light curves were rectified to spherical star systems so that the Russell-Merrill model could be applied. The resulting solutions indicated that the secondary eclipse was an occultation and that the stars were unusually different in size for this type of binary system. Although the solutions were not definitive, partly due to the small depth of the rectified eclipses, a general description of the system has been determined and is summarized by the following elements of the prolate ellipsoid model averaged over the three wavelength bands: $a_g = 0.53$, $a_s = 0.18$, $\epsilon = 0.16$, $j = 76^{\circ}.7$, $L_g = 0.920$, and $L_s = 0.080$. The maxima after primary eclipse was displaced from a phase of $0^{p}.25$ which could possibly indicate that the orbits are elliptical.

Although UZ Puppis had been studied spectroscopically and photometrically by photographic methods, no reports of photoelectric light curves were found in the Florida Card Catalogue of Eclipsing Binary Stars. The star was observed photoelectrically on thirteen nights. A period study did not reveal a significant change in the period from previously published values. The period derived from this photoelectric data and some old times of minimum light gave a refined period of $0^{d}.79485183 \pm 0^{d}.00000004$. The light curves were similar in shape to those of β Lyrae and indicated that the eclipses were partial. The center of the secondary eclipse was displaced from a phase of 0.5, and the star showed a significant "periastron effect." Solutions resulting from this investigation indicated that the secondary eclipse was an occultation of the smaller star and that there was a large amount of third light present in the system. Solutions both with and without

the assumption of third light were found; the solutions allowing third light resulted in the following elements based upon the prolate ellipsoid model and averaged over the three wavelength bands: $a_g = 0.37$, $a_s = 0.32$, $e = 0.14$, $j = 85\overset{\circ}{.}7$, $L_g = 0.505$, $L_s = 0.222$, and $L_3 = 0.273$. The inclination of the orbit from this solution, combined with O. Struve's radial velocity data, gave a mass for each star of about $1.1\odot$ and an orbital semi-major axis of approximately 1.6×10^6 km.

CHAPTER I

INTRODUCTION

In 1783 Goodricke published the first correct interpretation for the light variations of the eclipsing binary star, Algol. He explained that the periodic decrease in brightness of 1.2 magnitudes followed by a return to normal light within about ten hours could be caused by the eclipse of one star by another body. His insight (at the young age of nineteen) began a new field of study which has yielded a tremendous amount of information about the stars. However, 190 years later one finds that a great many old questions remain unanswered, e.g., the strange light variations of the bright system β Lyrae. In addition, new problems have arisen largely due to the rapid increase in the number of binary systems discovered and the improvement in the state-of-the-art of photometric and spectroscopic instrumentation.

A binary star system is defined here as two stars which are close enough in space to appreciably affect one another's motion by their gravitational fields. If the inclination of the plane of the orbit with respect to the plane of the sky is close enough to ninety degrees, each star will alternately eclipse the other with the subsequent loss of light. Just how small the inclination can be and still cause eclipses depends upon the sizes of the two stars relative to their separation.

There are several definitions of a "close" binary star system in use today. In the broadest sense, a binary star system is considered close if the two stars are close enough to affect one another's evolution at some point in their lifetimes. This definition, proposed by Plavec (1970), allows stars separated by many astronomical units to be considered close. In photometric investigations of eclipsing binary stars the term "close" usually describes a system which shows large light variations due to the changing aspect of stars which are tidally distorted by one another. In this investigation the latter more-restricted definition will be assumed unless otherwise stated.

In recent years the number of known eclipsing binary stars has increased very rapidly due, in part, to photographic sky patrols such as the one at the Dr. Remeis Sternwarte, Bamberg, West Germany, which is described in the next chapter. The dramatic increase in the estimates of the percentage of all stars which are actually multiple star systems has stimulated interest in the field. Other relatively recent developments have led to a greater emphasis on the study of close binary systems and, in particular, eclipsing systems: (1) the development of the photomultiplier tube, which has made possible photometric measurements routinely more precise than 0.01 magnitude in typical cases, thus making photometrically determined physical parameters for the system of higher precision and revealing heretofore hidden photometric complications; (2) photometric and spectroscopic evidences of gaseous streams, rings, disks, and other peculiarities in the system; (3) the suggestions that several types of cataclysmic variable stars may, in fact, all be close binary systems, according to Plavec's definition, such as the novae (Starfield, 1971) and the U Germinorum stars (Smak, 1969); and (4) the recent discovery that some binary stars may be radio (e.g., Algol), and x-ray sources.

With this increased activity in the more esoteric phenomena related to binary stars and the astrophysical insight which can be obtained from them it is of major importance that eclipsing binary stars provide the only direct method available for determining the dimensions of the stars (with the exception of the sun and inferences from interferometry of a small number of supergiant stars). Few research efforts in astronomy can be considered more important or fundamental than finding the dimensions of the stars in various categories and stages of evolution.

The dimensions extracted from the light variations are, however, only as meaningful as the model assumed in the analysis. Some models for eclipsing binary systems contain simplifying assumptions which demand that they be applied, in general, to well-separated binaries which have no strange peculiarities in their light variations. The model of Russell and Merrill (1952) used in this work applies to this situation. Since the majority of eclipsing binary stars do not fit in this category, schemes have been developed to "rectify" or change the system's light variations to ones which can be analyzed with a simple model. In the Russell-Merrill model, however, a third light (light which is emitted from a source other than one of the two stars mutually eclipsing one another) can be assumed. This assumption adds another degree of freedom to the model which could make up for improper rectification procedures with the result being the extraction of incorrect physical parameters or "elements" for the system. Many times this third light is a large fraction of the total light of the system and is not "visible" spectroscopically. Though today's procedures are undoubtedly far from being perfect, they must be applied and scrutinized until better methods can be developed to solve close binary star light curves.

New models have been developed based, for example, on the theoretical structure due to Lucy (1968); however, these models are imperfect also. Some problems in the analysis of close binary systems may not yield to any models, such as intrinsic random variability of the components and rapidly changing patterns of spots (bright or dark) on their surfaces. At present these problems are generally ignored and averaged to give some mean elements based upon several observing sessions. For lack of a better understanding of close binary stars, this seems to be the only recourse.

It was the intention of this work to investigate the light variations (including period studies) of two eclipsing binaries, one of which was discovered to be a variable by the author. The analysis of the light curves was done by conventional methods using the Russell-Merrill model. Certainly the observations of this epoch will continue to be of value even when eclipsing binaries are completely understood.

CHAPTER II

INSTRUMENTATION AND OBSERVATIONS

Dr. Remeis Sternwarte

The eclipsing binary star having Bamberg variable number 1481, now named AA Ceti (Kukarkin et al., 1972), was discovered to be variable by "blinking" sky patrol plates at the Dr. Remeis Sternwarte, Bamberg, West Germany. In this process two photographic plates of the same area of the sky taken at different times were viewed alternately in rapid succession through a microscope. If the plates were of similar quality and exposure, those objects which had not changed in brightness between the times that the two plates were exposed displayed no change in their image. Those objects which had varied in brightness appeared to "blink" as a result of the change of plate density and image diameter. The apparatus employed in the procedure described above is shown in Figure 1.

The plates were taken with four-inch f/6 Tessar lenses mounted either in six-camera units (at the Boyden Observatory, South Africa) or in four-camera units (at Mount John Observatory, New Zealand). Each camera covered a field of $13^{\circ} \times 13^{\circ}$, and the optical axes of the lenses were pointed thirteen degrees apart in declination. The typical one-hour exposure (one-half hour on each side of the meridian) reached a photographic magnitude of about 14.0.

After a search was made of the star catalogues and it was

Fig. 1. A blink microscope used for the routine search of sky patrol plates at the Dr. Remeis Sternwarte, Bamberg, West Germany

determined that the object had not been identified previously as a variable, the author then assigned a Bamberg variable number to the object, and a survey was then made of all available plates which contained the new variable. Such a search, along with spectral types available from star catalogues, gave clues as to the nature of the variation. For example, an object normally at maximum brightness fading only occasionally was probably an Algol-type or β Lyrae-type eclipsing system. Those objects which spent as much time "bright" as "faint" were probably either W UMa-type eclipsing stars or RR Lyrae-type stars. Spectral types available for the brighter stars (usually $m \leq 9^{m}_{.}0$) lent some key as to the nature of the variability.

From the times of faint light available a period for the variation was derived. This was done essentially by trial and error until a set of light elements was found which satisfied all available data. Unfortunately, the poor time precision of photographic methods often led to many possible periods, particularly for short period systems.

Rosemary Hill Observatory

The photoelectric observations were made with the thirty-inch Tinsley reflecting telescope at the Rosemary Hill Observatory of the University of Florida. Located approximately twenty-five miles southwest of Gainesville, Florida, the twenty-six-foot dome was constructed on a natural sand ridge at an elevation above sea level of about 130 feet, which is approximately fifty feet above the surrounding terrain. The elevation offered some protection from early morning ground fog so common in this subtropical climate. This pollutionfree rural site provided a very dark sky often of photometric quality. The seeing disks were typically two seconds of arc in diameter. Many of the characteristics of this location have recently been summarized by Dr. A. G. Smith (1972). The dome is shown in Figure 2.

The photometer base, made by the Astro Mechanics Company, and amplifiers were attached to the telescope at the Cassegrain focus in the configuration shown in Figure 3. After passing through a wide-field viewing mechanism, the f/16 light beam was brought to a focus at the diaphragm entrance to the photometer by moving the secondary mirror parallel to the optical axis of the telescope. The diaphragm, used to isolate the star being observed, was chosen to be either 25.0 or 32.5 seconds of arc in diameter depending upon how much sky brightness had to be eliminated to achieve a reasonably high sky-plus-star to sky-brightness ratio. Immediately after the diaphragm in the optical path was a small mirror which could be placed in the beam so that the diaphragm and star image could be viewed through an eyepiece to assure proper focus and centering of the image. After being reflected by two plane mirrors, the beam reached a six-position filter wheel in which were placed three wide-band transmission filters (a Corning 9863, a Corning 5030 and Schott GG 13, and a Corning 3384) which were the same filters used by Johnson and Morgan (1953) in the establishment of the standard UBV photometric system. The approximate effective wavelengths of the Johnson-Morgan system are 5480Å, 4400Å, and 3650Å; the filters are characteristically 700 - 900Å wide. Of course, the response of the system was slightly different from the standard system primarily due to the use of a different photomultiplier tube.

Fig. 2. The dome of the thirty-inch reflecting telescope at the Rosemary Hill Observatory

Fig. 3. The photometer base and amplifiers attached to the Cassegrain focus of the thirty-inch telescope

The filtered light beam then passed through a Fabry lens, which imaged the light on the photocathode of the photomultiplier tube, and then through a flat glass window at the entrace to the "cold box" which housed the photomultiplier tube. An EMI 6256 B photomultiplier tube was used during the 1971 observations of UZ Puppis, and a similar EMI 6256 S was used for all the other observations. These are two-inch-diameter thirteen-stage tubes with S-13 photocathodes. Operated at 1,000 volts (across the cathode, dynode chain, and anode), the dark current was always small compared to the star or sky signal, so the tubes were operated at ambient temperature rather than cooling with dry ice. The signal from the photomultiplier tube was then amplified by a d/c amplifier. All but a few observations were made with the PA-1 amplifier designed by J. P. Oliver and constructed at the University of Florida for the purpose of stellar photometry. The output was then displayed on one channel of the Honeywell ElectroniK 16 dual channel strip chart recorder. The paper transport was set at one inch per minute and was checked several times during each observing session with WWV, the national time standard, to insure that all times were accurate to better than five seconds. A typical example of a tracing is shown in Figure 4. At least once each night the coarse gain steps of the PA-1 amplifier were calibrated using a built-in current source. Fine gain steps were assumed to be of constant calibration since very stable resistors (5 ppm/°C drift) were used in the construction. A calibration made by D. H. Martins under typical temperature and humidity conditions was adopted. Drift of the resulting calibration of any gain setting was found to be never more than a few

Fig. 4. A chart-recorded tracing of photometric measurements on AA Ceti and its comparison star taken on the night of 10/29-30/72

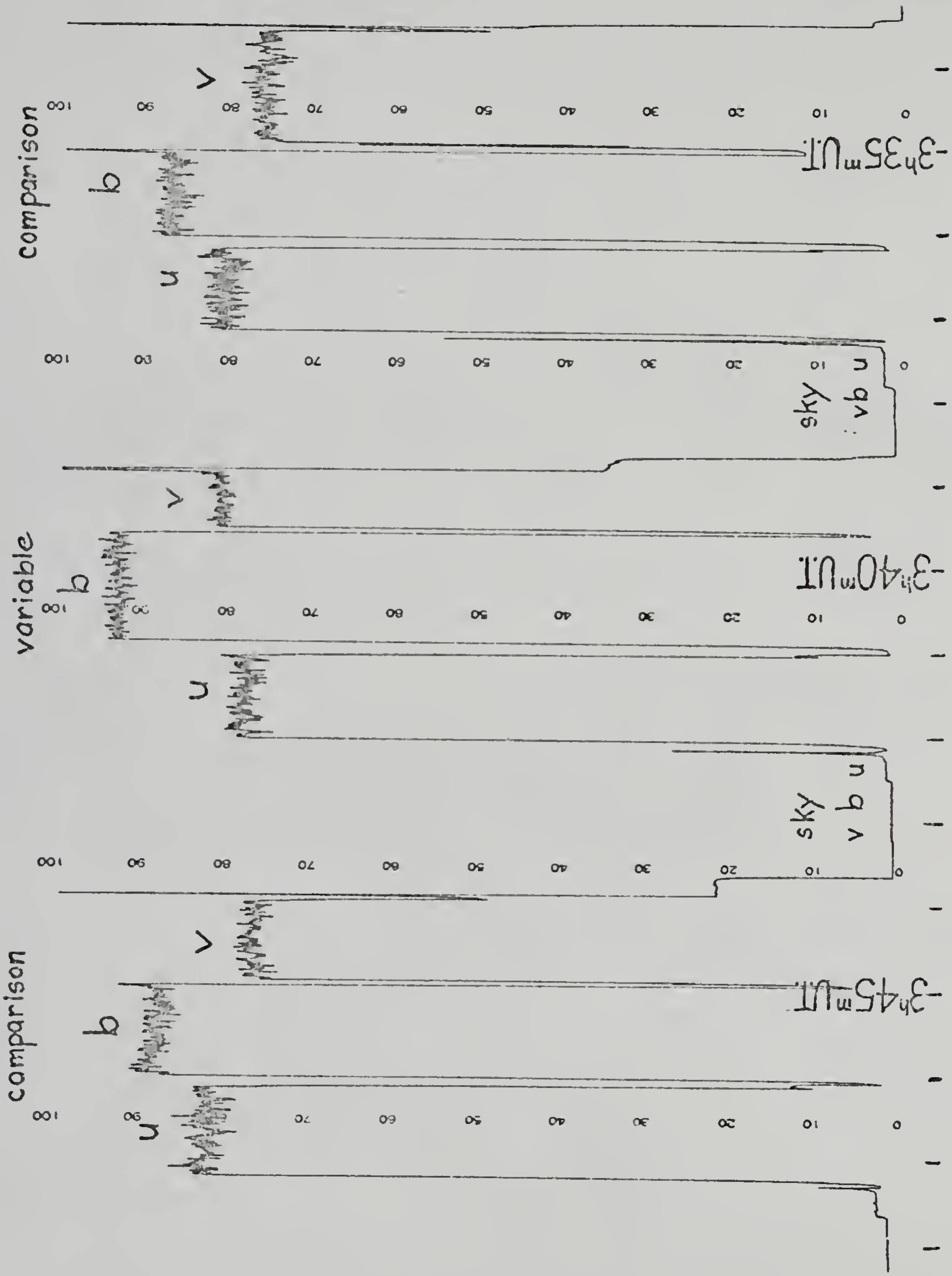
comparison
v
b
u
-3h35mUT
sky
v b u
variable
v
b
u
-3h40mUT
sky
v b u
comparison
v
b
u
-3h45mUT
100
90
80
70
60
50
40
30
20
10
0

thousandths of a magnitude, comparable to the reading error of the chart recording, so a mean calibration was used for all the observations.

Differential Photoelectric Photometry

The differential photoelectric photometry of variable stellar sources is a well-developed procedure capable of reaching precisions of the order of 0.01 magnitude or better with a minimum of systematic errors (Wood, 1963).

Due to small variations in the transparency of the atmosphere over a time scale of minutes, a differential measurement between a constant or "comparison" source (a near-by star) and the variable star was used in this work. In this procedure the light of the comparison star was measured before and after the variable star, and its brightness was linearly interpolated to the variable star reading so that a direct comparison could be made. This was done for each color, independently. It was common practice also to make occasional measurements of another star to "check" the constancy of the comparison source. Both the comparison and check stars were chosen for their similarity in brightness to the variable in order to reduce the demands of changing amplifier gains too often as well as for their similarity in color to simplify the reductions (see Chapter III).

Of course, significant transparency variations, perhaps due to a thin cloud, over a period of time shorter than the time between comparison star measurements (typically, three to ten minutes) result in an increase in the scatter of the data. In addition to this source of scatter, many components of close binary stars have been known to be intrinsically variable over time scales of hours or less. These facts contribute to the difficulty of a theoretical error analysis of photoelectric data. Further discussion of errors, except for chart recorder reading errors discussed in the next section, will be postponed until a discussion of the light curves.

General Observational Procedures

When the image of a star was centered and focused in the diaphragm of the photometer, readings were taken in yellow, blue, and then ultraviolet light. Before each reading the centering of the star was checked. This was necessary since the two stars of this investigation were always at a large zenith angle so that guiding corrections had to be made due to variable refraction of the image passing through the atmosphere. A thirty- to forty-five-second tracing was normally enough to establish the level of the noisy signal to an accuracy of about ±0.2 units ($\pm 0\overset{m}{.}002$ at full scale deflection) when one fitted a line through the reading by eye. Then, in reverse order, the same amplifier settings were used to measure the brightness of the sky (plus dark current and zero-point of the recorder) near the star. This procedure was followed for every star alternating between comparison and variable stars with an occasional set of deflections for the check stars and "standard" stars. On some occasions when the atmospheric transparency was reasonably constant and the comparison star readings were not changing significantly over a period of about five minutes, several sets of deflections were taken on the variable star between each comparison star set. In all cases an attempt was made to keep the deflections near full scale on the chart recorder since the inevitable error in reading the chart (approximately ±0.2 units) was a smaller fraction of the measurement at full scale than with a smaller signal. Although it has been shown that the time constant of the noisy signal has little effect upon the reading errors (Young, 1968), a time constant of 0.5 seconds was generally used as a comfortable compromise between large "grass" in the signal and too much smoothing, which could mask the effects of an unphotometric sky.

At the beginning of an observing session the Universal Time from radio station WWV was marked on the chart. The transport rate of the paper (one inch per minute) was chocked during the session several times. Then each deflection was assigned a time by estimating the center of the measurement. All times are accurate to better than five seconds.

CHAPTER III

REDUCTIONS OF THE DATA

Preliminary Steps

The tracings on the strip chart recording were measured using a strip of clear plastic scribed with a thin dark line. The line was visually fitted to the signal, and the deflection was estimated to the nearest 0.1 unit on a full scale of one hundred units. In most cases this procedure was reproducible to within ±0.2 units so that the reading error for a deflection near full scale corresponded to less than ±0.01 magnitude in most cases. This same measuring technique was applied to the sky readings, and they were linearly interpolated to the star readings. Since the same gain was used for the sky and star deflections, a direct subtraction could be made. This difference and the Universal Time at the mid-point of each reading were recorded and punched on computer cards for further reductions which were done primarily on the IBM 360/65 computer. The computer codes were initially developed at the University of Pennsylvania. Some of the calculations were done with the Hewlett-Packard 9820A calculator at the Air Force Weapons Laboratory, Kirtland Air Force Base, using programs written by the author.

Differential Magnitudes

The first step in the computer reductions was to calculate the first order extinction coefficients for each color on each night. The extinction coefficients were derived from the comparison star data. Those measurements which seemed obviously not to represent the general linear extinction were removed, and a linear least-squares fit to the remaining data (as a function of airmass) yielded the extinction coefficients. Since the extinction was found to vary by as much as a factor of two from one night to the next, it was felt that mean coefficients would not be adequate. This policy restricted useful nights to those in which enough comparison star data was taken to achieve some precision in the determination of the extinction coefficients.

The difference in magnitude between the comparison and variable star (or check star) was calculated allowing for differential extinction in light. If one defines the observed magnitude as m and the magnitude of the star outside the earth's atmosphere as m_o, then, to a good approximation,

$$m = m_o + kX$$

where k is a positive number in units of magnitudes/airmass and X is the airmass. The observed magnitude is, of course, dependent upon the gain of the amplifier (G), which is calibrated in magnitudes, and the deflection (S), such that

$$m = G - 2.5 \log(S/100) \quad .$$

For these calculations the expression for the airmass from Hardie (1962) was used:

$$X = \sec Z - 0.0018167(\sec Z - 1) - 0.002875(\sec Z - 1)^2 - 0.0008083(\sec Z - 1)^3$$

where Z is the zenith angle of the object. The zenith angle is related to the latitude (ϕ) of the observer and the declination (δ) and hour angle (h) by

$$\sec Z = [(\sin \phi \sin \delta) + (\cos \phi \cos \delta \cos h)]^{-1} .$$

The differential magnitude between the comparison star and variable star, corrected for first order extinction, is then

$$m_{var} - m_{comp} = m_{var_o} - m_{comp_o} + k(X_{var} - X_{comp}) .$$

Of course, k would be different in wide-band filter photometry for two stars of widely different color. In this work the comparison stars and variable stars were chosen to be similar in color so that second order extinction coefficients would be small and could be neglected. In this way the differential magnitudes between the comparison star and the variable and check stars were computed.

Light Time Correction

As the earth moves in its orbit, the distance from the object being observed changes. Since the velocity of light is finite, the position of the earth in its orbit would then affect the timing of an event such as an eclipse. To avoid this confusion, all times were reduced to the arrival time of the signal at the sun, i.e., to heliocentric time.

Following Binnendijk (1960), the correction added to the recorded geocentric time was Δt, where

$$\Delta t = -0.005770\, X_{\odot}(\cos \delta \cos \alpha) + Y_{\odot}(\tan \epsilon \sin \delta + \cos \delta \sin \alpha)$$

where $X_{\odot}$ and $Y_{\odot}$ are the Cartesian coordinates of the sun, α and δ the right ascension and declination of the variable star (precessed to the same equinox as $X_{\odot}$ and $Y_{\odot}$), and ϵ is the obliquity of the ecliptic.

The Period

Times of minimum light were found in two ways. On nights when data was available on both branches of an eclipse, the Hertzsprung (1928) method of finding the geometrical center of the eclipse was used. On nights when data was available on only one branch, the tracing paper method was used to visually fit the partial data to an eclipse whose mid-point was "known." Since this method is less precise than the Hertzsprung method, it was given lower weight in the calculations.

If a preliminary period was available from previous work, as it was for UZ Puppis, the relative cycle (or epoch) of each time of minimum could be calculated. For AA Ceti, however, the period had to be estimated such that phases predicted by the elements agreed with all the observations. A least-squares calculation was performed to find the period (P) and the initial epoch (T_o) (and their probable errors) so that times of future minima (T) could be predicted by the equation

$$T = T_o + P \cdot E$$

where E is obviously the number of cycles since the initial epoch.

Light and Color Curves

Once the light elements were found, the phase of each point was calculated and all the data assembled into light curves. No "night corrections" or adjustments were made between different sets of data.

If the comparison stars and variable stars had exactly the same color, then the light curves could be subtracted from one another directly to form the b-v and u-b vs. phase plots, i.e., the color curves. Since this is rarely the case, a correction should be made for each night's data based upon standard stars. However, these color-dependent constants were considered small, and a direct subtraction was made.

CHAPTER IV

AA CETI

History

The variable star BV 1481 was discovered to be a variable star at the Dr. Remeis Sternwarte in a routine search of sky patrol plates (Bloomer, 1971a). The object showed an amplitude of up to 0.5 magnitude, and on many plates (about 25 percent of them) the brightness was below maximum light by a significant amount indicating that the star was probably either a RR Lyrae-type star or a short period eclipsing binary star. The late spectral type (F2) tended to support the latter choice.

A set of light elements were calculated using times of faint light from the plates (Bloomer, 1971b):

$$\text{Min I} = \text{JD } 2440566 + 0\overset{d}{.}733282 \cdot E \quad .$$

Subsequent photometry showed these elements to be incorrect.

K. Locher (1972) published a light curve from visual estimates using these elements and pointed out that the eclipsing component is, in fact, a member of a visual binary system (SAO 167450/167451). The components do not differ greatly in brightness ($\Delta\text{mag} \approx 0\overset{m}{.}5$) and are separated by less than nine seconds of arc. He further identified the variable as the southern-most component of the visual pair.

Recently BV 1481 was named AA Ceti by Kukarkin et al. (1972).

The catalogue names of the individual stars and the visual pair as well as the coordinates of the stars are given in Table 1.

The visual binary system was first studied, according to the literature, in 1822 by J. Y. W. Herschel and James South (Burnham, 1880). Since then numerous publications concerning this pair have revealed no significant change in the separation (slightly less than nine seconds of arc according to most references) or position angle, which remains near 306 degrees. Some of these references and their results are given in Table 2.* In this table d is the separation of the stars, and θ is the position angle of the fainter star with respect to the brighter one and is measured counterclockwise from the northern direction. The proper motions in both right ascension and declination are so similar that the two stars are undoubtedly a physical pair with a very long period. The proper motion of the variable and companion stars according to the Smithsonian Astrophysical Observatory Star Catalog are

$$\sigma_{\mathrm{var},\alpha} = +0^{s}.0073/\mathrm{yr.} \pm{}''.010 \quad ,$$
$$\sigma_{\mathrm{comp},\alpha} = +0^{s}.0057/\mathrm{yr.} \pm{}''.010 \quad ,$$

and

$$\sigma_{\mathrm{var},\delta} = +0''.041 \pm{}''.007 \quad ,$$
$$\sigma_{\mathrm{comp},\delta} = +0''.058 \pm{}''.007 \quad .$$

Since no photometric studies other than those discussed above were found in the brief history of this variable star, the present investigation was begun to find the photometric elements for the system.

---

*It is interesting, indeed, that the variability of the brighter component was not mentioned in the major double star catalogues.

TABLE 1

THE EQUATORIAL COORDINATES, SPECTRAL TYPES, AND CATALOGUE DESIGNATIONS FOR AA CETI, ITS COMPANION STAR, AND THE COMPARISON AND CHECK STARS USED IN THIS INVESTIGATION

	$\alpha_{1950.0}$	$\delta_{1950.0}$	SAO	BD	GC	Spectral Type
AA Ceti	$1^{h}56^{m}40^{s}.6$	$-23^{\circ}\ 9'44''.9$	167451		2392 ($7^{m}.31$ vis.)	F2
Companion Star	$1^{h}56^{m}40^{s}.0$	$-23^{\circ}\ 9'41''.1$	167450		2391 ($7^{m}.7$ vis.) estimate	
Comparison Star	$1^{h}56^{m}33^{s}.3$	$-21^{\circ}22'33''.8$	167448 ($7^{m}.3$ vis.)	$-21^{\circ}352$		F5
Check Star	$1^{h}53^{m}27^{s}.4$	$-20^{\circ}48'21''.8$	167401 ($7^{m}.8$ vis.)	$-21^{\circ}339$		F2

AA Ceti + Companion = HD 12180 = CAP-23°227 = COD-23°737 = ADS 1581 = BDS 1047

BDS - Burnham's Double Star Catalogue
BD - Bonner Durchmusterung
ADS - Aitken's Double Star Catalogue
GC - General Catalogue
SAO - Smithsonian Astrophysical Observatory Star Catalog

TABLE 2

SOME EARLY OBSERVATIONS OF THE DOUBLE STAR ADS 1581

Epoch	d	θ	Magnitude	Reference
1822.89	9″.08	306°.5	$8^{m}.0-9^{m}.0$	Burnham (1880)
1877.86	8″.30	305°.0	---	Burnham (1880)
1895.86	8″.50	304°.4	---	Burnham (1880)
1897.893	8″.12	306°.2	$7^{m}.0-7^{m}.25$	Scott (1899)
1897.904	8″.49	306°.4	$7^{m}.0-7^{m}.25$	Scott (1899)
1902.895	8″.44	305°.0	$7^{m}.0-7^{m}.4$	Scott (1904)
1916.84	8″.47	306°.9	$7^{m}.2-7^{m}.4$	Franks (1918)

Photoelectric Observations

Useful photometric observations of AA Ceti were made on thirteen nights during 1971 and 1792. The comparison star used was BD-21°352. As a check on its constancy, occasional measurements were made of the check star BD-21°339 during the 1972 observing season. The catalogue names and the position of these stars are given in Table 1. Figure 5 is a finding chart for the stars.

As mentioned previously, the variable star is the brighter component of the visual binary Aitken 1581. Since the companion star of AA Ceti was so close (about nine seconds of arc), it was impractical to attempt to separate the stars in the diaphragm of the photometer, at least on a routine basis, so the great majority of the measurements were made with both stars in the diaphragm. On nights of good seeing one or more measurements were made with just the companion star in the diaphragm. This was done to have an empirical value of the third light of the system in each color and to act as a check on possible variability of the companion star. In addition to these special measurements, occasional measurements of the check star were made to check the constancy of the comparison star.

The first step of the reductions, as discussed in the previous chapters, was to find the first order extinction coefficients for each color on each night. Observations which were apparently not the result of smooth extinction effects were removed before the least-squares fit was performed. The results of these calculations (and the probable errors) are given in Table 3 in units of magnitudes per unit airmass. On the night of 12-31-71/1-1-72 an estimate of the

Fig. 5. A finding chart for AA Ceti, or BV 1481, and the comparison and check stars used in this investigation

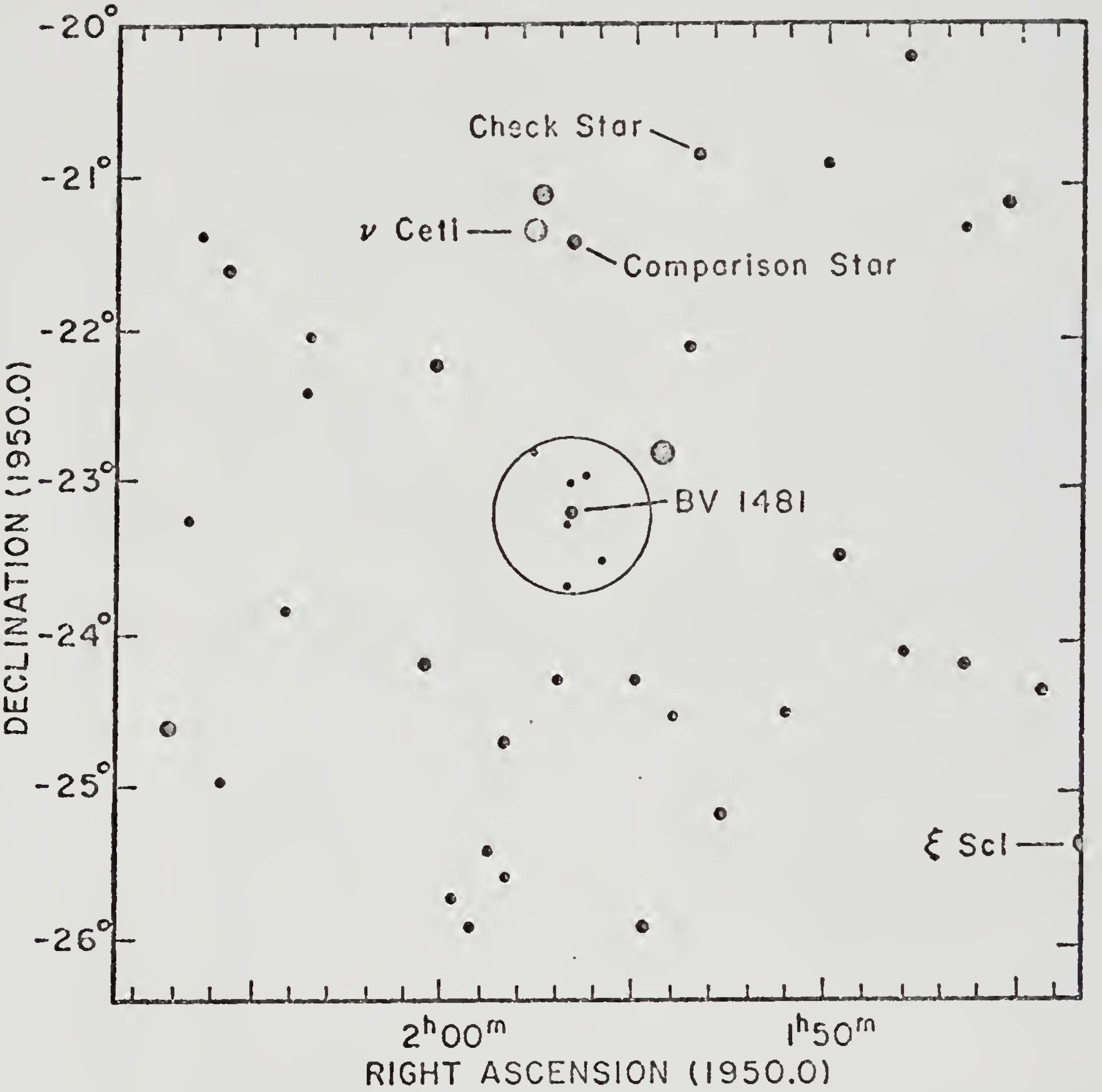
-20°
-21°
-22°
-23°
-24°
-25°
-26°
DECLINATION (1950.0)
Check Star
ν Ceti
Comparison Star
BV 1481
ξ Scl
2h00m
1h50m
RIGHT ASCENSION (1950.0)

TABLE 3

FIRST ORDER EXTINCTION COEFFICIENTS AND THEIR PROBABLE ERRORS USED IN THE REDUCTION OF DATA PERTAINING TO AA CETI

Date	k_v	k_b	k_u
11/ 5- 6/71	0.356 ±.018	0.517 ±.021	0.923 ±.023
11/ 6- 7/71	0.343 ±.015	0.515 ±.027	0.902 ±.032
11/ 8- 9/71	0.409 ±.025	0.609 ±.028	1.016 ±.029
11/12-13/71	0.243 ±.011	0.394 ±.013	0.777 ±.012
11/25-26/71	0.275 ±.020	0.436 ±.019	0.822 ±.027
12/29-30/71	0.274 ±.009	0.437 ±.014	0.812 ±.011
12/31/71- 1/1/72	(est.) 0.35	(est.) 0.60	(est.) 1.00
9/ 2- 3/72	0.451 ±.031	0.693 ±.035	1.099 ±.010
9/ 4- 5/72	0.260 ±.035	0.422 ±.023	0.780 ±.067
10/28-29/72	0.253 ±.026	0.406 ±.043	0.805 ±.059
10/29-30/72	0.230 ±.019	0.391 ±.022	0.767 ±.030
11/ 8- 9/72 East Side	0.244 ±.021	0.368 ±.011	0.721 ±.070
West Side	0.157 ±.028	0.286 ±.021	0.670 ±.015
*12/ 8- 9/72	0.313 ±1.169	0.475 ±1.480	No usable data

*Very poor quality data

extinction was made due to the lack of data necessary to perform a meaningful least-squares fit. With these extinction coefficients the differential magnitudes between the comparison star and the combined variable and companion, companion, and check stars were calculated as described in Chapter III.

Table 4 lists the differential magnitudes (Δmag) between the comparison star and check star. It is defined as the magnitude of the check star minus the comparison star. The probable errors listed at the bottom of each column are the maximum likely intrinsic variations of the comparison star or the check star. They are sufficiently small that it can be said, at least on nights of observation, that the comparison star was suitably constant.

In an attempt to find an empirical value for the third light of the system (that of the companion star), occasional measurements were made on nights of good seeing. Unfortunately, nights of good seeing were often of poor photometric quality. For example, a thin layer of clouds may cause reduction of turbulence, thus improving the seeing, but these clouds also cause a varying transparency of the atmosphere making the night of poor photometric quality. Also the quality of the tracing (due to imperfect centering of the companion star while attempting to prevent light of the variable star from "leaking in") was critical. For these two reasons, each measurement was weighted with a number between one and five giving some indication of the quality of the observation due to the photometric quality of the night and the quality of the tracing. The product of these two numbers (divided by ten) was the adopted weight for the measurement in

TABLE 4

THE DIFFERENTIAL MAGNITUDES BETWEEN THE COMPARISON AND CHECK STARS USED DURING THE PHOTOMETRIC INVESTIGATION OF AA CETI

Date	Δmag_v	Δmag_b	Δmag_u
9/ 2- 3/72	0.692	0.679	0.694
	0.721	0.644	0.678
	0.668		
9/ 4- 5/72	0.698	0.671	0.685
*10/14-15/72	0.662	0.645	0.664
*10/16-17/72	0.733	0.701	0.692
10/28-29/72	0.712	0.676	0.662
10/29-30/72	0.703	0.664	0.690
	0.703	0.676	
11/ 8- 9/72	0.718	0.681	0.699
	0.700	0.665	0.677
	0.699	0.667	0.681
*12/ 8- 9/72	0.675	0.689	**
*12/ 9-10/72	0.704	0.649	0.641
Average	0.704	0.670	0.680
Probable Error	±.012	±.010	±.010

*Very poor night; one-half weight

**No extinction information

TABLE 5

THE DIFFERENTIAL MAGNITUDES BETWEEN THE COMPANION AND COMPARISON STARS AND THE WEIGHTS USED FOR EACH MEASUREMENT TO CALCULATE THE AVERAGE AND PROBABLE ERROR

Date	Δmag_v	Δmag_b	Δmag_u	Weight
11/12-13/71	0.218			1.0
	0.302			1.5
	0.307			2.0
	0.359			1.0
	0.367			1.0
11/25-26/71	0.385			0.5
	0.352			0.5
12/29-30/71	0.252	0.314	0.424	2.0
	0.231	0.295	0.412	2.5
12/31/71-1/1/72	0.254	0.298	0.394	2.0
9/ 2- 3/72	0.287	0.318	0.438	0.3
9/ 4- 5/72	0.191	0.251	0.428	0.9
10/14-15/72	0.185	0.191	0.289	0.4
	0.162	0.207	0.316	0.4
10/16-17/72	0.206	0.243	0.342	0.8
10/29-30/72	0.242	0.335	0.429	1.2
	0.269	0.355	0.448	1.2
11/ 8- 9/72	0.233	0.321	0.437	2.5
Average	0.264	0.300	0.411	
Probable Error	±.036	±.026	±.025	

each color, and that number is given in Table 5 along with the individual observations, their weighted averages and probable errors. The differential magnitudes are defined in the sense of companion star minus comparison star.

It is apparent from the probable errors shown in Table 5 that there is a great deal of scatter in the data possibly due to the difficulty of the measurement. However, the uncertainty in the third light which was subtracted in the yellow results in a probable error in the depth of the primary eclipse of only ±0.017 magnitude for the final light curve. Likewise for the blue and ultraviolet the uncertainty in the final primary eclipse depths are only ±0.011 and ±0.010 magnitudes respectively. A careful study of the correlation of the apparent "fluctuation" of the companion star's light from these measurements with respect to scatter in the light curve of both stars of the visual binary seems to indicate that the variations are not "real," i.e., not attributable to intrinsic variations of the companion, but rather caused by the difficulty of the measurement. The apparent fading trend of the companion star on the night of 11/12-13/71, however, is difficult to explain in terms of observational difficulties which would cause random scatter in the measurements. It would appear then that extensive measurements should be made of the companion star if improvement in the light curve of the visual binary system is attempted. Since these measurements do not demonstrate that the "fluctuations" of the light of the companion are systematic, it will be assumed here that the companion star represented a constant source of light. The best values of the third light given in Table 5 were then subtracted to give the light of the variable component alone.

Light Elements

As was pointed out in a previous section, preliminary light elements were found based upon times of faint light on the Bamberg plates. Subsequent photoelectric observations showed these elements to be incorrect.

Individual times of mid-eclipse were determined from the photoelectric data by the Hertzsprung (1928) method if sufficient data was available on both branches of the eclipse. Otherwise, an estimate was made using the tracing paper method of fitting the partial data to an eclipse whose mid-point was "known." The approximate period was found by assuming for each available pair of times that exactly n cycles (for two primary minima or two secondary minima) or n plus one-half cycles (for a primary and a secondary) had taken place. Solving for several values of n (for each pair) revealed one common period in the vicinity of 0.5 to 1.25 days. With this approximation the epoch of each observed eclipse was determined, and a linear least-squares calculation was done to refine the elements. The final set of elements were calculated using the best times available from the Bamberg plates and all the photoelectric times of minimum light weighted as shown in Table 6 (Bloomer, 1972a). The final light elements (and probable errors) derived for this system were

$$\begin{array}{lll} \text{Min I} = \text{JD(hel.)}\ 2441268.6869 & + & 0\overset{d}{.}53617353 \cdot E \\ \qquad\qquad\qquad\qquad\quad \pm.0007 & & \pm.00000050 \end{array} .$$

The observed minus the calculated times of minimum light given in Table 6 are plotted in Figures 6 and 7.

TABLE 6

TIMES OF MINIMUM LIGHT OF AA CETI AND THE WEIGHTS USED TO CALCULATE THE LIGHT ELEMENTS

Julian Date (hel.)	Epoch	Weight	O-C(days)*
2438728.319	-4738.0	2	+0.022
38995.594	-4239.5	1	+0.015
39006.549	-4219.0	1	-0.022
39060.417	-4118.5	1	-0.039
39383.507	-3516.0	1	+0.006
39404.394	-3477.0	2	-0.018
39444.359	-3402.5	1	+0.003
39761.491	-2811.0	2	-0.012
39768.483	-2798.0	1	+0.010
39771.463	-2792.5	1	+0.041
40530.392	-1377.0	1	+0.016
40566.285	-1310.0	2	-0.015
41261.7176	- 13.0	5	+0.0010
.7176	- 13.0	5	+0.0010
.7155	- 13.0	5	-0.0011
41264.6665	- 7.5	4	+0.0009
.6687	- 7.5	4	+0.0030
.6664	- 7.5	4	+0.0008
41268.6866	0.0	5	-0.0003
.6869	0.0	5	0.0000
.6860	0.0	5	-0.0009
41281.5571	+ 24.0	4	+0.0020
.5566	+ 24.0	4	+0.0015
.5561	+ 24.0	4	+0.0010
41315.6031	+ 87.5	4	+0.0010
.6022	+ 87.5	4	+0.0001
.6012	+ 87.5	4	-0.0009

TABLE 6 CONTINUED

Julian Date (hel.)	Epoch	Weight	O-C(days)*
2441317.481	+ 91.0	2	+0.002
41563.853	+ 550.5	2	+0.002
41607.836	+ 632.5	1	+0.019
41620.664	+ 656.5	2	-0.021
41630.603	+ 675.0	3	-0.002

* Observed minus calculated time of minimum predicted from Min I = JD(hel.) 2441268.6869 + $0\overset{d}{.}53617353 \cdot E$

Fig. 6. The observed minus the calculated times of minimum light of AA Ceti used in the calculation of the light elements

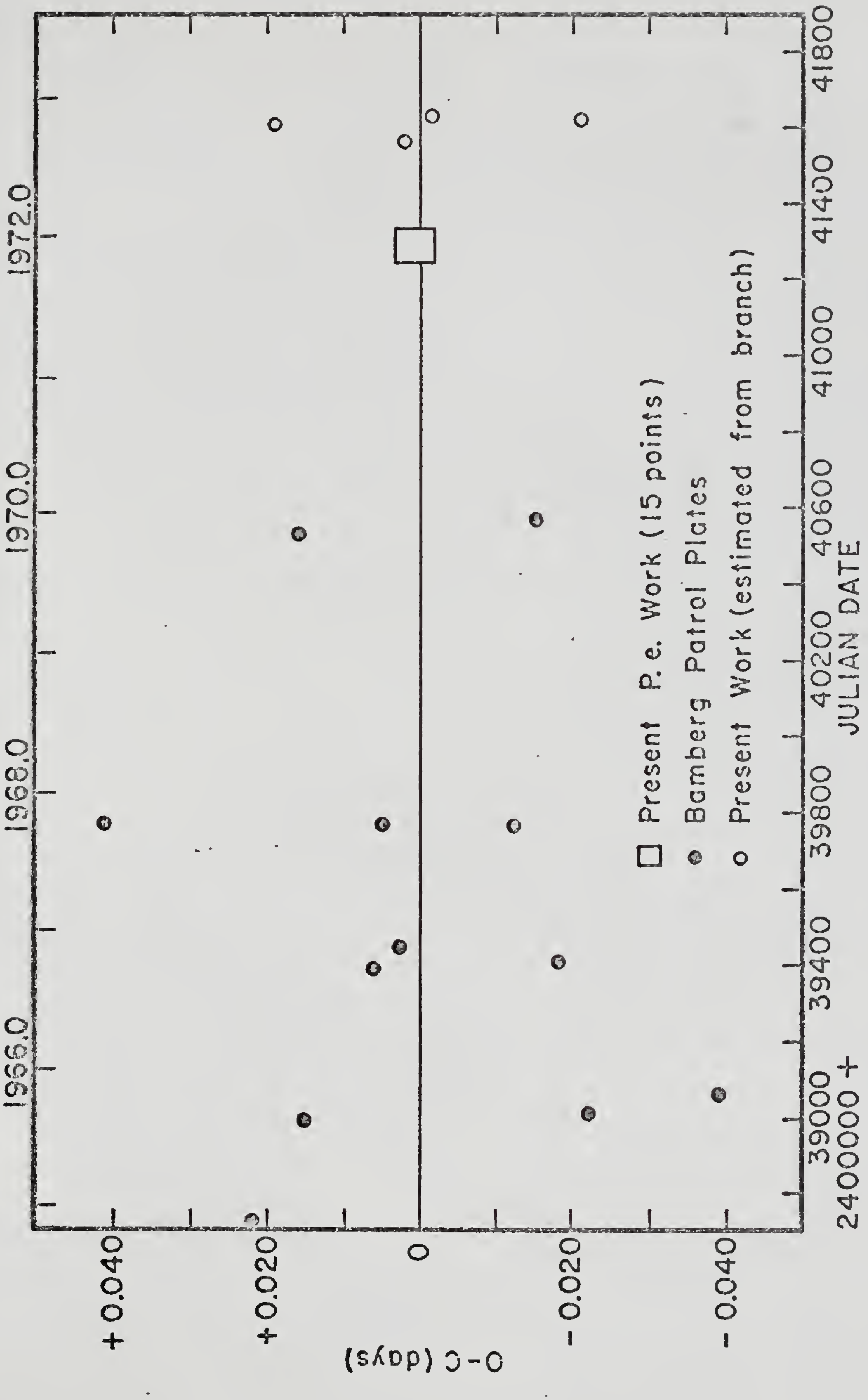
O-C (days)
+0.040
+0.020
0
-0.020
-0.040
1966.0
1968.0
1970.0
1972.0
39000
39400
39800
40200
40600
41000
41400
41800
2400000 +
JULIAN DATE
□ Present P.e. Work (15 points)
● Bamberg Patrol Plates
○ Present Work (estimated from branch)

Fig. 7. The observed minus the calculated times of minimum light of AA Ceti derived from the photoelectric data only

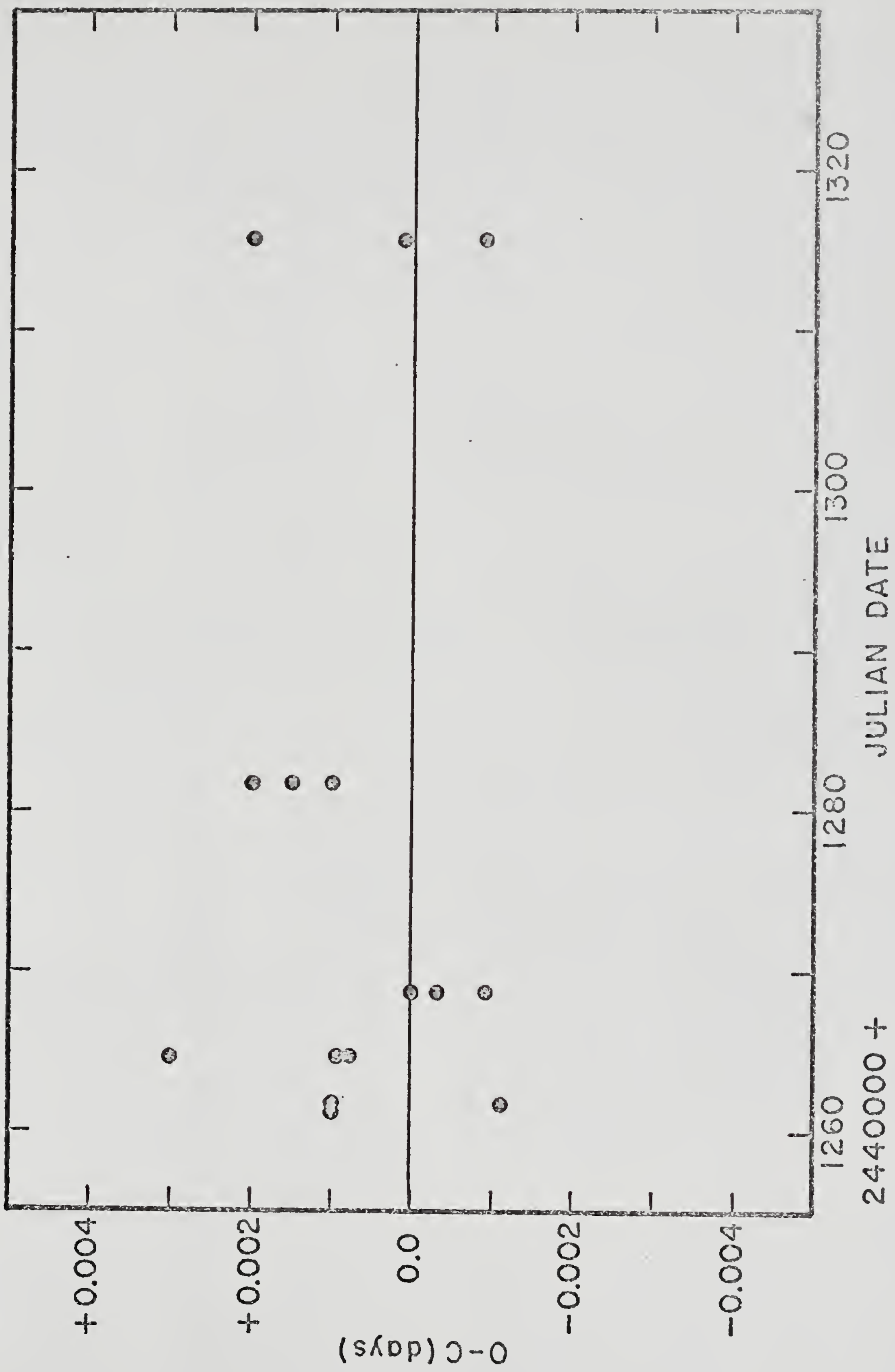
O-C (days)
+0.004
+0.002
0.0
-0.002
-0.004
1260
1280
1300
1320
2440000 +
JULIAN DATE

Color Curves

In order to display the average change in color of the star system during a cycle, b-v and u-b curves were constructed after the third light subtraction had been made. First, the phase of each observation was calculated using the light elements discussed previously. Then, since the b and v measurements were not made simultaneously, the blue magnitudes were linearly interpolated to the yellow measurements so that the subtraction could be made. The same procedure was followed for the u-b curve. No night corrections or seasonal adjustments were made in plotting all the data together.

The b-v curve shown in Figure 8 exhibits a distinct reddening of the system by about 0.06 magnitude during the primary eclipse. Since the primary eclipse is, in most cases, the eclipse of the hotter star, this is an expected result. There does not seem to be a significant change during the secondary eclipse.

The u-b curve (Figure 9) shows the same general characteristics although the reddening during the eclipse is only one-half as large, and the scatter of the data seems greater.

The fact that the system does not become more blue during the secondary eclipse (the eclipse of the cooler star) tends to indicate that the relative contribution of the cooler star to the total light of the system is small at all the wavelengths investigated.

Fig. 8. The b-v curve for AA Ceti after subtraction of the third light of the companion star

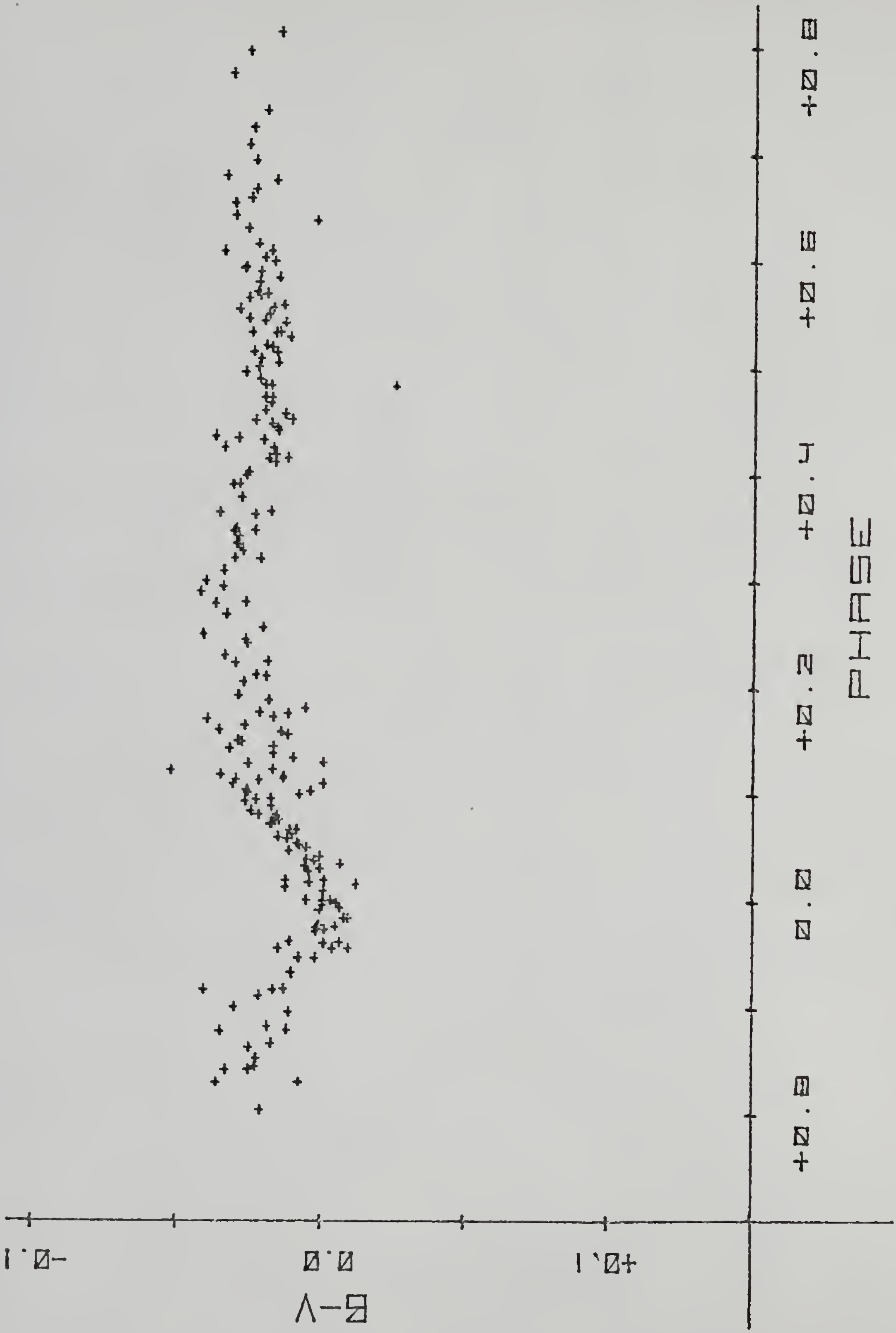
B-V
-0.1
0.0
+0.1
PHASE
+0.8
0.0
+0.2
+0.4
+0.6
+0.8

Fig. 9. The u-b curve for AA Ceti after subtraction of the third light of the companion star

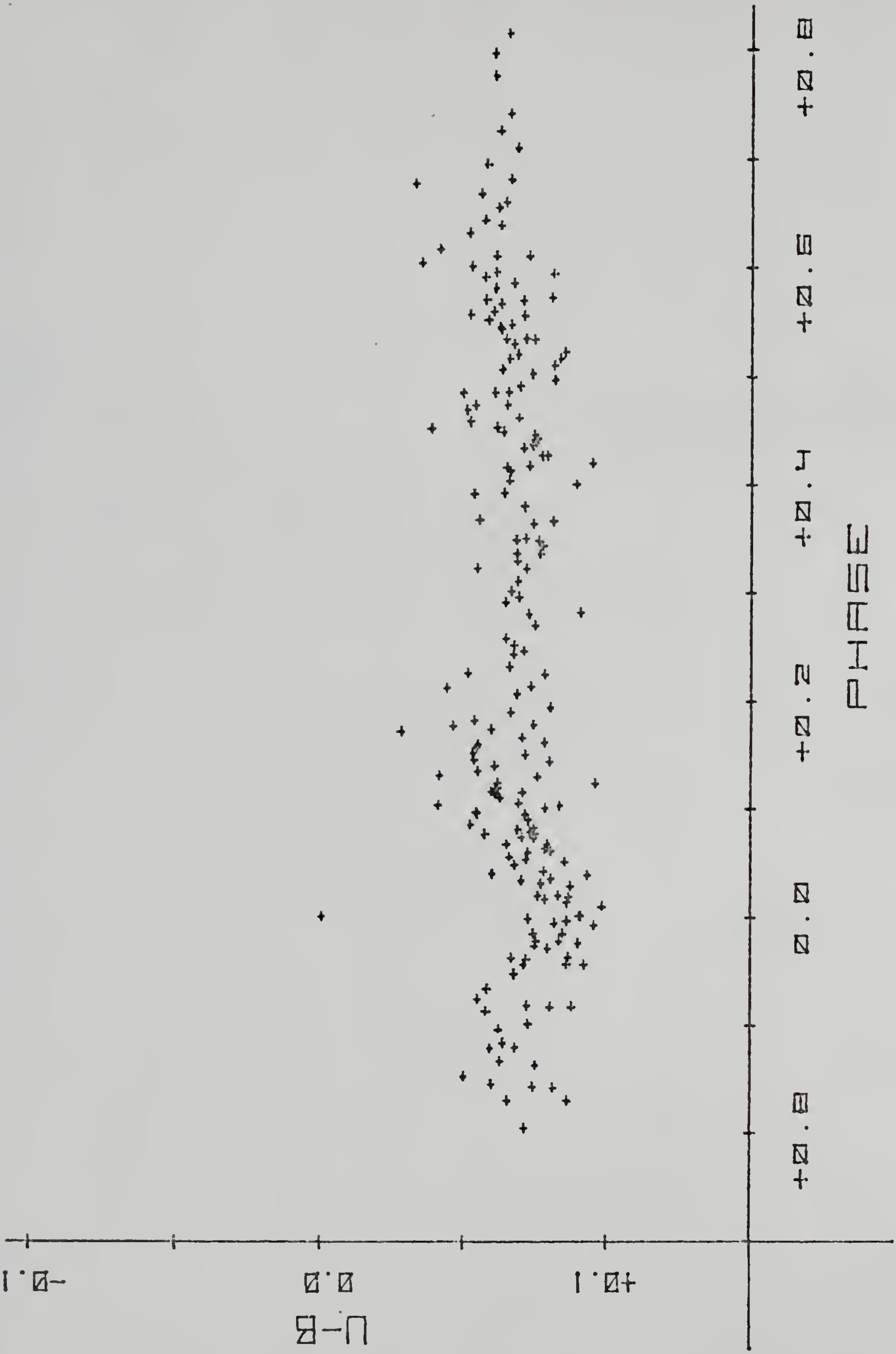
+0.8
0.0
+0.2
+0.4
+0.6
+0.8
PHASE
+0.1
0.0
-0.1
U-B

Light Curves

The data points were plotted into light curves. No night corrections or seasonal adjustments were made. The resulting curves are shown in Figures 10 through 12. All the curves showed a continuous variation between the eclipses and a period of constant light which lasted approximately fifty minutes during the secondary eclipse with the exception of the ultraviolet light, which faded linearly with phase as the eclipse progressed. There was a larger apparent scatter during the secondary eclipse than in the rest of the curves. However, an analysis of this region showed that there were night-to-night changes in the level and shape of the light variations at the bottom of the eclipse. Although there were indications, then, of intrinsic variability of the stars, an average of all the data was used for the solution as if the scatter had been random.

There were no significant indications of a "periastron effect" or of a displacement of the secondary minimum from a linear phase of 0.5. It is apparent, however, that maximum light after primary eclipse came later than a phase of 0.25.

The light curves can then be classified as essentially W UMa-type curves with a total secondary eclipse (and annular primary) with some photometric complications.

Fig. 10. The v light curve of AA Ceti after subtraction of the third light of the companion star and adjustment of the magnitude scale to 0.0 magnitude at maximum light

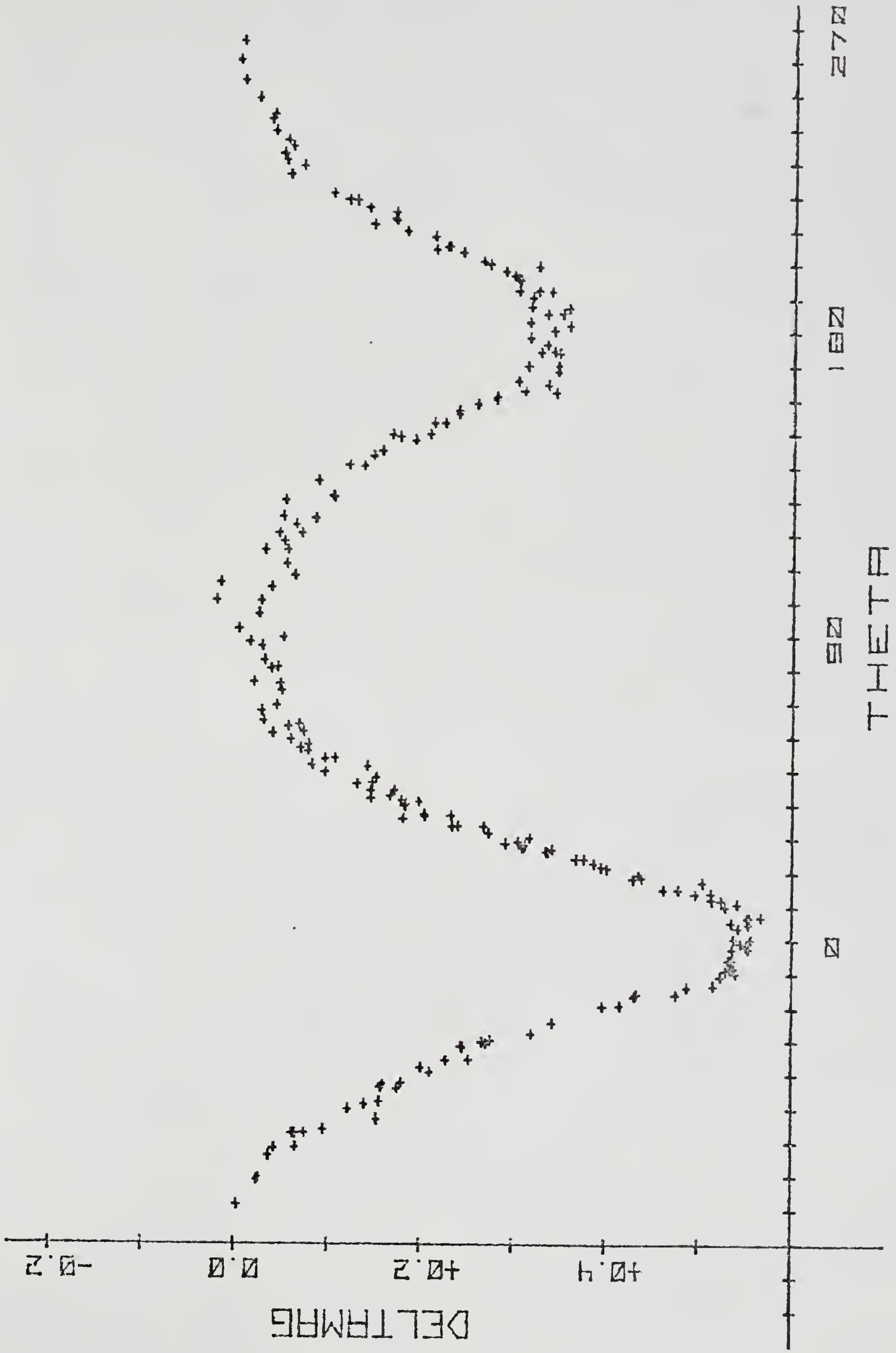
DELTAMAG
-0.2
0.0
+0.2
+0.4
THETA
0
90
180
270

Fig. 11. The b light curve of AA Ceti after subtraction of the third light of the companion star and adjustment of the magnitude scale to 0.0 magnitude at maximum light

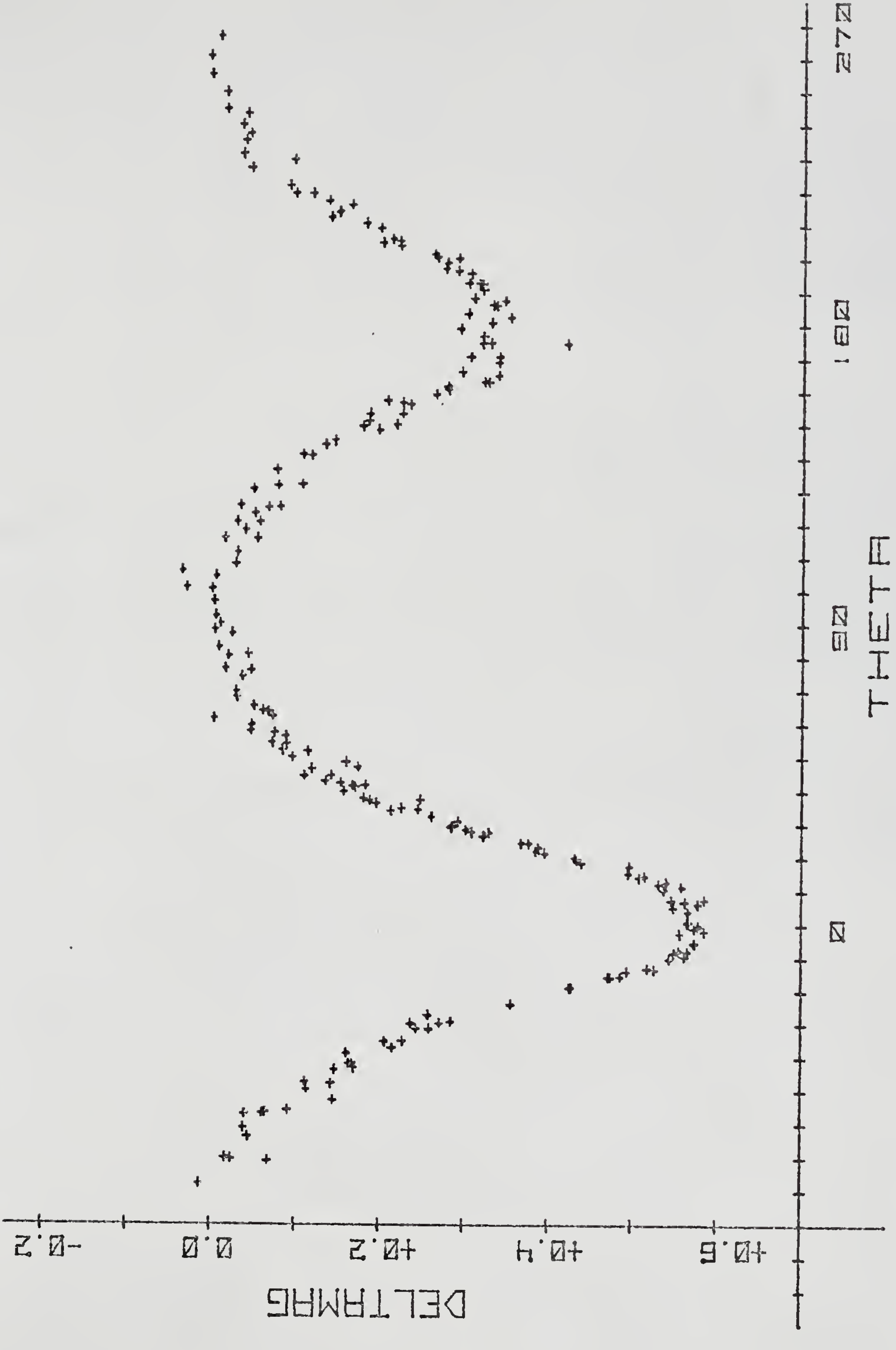
DELTAMAG
-0.2
0.0
+0.2
+0.4
+0.6
THETA
0
90
180
270

Fig. 12. The u light curve of AA Ceti after subtraction of the third light of the companion star and adjustment of the magnitude scale to 0.0 magnitude at maximum light

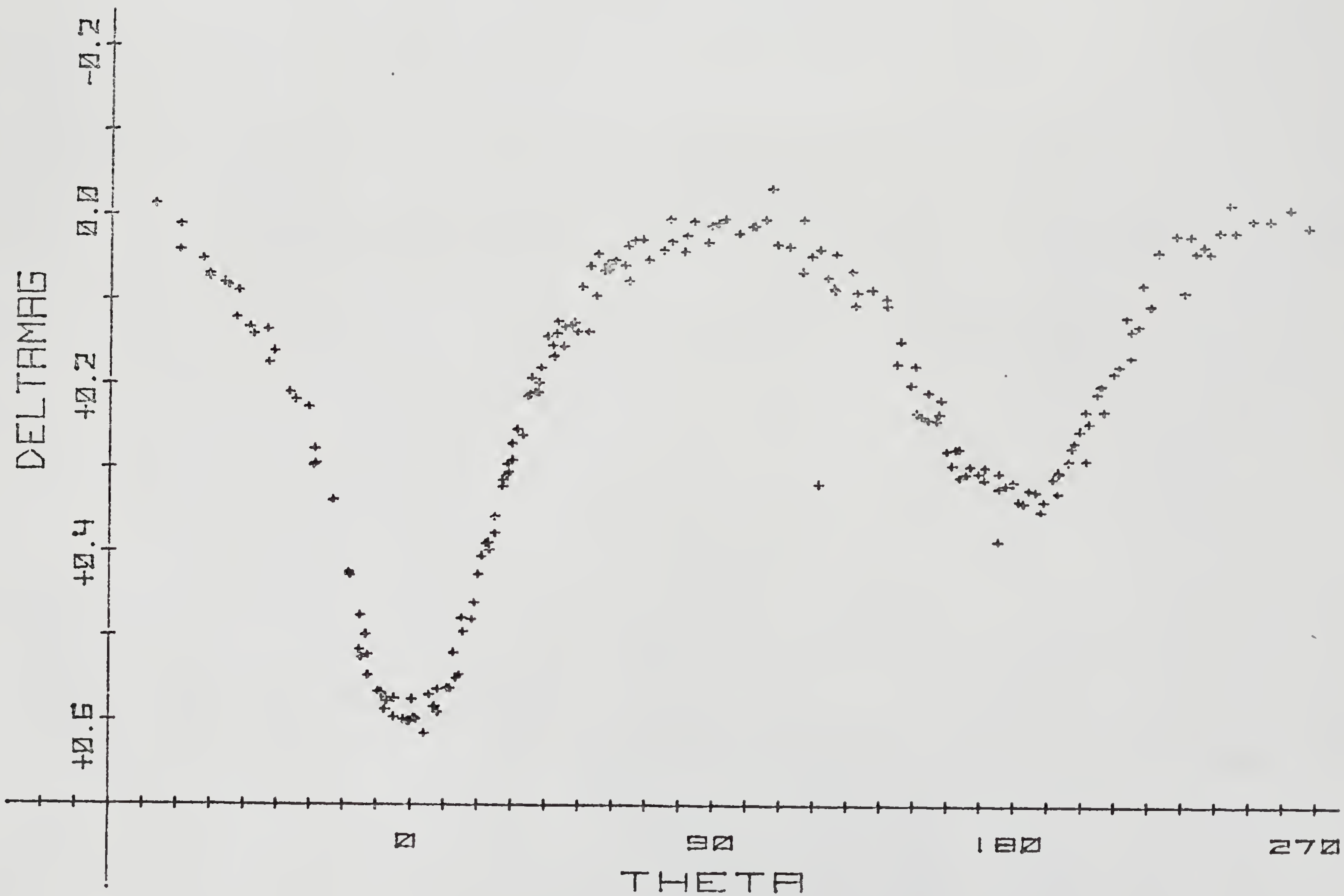
DELTAMAG
-0.2
0.0
+0.2
+0.4
+0.6
0
90
180
270
THETA

The Model

In order to deduce the photometric elements or parameters describing a physical binary system, some model must be employed. The model of Russell and Merrill (1952) adopted here assumes two spherical stars which are darkened at the limb by a linear cosine relation and which are moving in circular orbits. The darkening equation relates the observed surface brightness (J) at some point on the disk described by the angle γ (the angle measured at the center of the star between the direction of the observer and the point on the surface) and the surface brightness at the center of the observed disk (J_c); specifically

$$J = J_c(1 - x + x \cos\gamma)$$

where x is the limb darkening coefficient, which may have a value between zero and one.

Merrill (1950) has calculated tables of functions which describe the shapes of eclipses in terms of the tabular values of the ratio of the radii of the two stars, a quantity which describes the "depth" or geometrical degree of eclipse taking place, and values of the darkening coefficient 0.0, 0.2, 0.4, 0.6, 0.8, and 1.0. Finding a solution, then, is a multiparameter fitting problem. In order to discuss the solution, the parameters involved must be enumerated.*

For the case of spherical stars moving in circular orbits and darkened at the limb by the aforementioned linear cosine relation, the following parameters must be determined:

P - the orbital period of the two stars,

---

*For a detailed explanation of the model the original papers of Russell and Merrill are referenced here.

T_o - the initial epoch necessary to predict the relative positions of the stars at some time; the initial epoch and period are usually referred to as the "light elements,"

i - the inclination of the orbit of the spherical star system with respect to the plane of the sky,

L_s - the fractional luminosity contribution of the smaller star to the total light of the system,

L_g - the fractional luminosity contribution of the "greater" or larger star to the total light of the system,

L_3 - the light of a supposed third body if the solution does not satisfy $L_s + L_g = 1.0$,

r_g - the radius of the larger star in units of the separation of their centers,

r_s - the radius of the smaller star in units of the separation of their centers,

or $k = r_s/r_g$,

x_s - the darkening coefficient of the smaller star,

and

x_g - the darkening coefficient of the larger star.

The darkening coefficients are usually assumed a priori based upon theoretical considerations, although they are sometimes changed to achieve a better fit to the data. If one of the eclipses is total, i.e., a smaller star is completely eclipsed by a larger one, then L_s is determined, and $L_g = 1 - L_s$ unless there is a third light known or suspected. Since the period and initial epoch are determined beforehand, a star with a total eclipse has only three parameters to be determined from the shape of the eclipse: i, r_g and r_s, or k. For a system in which partial eclipses take place, four parameters must be found with the addition of L_s or L_g (assuming $L_3 = 0$).

The extent of eclipse may be described by the quantity

$$p = \frac{\delta - r_g}{r_s}$$

where δ is the apparent or projected separation of the centers of the two stars, and p_o is defined so that when the eclipsed area is maximum (and light is minimum), $p = p_o$. Then

$p_o > 1$ for no eclipse,

$1 > p_o > -1$ for a partial eclipse,

and

$p_o < -1$ for a complete eclipse.

Another quantity which describes the degree of eclipse is α_o. It is expressed in terms of the light lost at internal tangency $(1 - \ell_i)$. If the light lost in mid-eclipse is $(1 - \ell_o)$, then

$$\alpha_o = \frac{1 - \ell_o}{1 - \ell_i} \quad .$$

During a partial eclipse ℓ_o never reaches ℓ_i, and therefore $\alpha_o < 1$. For an eclipse which is total, i.e., a total occultation of a smaller star, $\alpha_o^{oc} = 1$. An eclipse which is annular, i.e., the transit of the smaller star across the face of the larger, will have $\alpha_o^{tr} > 1$.

The problem reduces, then, essentially to choosing the proper values of k, α_o^{tr}, and α_o^{oc} (or p_o in the case of total eclipses since α_o^{oc} then is fixed at unity) which describe the data of both eclipses. A great deal of time and insight is gained by utilizing the nomographs of Merrill (1953) which graphically display the "shape functions" on a grid of possible solutions (k's and p_o's). These functions, ${}^x\chi(k,\alpha_o,n)$ and ${}^x\Psi(k,\alpha)$, were tabulated by Merrill (1950) as mentioned at the beginning of this chapter.

Once the best values of k and p_o are found, then the physical elements of the system may be calculated by solving the equations below.

$$L_s = \frac{1 - \ell_o^{oc}}{\alpha_o^{oc}} \qquad (\alpha_o^{oc} = 1 \text{ for total eclipses})$$

$$L_g = 1 - L_s \text{ if } L_3 = 0$$

$$r_g^2 \operatorname{cosec}^2 i = \sin^2\theta_e / \left[k(1 - p_o)(2 + k + kp_o)\right]$$

$$r_g^2 \operatorname{cosec}^2 i (1 + kp_o)^2 = \cot^2 i$$

The angle θ_e is the point of external contact or the phase angle at which the eclipse begins.

On the nomographs a possible solution is described by coordinates V and H, and then

$$L_g = \frac{1 - \ell_o^{tr}}{V} \quad \text{and} \quad L_s = \frac{1 - \ell_o^{oc}}{\alpha_o^{oc}} \quad .$$

If a solution is chosen which satisfies the so-called "depth equation" that relates the maximum light lost in the eclipses, then V will have a value such that $L_g + L_s = 1$. However, if the shape functions require a solution at a different value of V, then $L_s + L_g < 1$, and the solution requires that $L_3 > 0$. A solution which causes $L_s + L_g > 1$ is clearly spurious.

Although the linear cosine law of darkening and the assumption of circular orbits are usually adequate for close binaries, the extreme proximity of the stars and the resulting huge tidal distortions make the assumption of spherical stars very poor indeed. This is evidenced by the fact that the major light changes are sometimes due not to eclipse effects but to changing aspects of the highly distorted stars. In order to remove non-eclipse effects, a "rectification" or transformation is performed.

It has been demonstrated by Russell and Merrill (1952) that the distortion of the component stars can be approximated by two similar tri-axial ellipsoids. In fact, the stars will assume the shape of their Roche limiting surfaces (the equipotential contours around the stars); however, similar ellipsoids have been assumed in the interest of tractability.

Russell and Merrill have also shown that the ellipsoids cause distortions of the light curve (generally referred to as the "ellipticity effect") which can be described by a truncated Fourier series:

$$\ell = a_0 + a_1 \cos \theta + a_2 \cos 2\theta \ldots .$$

Actually the effects of limb darkening and gravity darkening (brightening of the star's surface at the poles due to centripital flattening which results in a higher acceleration of gravity) complicate the transformation somewhat, and a rectification of the phase as well as of the light is necessary.

The so-called "reflection effect," a heating up of the facing surfaces of the stars, also contributes cos $n\theta$ terms to the light variations. The coefficients can be estimated from theory (Russell and Merrill, 1952) and are generally designated by C_n.

None of these effects cause $B_n \sin n\theta$ variations in the light although they are sometimes observed to be present. Conventionally, these "complications" in the light curve are simply subtracted in the rectification process. This assumes that the complications extend through the entire cycle.

The rectification process, then, consists of, first, fitting by the method of least-squares a truncated Fourier series to the light variations outside of eclipse and finding the coefficients of the series:

$$\ell = A_0 + \sum_{n=1}^{4} A_n \cos n\theta + \sum_{n=1}^{4} B_n \sin n\theta \quad .$$

These coefficients include the algebraic sum of the effects of ellipticity and reflection. The reflection coefficients are found from the theory as described by Russell and Merrill, and then the rectified light (ℓ') and the rectified phase (θ') of each observed ℓ and θ are found by the following equations:

$$\begin{aligned}\ell' = (&\ell + C_0 + C_1 \cos\theta + C_2 \cos 2\theta - A_3 \cos 3\theta \\ &- A_4 \cos 4\theta - B_1 \sin\theta - B_2 \sin 2\theta - B_3 \sin 3\theta \\ &- B_4 \sin 4\theta) \; / \; (A_0 + C_0 + (A_2 + C_2) \cos 2\theta)\end{aligned}$$

and

$$\sin^2\theta' = \frac{\sin^2\theta}{1 - Z\cos^2\theta} \qquad \text{where} \qquad Z = \frac{-4(A_2 - C_2)}{(A_0 - C_0 - A_2 + C_2)N} \quad .$$

The quantity N is estimated to be 2.0, 2.2, 2.6, and 3.2 for the values of x of 0.2, 0.4, 0.6, and 0.8 respectively. In these equations the value of $-A_1$ is substituted for C_1 so that the entire cos θ variation is removed. The resulting light is presumably the light of two spherical stars whose radii have a ratio (k) which corresponds to two ellipsoids whose similar axes have the ratio of k, also. Likewise, the other spherical star elements of the system have an interpretation in terms of the "real" ellipsoidal system initially assumed.

The Rectification of the Light Curves of AA Ceti

The Fourier coefficients were found for all three light curves by estimating the point of external contact to be $0\overset{p}{.}12 = 43\overset{\circ}{.}2$ and by performing a least-squares fit to the data outside of eclipse. With the values of A_2 resulting from this calculation, the cos 2θ terms were removed from the unrectified light curves revealing a change in the slope at a phase of slightly greater than $0\overset{p}{.}111 = 40^\circ$. The sine and cosine coefficients were found through $n = 4$ since the exclusion of the higher order terms ($n = 3$ and 4) could result in spurious values of the lower order terms as pointed out by Merrill (1970).

From an initial rectification of each light curve the relative depths of the primary and secondary eclipses were found. The ratio of the depths approximates the surface brightness ratio of the two components, and from this the theoretical reflection coefficients were found.

A rectification was performed with the equations discussed in the previous section assuming limb darkenings of 0.4, 0.6, and 0.6 for the v, b, and u curves respectively. The preliminary solutions indicated that the darkening coefficients should have been chosen to be smaller in order to achieve a good fit to the data, and so the final rectification assumed darkenings of 0.2, 0.4, and 0.4. The coefficients used for the final rectification are given in Table

7. Since the sine terms were all small, they were set equal to zero in the final rectification.

In the process of finding the reflection coefficients using the graphical method of Russell and Merrill (1952), an attempt was made to find the spectral type of the fainter star; however, this procedure depended very critically upon the rectification done, particularly since the eclipses were extremely shallow. The primary component was assumed to be F2, and the secondary component was found to have a spectral type of F2, F6, and F9 based upon the v, b, and u curves respectively.

This same problem of achieving a consistent and reliable result for all the light curves occurred for another essentially W UMa-type star, RR Centauri. This star was found by several investigators (Knipe, 1965, and Bookmeyer, 1968) to be very difficult to solve, partly because the shallow eclipses did not allow definitive values of the ratio of surface brightnesses to be determined. Merrill (1970) found the spectral type of the smaller star in RR Centauri to be F3 if the brighter component were F2. However, Koch _et al_. (1970) stated that the secondary spectrum was F9. Both were considering only yellow observations.

The disparity of results for both AA Ceti and RR Centauri tends to make the determination of the spectrum of the fainter component of little value. In AA Ceti the secondary component is probably several sub-classes later than the primary component. The many other similarities between RR Centauri and AA Ceti will be discussed in the next section.

TABLE 7

COEFFICIENTS USED IN THE RECTIFICATION OF THE LIGHT CURVES OF AA CETI

	v	b	u
A_0	+0.87319 ±0.00607	+0.88441 ±0.00697	+0.89095 ±0.00700
A_1	-0.05371 ±0.00611	-0.04703 ±0.00697	-0.04197 ±0.00718
A_2	-0.13546 ±0.00943	-0.13551 ±0.01087	-0.11958 ±0.01094
A_3	-0.01735 ±0.00390	-0.01132 ±0.00447	-0.00840 ±0.00457
A_4	-0.01774 ±0.00498	-0.01494 ±0.00576	-0.01111 ±0.00575
B_1	-0.00245* ±0.00134	-0.00085* ±0.00154	-0.00423* ±0.00156
B_2	+0.00452* ±0.00203	+0.00302* ±0.00228	+0.00840* ±0.00233
B_3	+0.00672* ±0.00206	+0.00413* ±0.00234	+0.00295* ±0.00236
B_4	+0.00233* ±0.00244	+0.00521* ±0.00274	+0.00221* ±0.00282
Z	+0.3083 (x=0.2)	+0.2620 (x=0.4)	+0.2504 (x=0.4)
C_0	+0.03100	+0.03200	+0.03270
C_1	+0.05371	+0.04703	+0.04197
C_2	+0.01030	+0.01070	+0.01090

*Set equal to zero in rectification

Solutions of the Light Curves of AA Ceti

The rectified light curves were solved using the χ functions and nomographs. It was apparent from the values of χ that the primary eclipse was the transit and the secondary eclipse the occultation of the somewhat cooler and smaller star. The nomographic solutions revealed that the ratio of the radii was a small number and that the eclipses were total, which agreed with the appearance of the unrectified light curves. Independent solutions for each color were found using the χ functions, and a summary of the results is shown in Table 8. The values of $\bar{\theta}_e$, which seemed to become larger at shorter wavelengths, are an average of the θ_e from the primary and secondary eclipses. Figures 13 through 18 show the fit of the theoretical curves generated by the elements in Table 7 and the rectified data.

The inclination of the orbit for the ellipsoidal system (j) was found from the equation

$$\cos^2 j = \cos^2 i(1 - Z) \quad .$$

It was assumed that the semi-major axis of the ellipsoid of revolution (a) was the value of r resulting from the model. Then, the other axis of the equatorial cross section of the star (b) was found from

$$b = a \frac{\tan i}{\tan j} \quad .$$

It is possible to find the third dimension (c) of tri-axial stars; however, with the uncertainties in these solutions based upon somewhat uncertain rectification procedures, the calculation would be of little value.

It is customary to solve the light curves of totally eclipsing

TABLE 8

ELEMENTS OF THE SYSTEM AA CETI

	v	b	u
$x_s = x_g$	0.2	0.4	0.4
k	0.26	0.34	0.41
p_o	-1.50	-1.54	-1.37
α_o^{tr}	1.030	1.069	1.050
α_o^{oc}	1.000	1.000	1.000
r_g	0.55	0.53	0.52
r_s	0.14	0.18	0.21
i	70°.3	75°.4	76°.9
j	73°.7	77°.5	78°.7
$\bar{\theta}_e$	40°.7	43°.4	45°.6
$\bar{\theta}_i$ (Ψ solutions)	14°.7	14°.4	12°.2
a_g	0.55	0.53	0.52
b_g	0.45	0.45	0.45
a_s	0.14	0.18	0.21
b_s	0.12	0.15	0.18
$\epsilon = \frac{a-b}{a}$	0.184	0.150	0.141
$1-\ell_o^{tr}$	0.065	0.115	0.165
$1-\ell_o^{oc}$	0.079	0.073	0.089
L_g	0.921	0.927	0.912
L_s	0.079	0.073	0.089
$\bar{J}_g/\bar{J}_s$	0.786	1.475	1.727

Fig. 13. The theoretical solution of the yellow light curve plotted with the rectified data of the primary eclipse of AA Ceti

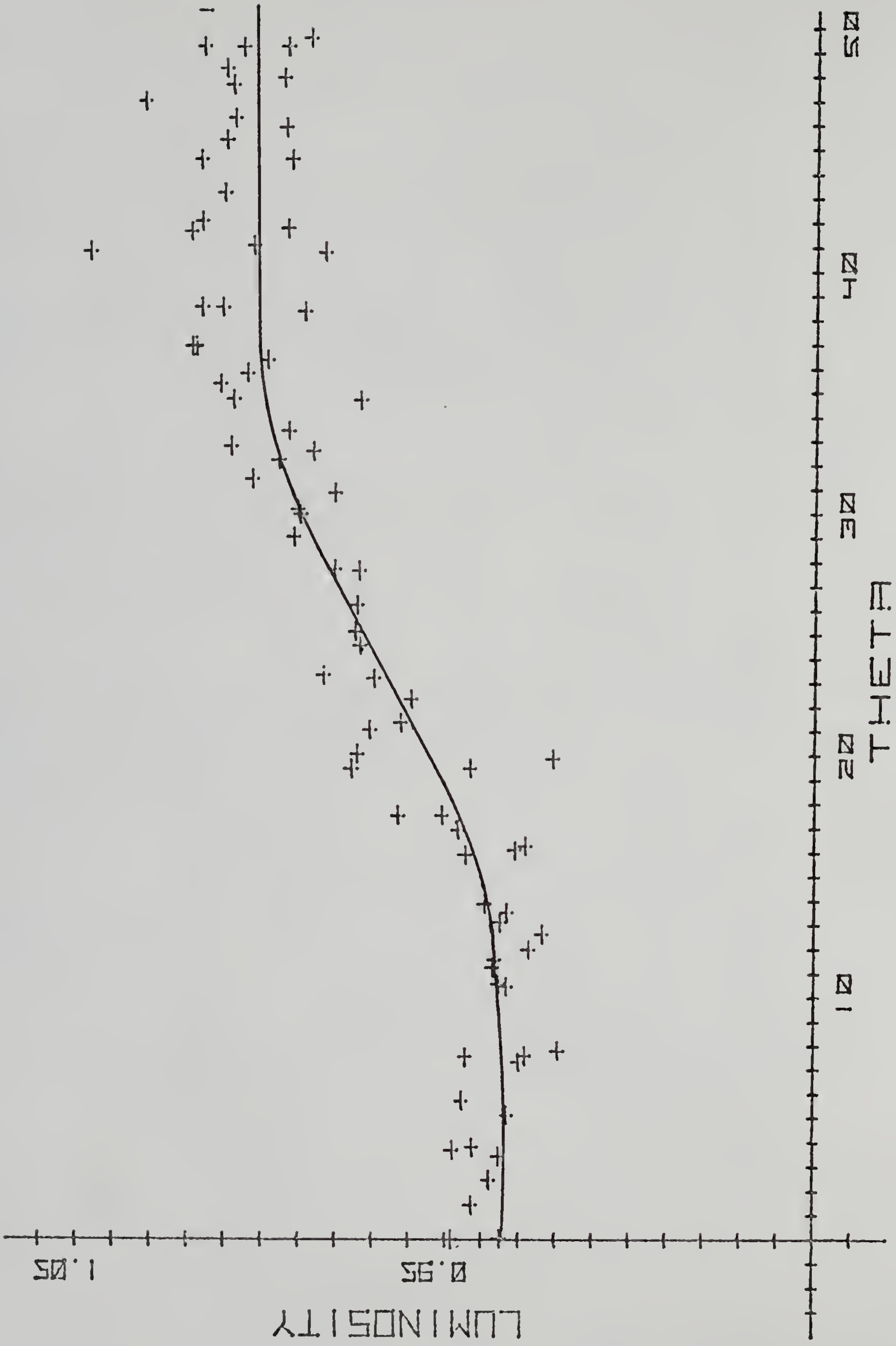
LUMINOSITY
1.05
0.95
THETA
10
20
30
40
50

Fig. 14. The theoretical solution of the yellow light curve plotted with the rectified data of the secondary eclipse of AA Ceti

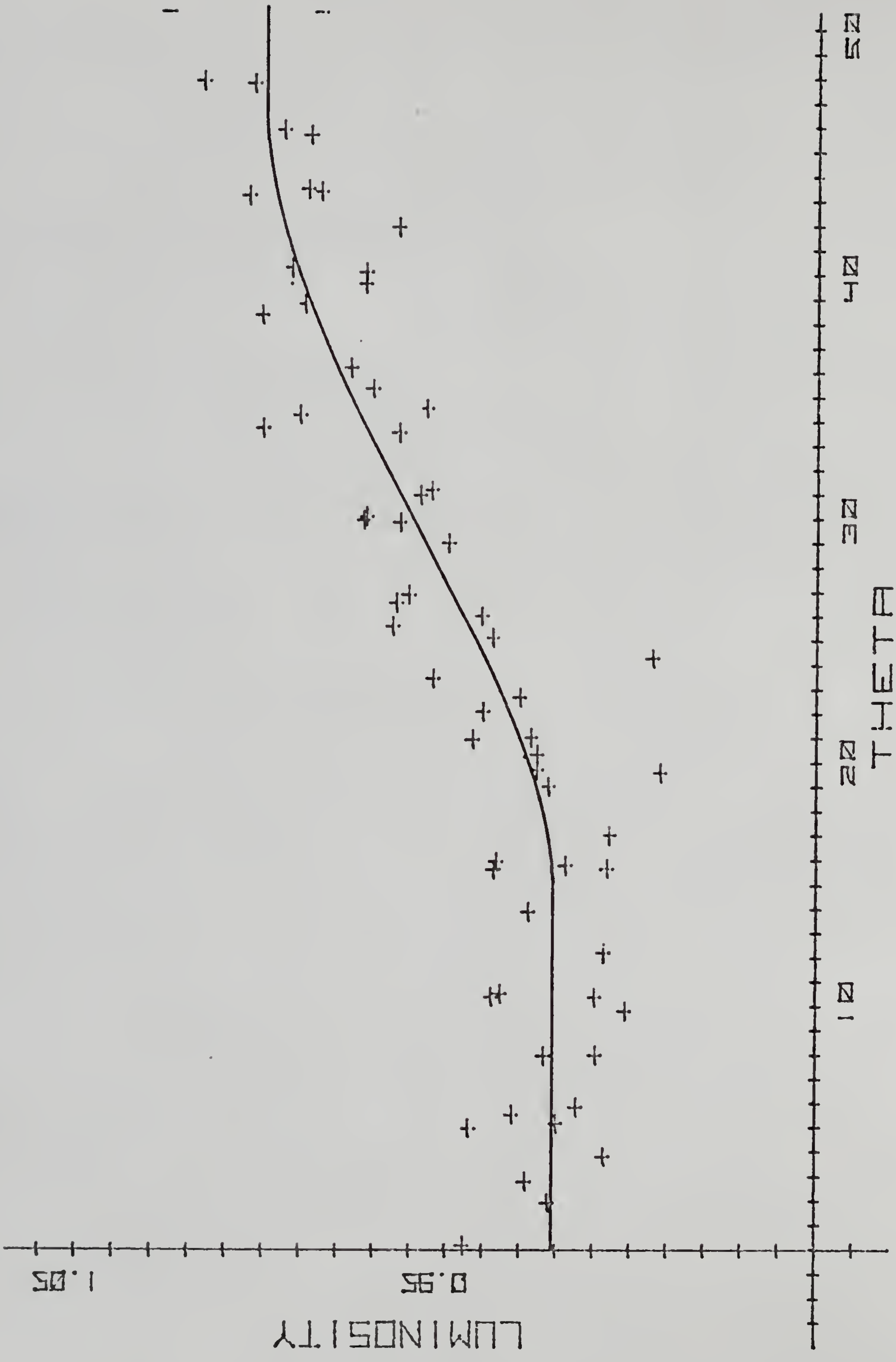
LUMINOSITY
1.05
0.95
THETA
10
20
30
40
50

Fig. 15. The theoretical solution of the blue light curve plotted with the rectified data of the primary eclipse of AA Ceti

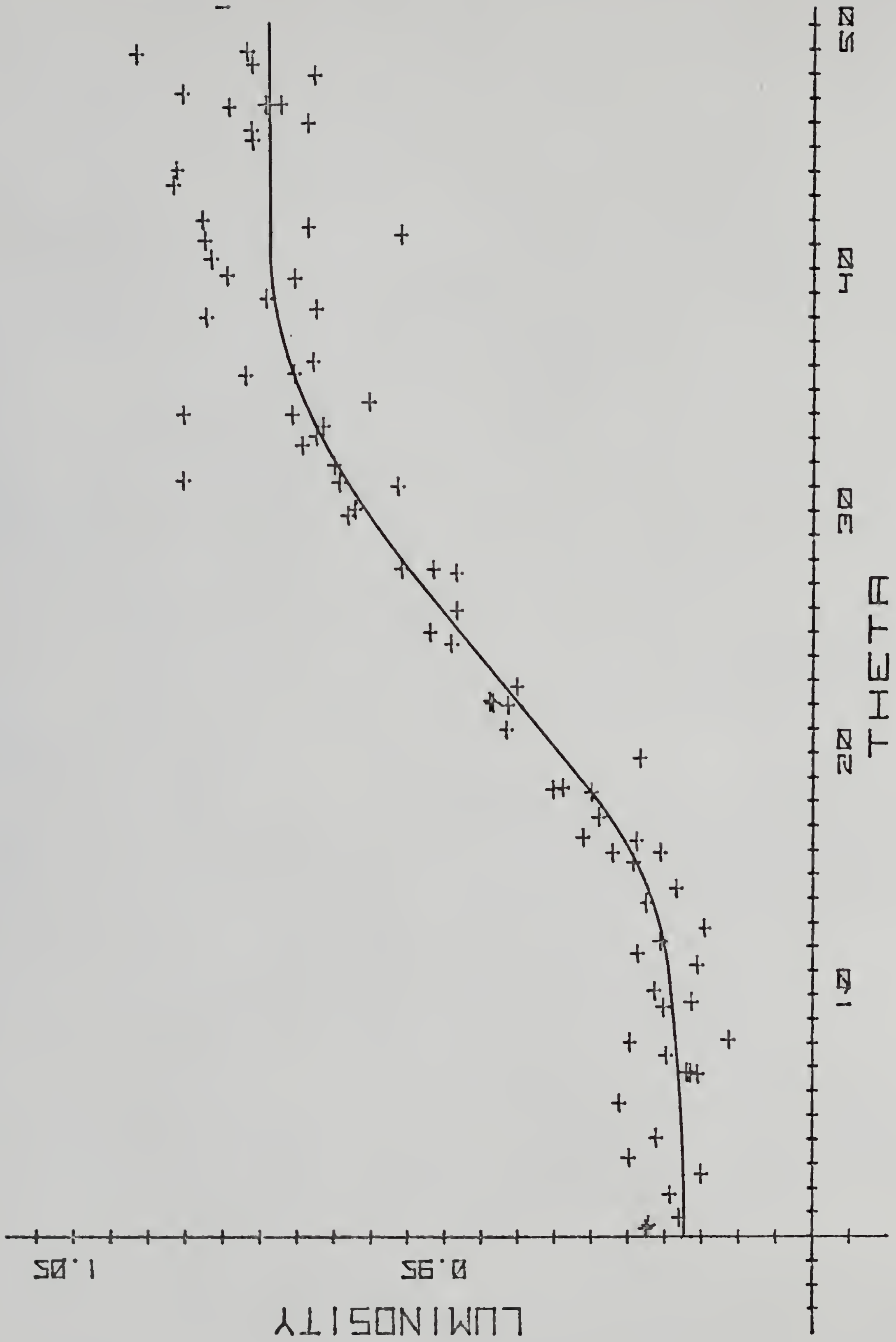
LUMINOSITY
1.05
0.95
THETA
10
20
30
40
50

Fig. 16. The theoretical solution of the blue light curve plotted with the rectified data of the secondary eclipse of AA Ceti

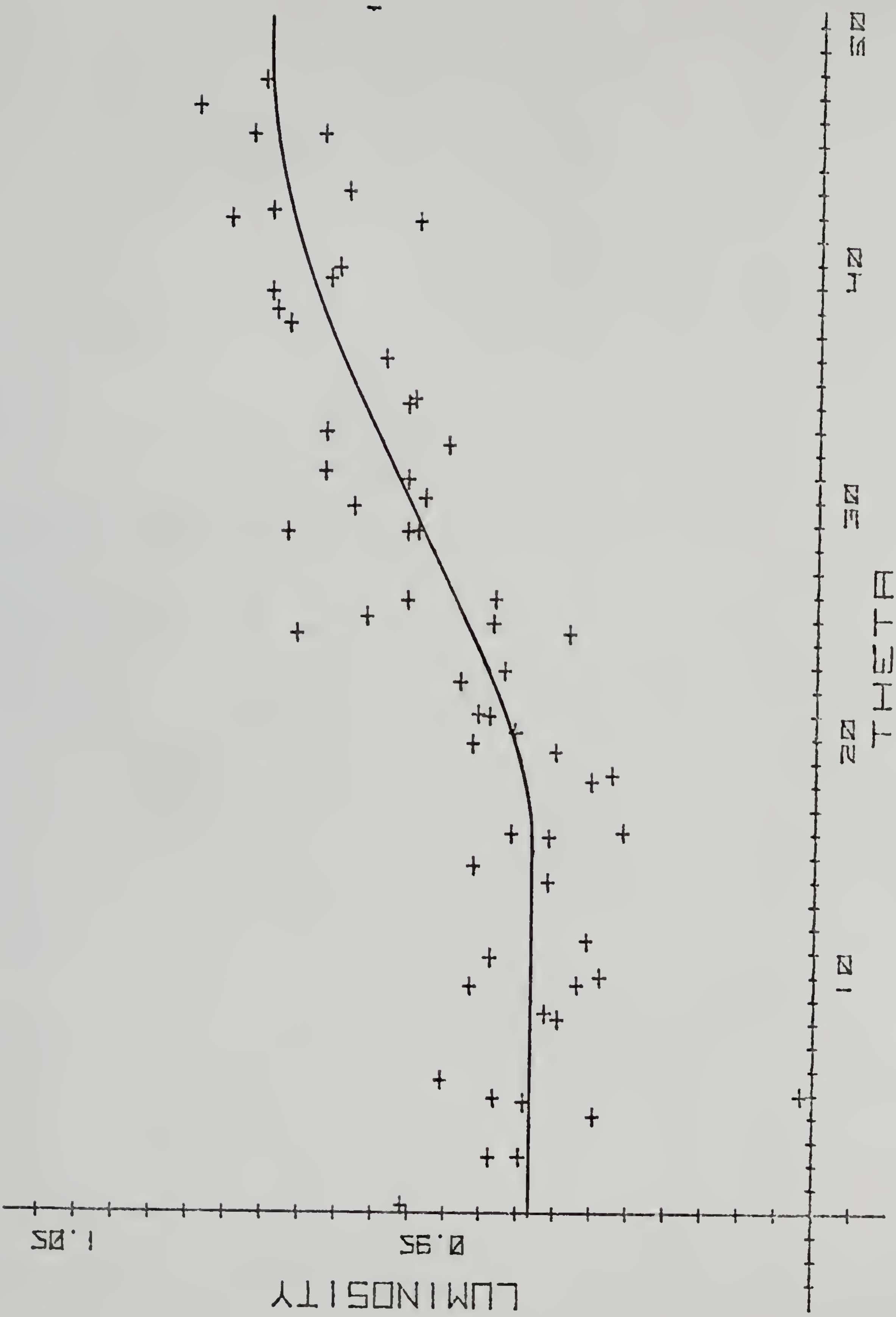
LUMINOSITY
1.05
0.95
THETA
10
20
30
40
50

Fig. 17. The theoretical solution of the ultraviolet light curve plotted with the rectified data of the primary eclipse of AA Ceti

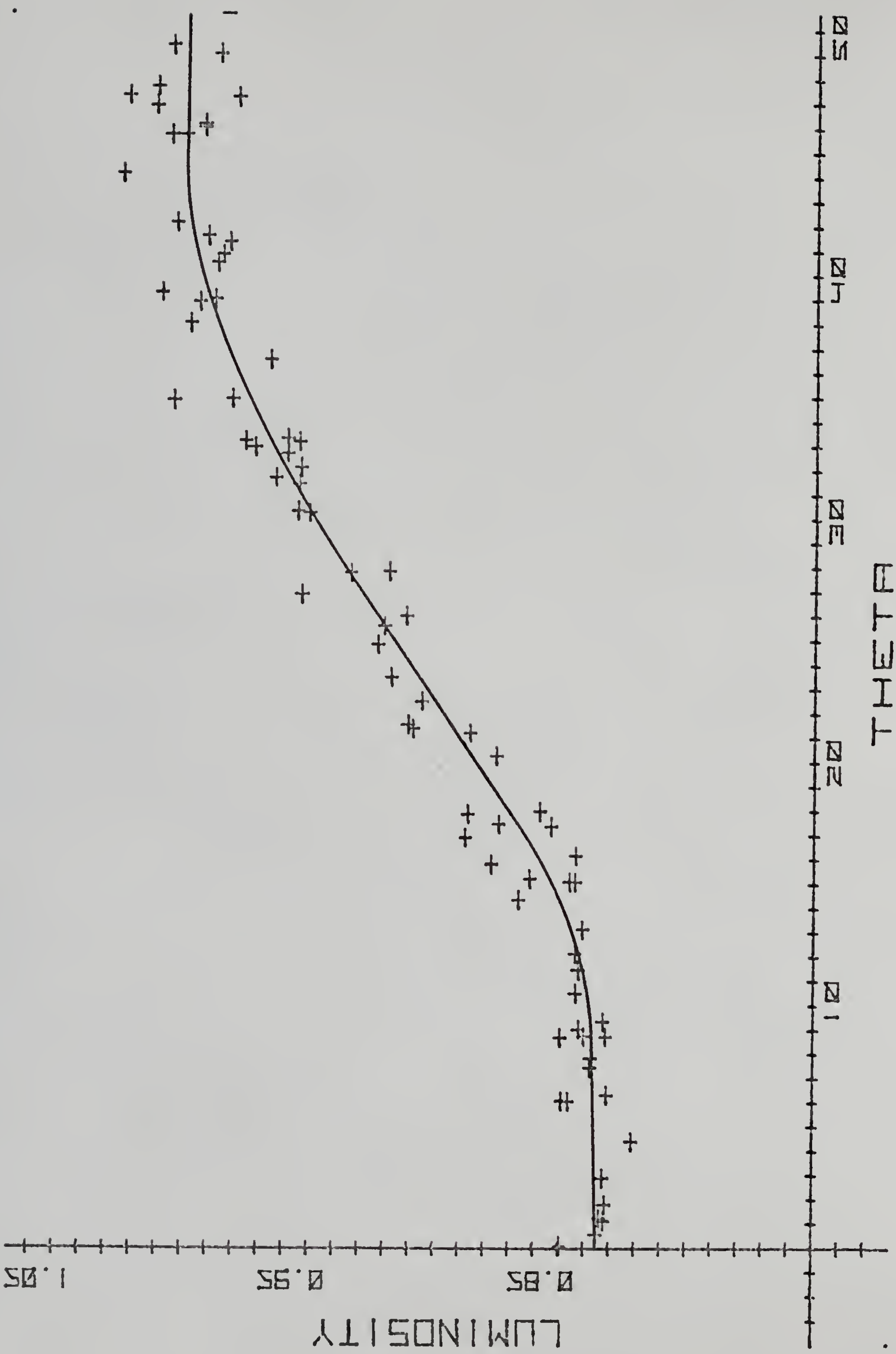
LUMINOSITY
0.85
0.95
1.05
THETA
10
20
30
40
50

Fig. 18. The theoretical solution of the ultraviolet light curve plotted with the rectified data of the secondary eclipse of AA Ceti

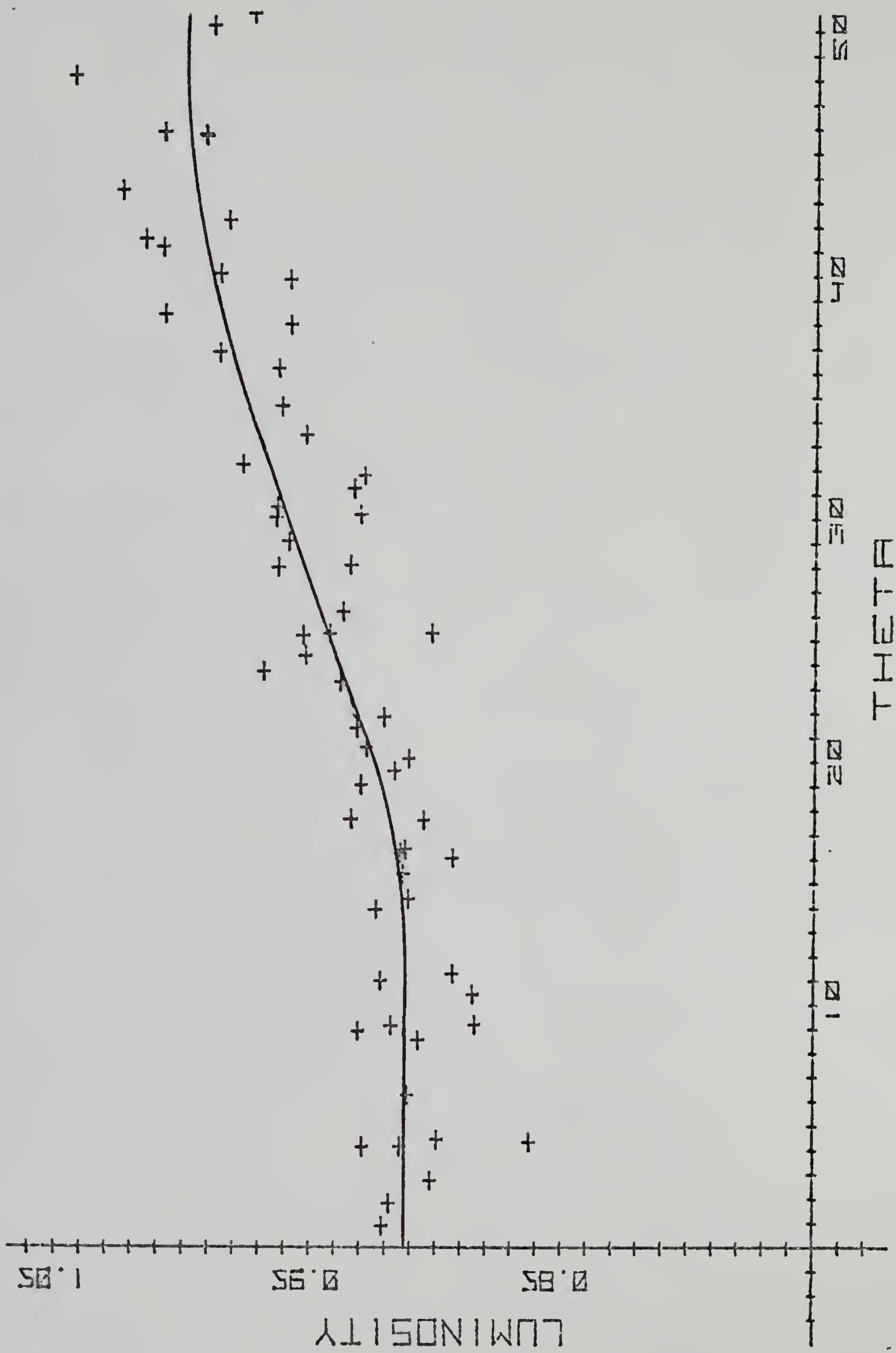
LUMINOSITY
1.05
0.95
0.85
THETA
10
20
30
40
50

stars using the Ψ functions of Russell and Merrill (1952). For light curves of high precision this is advisable since the Ψ tables can be linearly interpolated with higher precision than the χ functions. It was felt that the χ functions were sufficient for the eclipses being discussed here. As a check, however, the final solutions (k's, α_o^{tr}'s, and p_o's) were used to generate the Ψ functions, and they were plotted against the rectified data. These theoretical fits were almost identical with those generated by the χ functions. Also, the elements resulting from the Ψ procedure were almost exactly the same as those resulting from the initial χ solutions.

The approximate functions which describe the shapes of the eclipses in terms of the ${}^{x}\Psi(k,\alpha)$ functions were:

v Primary $\quad \sin^2\theta(\alpha^{tr}) = 0.0670\ {}^{0.2}\Psi(0.26,\ \alpha^{tr}) + 0.1500$

v Secondary $\quad \sin^2\theta(\alpha^{oc}) = 0.0960\ {}^{0.2}\Psi(0.26,\ \alpha^{oc}) + 0.2180$

b Primary $\quad \sin^2\theta(\alpha^{tr}) = 0.0690\ {}^{0.4}\Psi(0.34,\ \alpha^{tr}) + 0.1500$

b Secondary $\quad \sin^2\theta(\alpha^{oc}) = 0.0990\ {}^{0.4}\Psi(0.34,\ \alpha^{oc}) + 0.2220$

u Primary $\quad \sin^2\theta(\alpha^{tr}) = 0.0830\ {}^{0.4}\Psi(0.41,\ \alpha^{tr}) + 0.1550$

u Secondary $\quad \sin^2\theta(\alpha^{oc}) = 0.1007\ {}^{0.4}\Psi(0.41,\ \alpha^{oc}) + 0.1981$

Since Ψ functions are more easily interpolated at large α, the values of $\bar{\theta}_i$, the points of internal tangency, in Table 8 are based upon these functions.

Due to the uncertainties in subtraction of third light, the shallow eclipses, and the difficulty in the rectification procedures, these solutions must be considered only preliminary.

It is interesting to note the similarities between the well-known eclipsing binary RR Centauri and AA Ceti. Extensive photoelectric yellow observations of RR Centauri by Knipe (1965) were analyzed by Bookmeyer (1968) utilizing the Russell model and are repeated here in Table 9 along with the results of the present analysis of the yellow light curve of AA Ceti. The problems encountered by Knipe and later by Bookmeyer in rectification and solution of RR Centauri are summarized by Koch _et al._ (1970, p. 60):

> Her work did not lead to a unique solution, and the choice of rectification procedures affects the ratio J_g/J_s. In the first solution given in our catalogue the Fourier series was truncated after cos 2θ which resulted in a positive but rather small A_1 term. If the third harmonic is included, one obtains $A_3 = -0.0110$ and $A_1 < 0$. Neither solution appears quite satisfactory although a general picture of the system is fairly well-defined for such a closely-interacting binary.

It would seem that some of the problems which afflict the solutions of RR Centauri are present in AA Ceti. Of particular note is the large size of A_3 in both stars. Although there seems to be no shift of the secondary minimum from a phase of $0\overset{p}{.}5$, the maximum after primary is definitely shifted in AA Ceti to a later phase than the expected $0\overset{p}{.}25$. As Bookmeyer points out in regard to RR Centauri, this could be indicative of an eccentric orbit. If the orbit were eccentric and viewed along the semi-major axis, then: (1) the eclipses would not be of equal duration; (2) the secondary minimum would not be displaced from a phase of $0\overset{p}{.}5$; and (3) the maximum light would occur at a true anomaly of 0.25 in phase, not at the

TABLE 9

RESULTS OF ANALYSIS OF THE YELLOW LIGHT CURVES OF AA CETI AND RR CENTAURI

	AA Ceti (Present Work)	RR Centauri (Bookmeyer, 1968) Solution B
L_g	0.921	0.889
L_s	0.079	0.111
a_g	0.55	0.58
b_g	0.45	0.52
a_s	0.14	0.21
b_s	0.12	0.19
x	0.2	0.6
k	0.26	0.36
i	$70\overset{\circ}{.}3$	$72\overset{\circ}{.}4$
$\bar{\theta}_e$	$40\overset{\circ}{.}7$	$49\overset{\circ}{.}2$
$\bar{\theta}_i$	$14\overset{\circ}{.}7$	$9\overset{\circ}{.}8$
α_o^{tr}	1.03	1.043
α_o^{oc}	1.00	1.00

mean anomaly of $0^{P}.25$ as predicted by the linear light elements. These three conditions are evident in the light curves of both stars. In the case of RR Centauri there is some evidence to deny that the apparent eccentricity is real; this is not yet the case of AA Ceti, and so the possibility remains. From the duration of the primary (t_1) and the secondary (t_2) one can extract the eccentricity (e) using the following equation:

$$\frac{1 + e}{1 - e} = \frac{t_1}{t_2}$$

if the angle from the ascending node to the periastron point is ninety degrees.

From the yellow curve e = 0.12, from the blue e = 0.10, and from the ultraviolet e = 0.06, all of which are extremely large for this type of binary. If the eccentricity is real, the star, of course, would be valuable for apsidal motion studies; however, it is felt in this investigation that the problems of rectification and the third light subtraction are sufficiently severe to make a determination of the eccentricity dubious, at best.

There appeared to be an inconsistency in the values of $\bar{J}_g/\bar{J}_s$ for the components of AA Ceti, which were calculated from

$$\frac{\bar{J}_g}{\bar{J}_s} = \frac{L_g}{L_s} \cdot \frac{r_s^2}{r_g^2} \quad .$$

The value for the v curve was less than 1.0, which implied that the larger star was the cooler one, and thus that the secondary eclipse was a transit. This implication was just the opposite of what had been assumed from the beginning of this investigation.

However, inspection of the rectified light curves revealed that the rectified primary was indeed the shallower eclipse, and so the solutions were internally consistent. It was just such an inconsistency which caused Bookmeyer to re-analyze the light curves of RR Centauri in the first place. Whether the roles of the two stars did reverse between the v and b bands (which is a physical possibility) or whether the problems involved in rectification were asserting themselves was not clear.

In order to evaluate the fit of the theoretical shapes to the data, a program was written for the Hewlett-Packard 9820A calculator to find the average difference between the individual rectified data points and the value of the theory at that phase. These average (O - C)'s and the average of their phases were found over ten-degree intervals. They are shown in Tables 10 through 12, including the number of data points (n) in each interval. Then the program "de-rectified" the theoretical values using the final set of coefficients from Table 7, and the average differences were calculated for the unrectified light over the entire period.

It is apparent that the residuals are generally small and change sign often, indicating that the fit is good over the entire light variation. As was stated previously, ignoring the sine terms in the rectification has little effect on the ultimate results as is indicated by the small (O - C)'s.

A statistical study of the fit is shown in Table 30 in the Appendix where the root-mean-square deviations of the data from the theoretical shape are given for the rectified primary eclipse, first maximum, secondary eclipse, and second maximum in each color.

TABLE 10

AVERAGE DIFFERENCES OF THE OBSERVED DATA AND THE THEORETICAL SHAPES OVER THE YELLOW LIGHT CURVE OF AA CETI

Rectified Light			Un-Rectified Light	
Average θ'	Average (O-C)	n	Average θ	Average (O-C)
5°.43	-0.002	7	4°.52	-0.001
14°.58	-0.006	7	12°.21	-0.004
24°.18	-0.005	9	20°.49	-0.004
34°.19	-0.001	12	29°.49	-0.001
45°.43	+0.013	12	40°.19	+0.011
55°.38	+0.003	8	50°.33	+0.003
65°.02	+0.005	9	60°.77	+0.005
75°.78	-0.008	5	73°.08	-0.008
85°.28	-0.015	5	84°.34	-0.015
95°.49	-0.002	5	96°.58	-0.002
105°.28	-0.008	4	108°.17	-0.008
115°.36	-0.006	6	119°.66	-0.006
123°.97	-0.006	6	128°.98	-0.005
135°.97	+0.002	4	141°.17	+0.008
146°.10	+0.004	7	150°.78	+0.003
155°.53	+0.012	6	159°.26	+0.010
164°.95	-0.008	7	167°.38	-0.007
175°.99	+0.006	5	176°.67	+0.004
186°.19	-0.005	6	185°.16	-0.004
195°.41	+0.001	6	192°.92	+0.001
204°.29	-0.013	7	200°.59	-0.010

TABLE 10 CONTINUED

Rectified Light			Un-Rectified Light	
Average θ'	Average(O-C)	n	Average θ	Average(O-C)
214°.69	-0.007	7	209°.96	-0.006
224°.45	-0.014	6	219°.23	-0.013
236°.80	+0.014	4	231°.82	+0.013
245°.88	-0.001	5	241°.73	-0.001
270°.70	+0.008	7	270°.83	+0.008
295°.45	+0.005	7	299°.76	+0.005
304°.26	-0.021	4	309°.30	-0.019
314°.10	-0.002	8	319°.33	-0.002
324°.36	+0.009	6	329°.19	+0.007
335°.90	+0.010	4	339°.57	+0.008
345°.15	-0.002	10	347°.55	-0.001
356°.19	+0.004	7	351°.83	+0.003

TABLE 11

AVERAGE DIFFERENCES OF THE OBSERVED DATA AND THE THEORETICAL SHAPES OVER THE BLUE LIGHT CURVE OF AA CETI

Rectified Light			Un-Rectified Light	
Average θ'	Average(O-C)	n	Average θ	Average(O-C)
5°.14	+0.003	8	4°.42	+0.003
15°.37	-0.004	8	13°.29	-0.003
25°.25	-0.001	9	22°.07	-0.001
34°.35	-0.004	11	30°.26	-0.002
45°.03	+0.009	12	40°.71	+0.008
55°.17	-0.004	8	50°.91	-0.003
64°.84	-0.001	9	61°.35	-0.001
75°.71	-0.013	5	73°.50	-0.013
85°.55	-0.017	5	84°.83	-0.018
95°.11	-0.006	4	95°.93	-0.006
104°.98	+0.008	4	107°.29	+0.008
115°.74	-0.006	5	119°.29	-0.006
124°.58	-0.004	7	128°.71	-0.004
142°.28	+0.008	9	146°.34	+0.007
154°.67	+0.019	7	157°.86	+0.016
163°.45	-0.009	6	165°.67	-0.007
173°.94	-0.007	6	174°.79	-0.006
184°.87	+0.007	6	184°.19	+0.005
194°.63	-0.008	7	192°.65	-0.006
204°.89	-0.003	8	201°.74	-0.003
215°.00	-0.004	6	211°.05	-0.004

TABLE 11 CONTINUED

Rectified Light			Un-Rectified Light	
Average θ'	Average (O-C)	n	Average θ	Average (O-C)
224°.08	-0.010	6	219°.77	-0.009
241°.82	-0.002	8	238°.13	-0.002
271°.24	+0.002	7	271°.42	+0.002
296°.64	+0.004	7	300°.26	+0.003
305°.63	-0.013	4	309°.83	-0.013
313°.92	0.000	6	318°.25	0.000
324°.40	+0.010	8	328°.38	+0.008
335°.91	+0.003	3	338°.98	+0.003
344°.67	+0.001	9	346°.74	+0.001
354°.81	-0.001	8	355°.53	-0.001

TABLE 12

AVERAGE DIFFERENCES OF THE OBSERVED DATA AND THE THEORETICAL SHAPES OVER THE ULTRAVIOLET LIGHT CURVE OF AA CETI

Rectified Light			Un-Rectified Light	
Average θ'	Average(O-C)	n	Average θ	Average(O-C)
6°.40	+0.001	9	5°.55	+0.001
15°.63	+0.001	6	13°.62	+0.001
24°.57	-0.004	9	21°.61	-0.003
34°.40	+0.002	12	30°.68	+0.001
45°.32	+0.002	12	41°.22	+0.002
55°.46	+0.003	8	51°.53	+0.003
65°.07	+0.004	8	61°.78	+0.003
76°.03	-0.007	5	73°.98	-0.007
85°.95	-0.014	5	85°.33	-0.015
93°.99	-0.007	3	94°.48	-0.007
103°.60	+0.004	5	105°.61	+0.004
115°.38	-0.010	6	118°.69	-0.010
125°.26	-0.013	7	129°.21	-0.012
136°.94	+0.018	3	141°.01	+0.016
146°.07	-0.015	6	149°.77	-0.013
155°.36	+0.003	7	158°.33	+0.002
164°.13	+0.007	6	166°.17	+0.005
174°.54	+0.002	6	175°.27	+0.001
185°.38	-0.006	6	184°.67	-0.005
195°.01	-0.010	7	193°.08	-0.008
204°.57	-0.004	7	201°.61	-0.003

TABLE 12 CONTINUED

Rectified Light			Un-Rectified Light	
Average θ'	Average(O-C)	n	Average θ	Average(O-C)
213°.67	-0.004	6	210°.00	-0.003
223°.83	+0.003	7	219°.75	+0.003
236°.70	+0.014	4	232°.83	+0.013
244°.90	+0.013	4	241°.60	+0.013
254°.80	+0.005	3	252°.60	+0.005
277°.78	+0.008	5	278°.91	+0.008
296°.51	-0.007	5	299°.93	-0.007
309°.33	-0.009	8	313°.33	-0.008
325°.22	+0.003	5	328°.97	+0.003
336°.56	+0.018	3	339°.42	+0.015
344°.72	+0.001	8	346°.69	0.000
354°.91	+0.001	9	355°.59	+0.001

Summary of Results and Suggestions for Further Work

The variable star AA Ceti is an eclipsing binary of essentially the W UMa-type and is a member of a common proper motion visual binary. The period of the star is $0\overset{d}{.}53617353 \pm 0\overset{d}{.}00000050$, and the secondary eclipse is a total occultation of the cooler star. The secondary component is probably only a few sub-classes later than the primary, which is about F2. Photometric complications and the possibility of intrinsic variability of the stars are also present.

Rectification in the conventional way showed that although the sine terms were small, higher order cosine terms were relatively large. The rectified eclipses were extremely shallow, and therefore definitive solutions were not possible. The ellipticity of the system was quite large.

The solutions based upon the Russell model indicated that k was a small number (about 0.3) and that the darkening coefficients necessary to achieve a reasonable solution were also smaller than generally expected. The system is very similar to RR Centauri, which also has not yielded to a definitive solution. It was found that the orbit of AA Ceti may be eccentric.

Further photometric work is warranted only after the light of the companion star is demonstrated to be constant through more extensive measurements, or only if measurements of the variable are made with the companion star excluded from the diaphragm. It is felt that higher quality light curves and solutions would be worthwhile although our understanding of the theory of close binaries, particularly that of rectification, would limit the precision of the final results in almost every case.

It has been suggested by Merrill (1970) that the spectral type of the secondary component of RR Centauri may be found from spectroscopy. Since AA Ceti is so similar, it seems that a spectroscopic study would be useful in finding the spectral type of the secondary star, and thus more accurate reflection coefficients so critical in the rectification process.

It would seem unlikely, judging from the relative luminosities of the two stars derived from this study, that both spectra would be sufficiently visible to permit high quality radial velocity curves for both components to be found. However, the star is sufficiently bright that a telescope of moderate aperture could be applied to find: (1) the mass function of the system, (2) the spectral type of the secondary component, and (3) the eccentricity of the orbit if, indeed, it is non-zero.

CHAPTER V

UZ PUPPIS

History

The eclipsing variable star UZ Puppis (BD-13°2170) was discovered to be a variable star by C. Hoffmeister (1929) and was assigned the discovery number 64.1929. A year later Mergentaler (1930) published provisional light elements based upon ninety-three photographic observations made between December 20, 1929, and March 2, 1930. A subsequent set of thirty-three observations confirmed the period he had found: $0^{d}.7944$ (±$0^{d}.0005$). With the total set of 126 observations Mergentaler then formed the first light curve found in the literature for UZ Puppis revealing β Lyrae-type variations. The star showed a maximum brightness of 9.1 magnitudes (visual) and faded approximately one magnitude during its primary eclipse. He also pointed out that the star exhibited a faint periastron effect (one maximum brighter than the other). Lause (1933) later confirmed this fact and measured it to be 0.02 magnitude.

In a series of papers by Florja (1932, 1933, 1937) the period was refined based upon observations made between 1931 and 1935, and a light curve was constructed. This early light curve is reproduced in Figure 19. The periastron effect is not apparent in this curve. In the last of this series of publications he gave the

Fig. 19. An early light curve of UZ Puppis by Florja (1937)

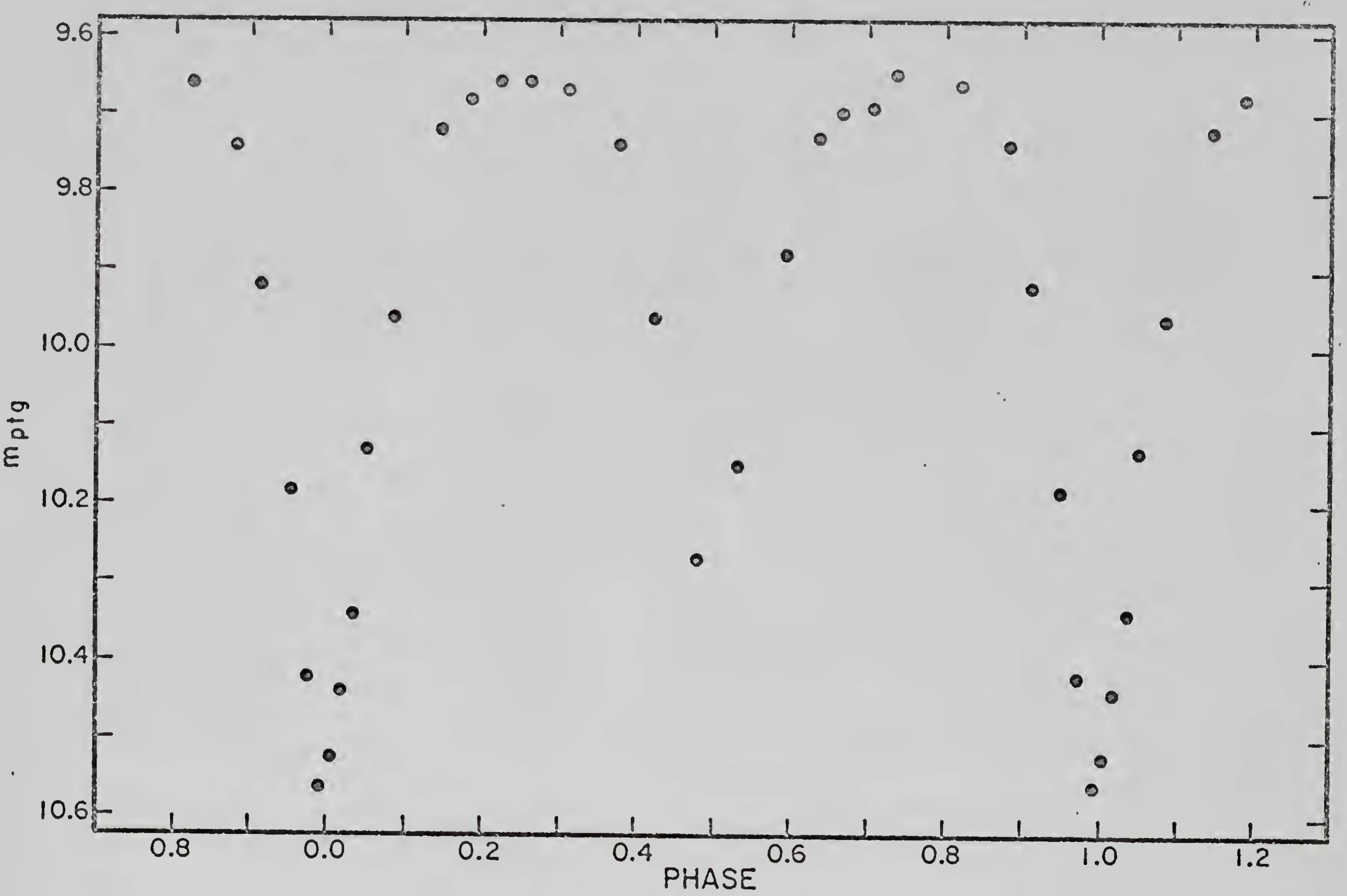
9.6
9.8
10.0
10.2
10.4
10.6
m_{ptg}
0.8
0.0
0.2
0.4
0.6
0.8
1.0
1.2
PHASE

refined light elements

$$\text{Min I} = \text{JD(hel.) } 2426033.251 + 0\overset{d}{.}794853 \cdot E \quad .$$

More recent light elements have been given by Soloviev (1943)

$$\text{Min I} = \text{JD(hel.) } 2426033.251 + 0\overset{d}{.}7948495 \cdot E \quad .$$

Further photographic photometry was done by Gaposchkin (1952, 1953). From 1,342 photographic observations a light curve was constructed, and a new period found: $0\overset{d}{.}79485041$.

The only spectroscopic study of UZ Puppis is that of O. Struve (1945). Using a dispersion of 76Å/mm at Hγ, forty-two spectra were taken and radial velocities determined based upon measurements of nine lines. Near conjunctions the great difference in luminosity of the two stars made the lines of the secondary component difficult to measure. The results of an analysis done by Struve are given in Table 13 and the curves themselves in Figure 20. He found that the system seemed to be of later spectral type during conjunctions, and the average spectral types of both stars were between A5 and A7. According to the Sixth Catalogue of Orbital Elements of Spectroscopic Binaries, the elements are listed as "poor" partly due to the large scatter in the radial velocities of the secondary component.

TABLE 13

SPECTROSCOPIC ORBITAL ELEMENTS OF UZ PUPPIS FROM STRUVE (1945)

$P = 0\overset{d}{.}795$ (assumed)

$\gamma = +25$ km/sec

$K_1 = K_2 = 150$ km/sec

$e = 0$ (assumed)

T (max. vel.) = phase 0.75

$M_1 \sin^3 i = 1.1 \odot$

$M_2 \sin^3 i = 1.1 \odot$

$a_1 \sin i = 1.6 \times 10^6$ km
$= a_2 \sin i$

Fig. 20. Radial velocity curves of UZ Puppis by Struve (1945). The symbol O represents the velocity measurements of the primary or brighter component while + represents the radial velocities of the fainter component.

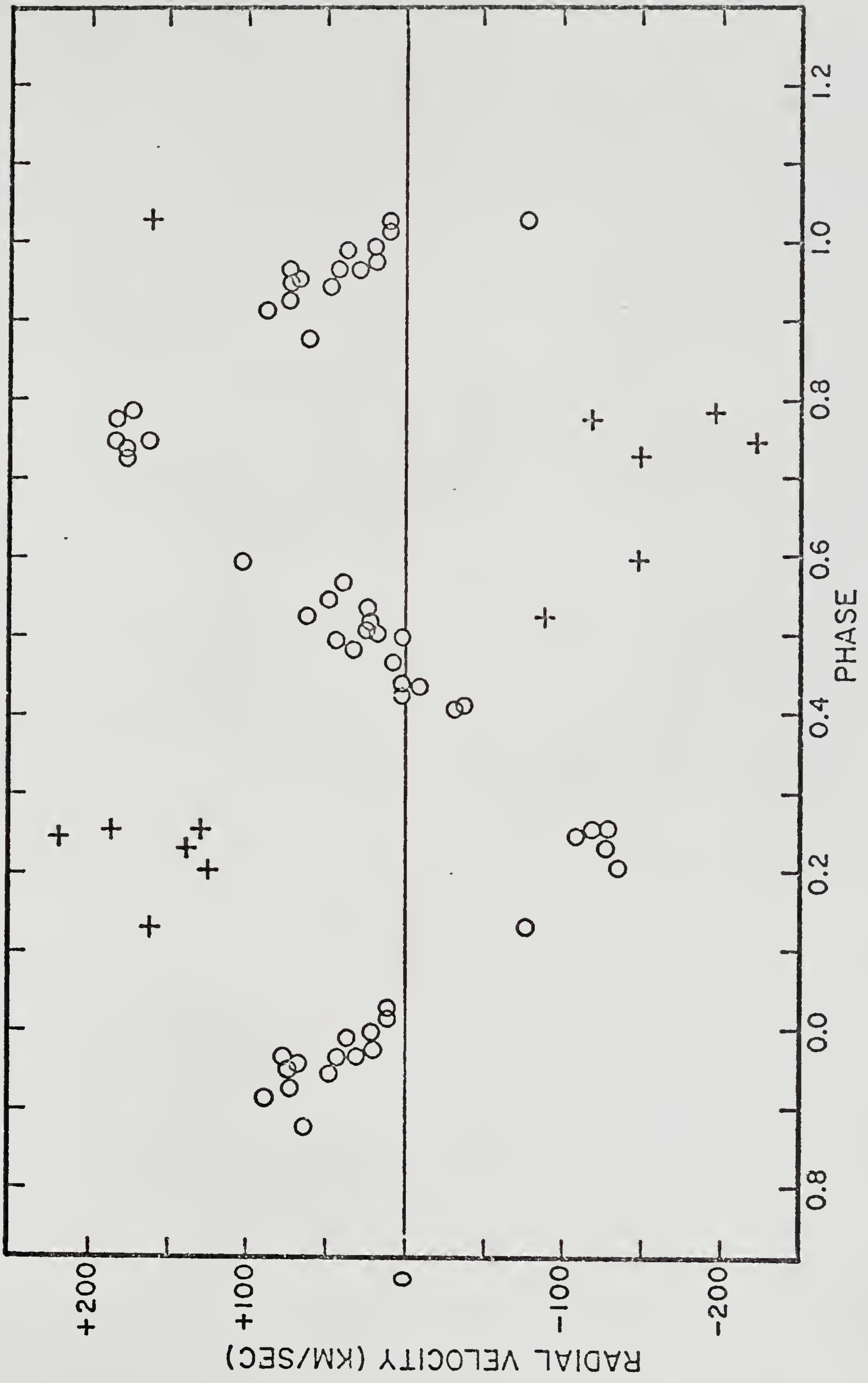
RADIAL VELOCITY (KM/SEC)
+200
+100
0
-100
-200
PHASE
0.8
0.0
0.2
0.4
0.6
0.8
1.0
1.2

The present work was undertaken since no reports of photoelectric light curves were found in the Florida Card Catalogue of Eclipsing Binary Stars.

Photoelectric Observations

The star BD-12°2092, chosen as a comparison star for observations of UZ Puppis, showed no signs of variability during any of the observations. This is substantiated by the check star readings given in Table 15. The check star was BD-13°2180. A finding chart for the variable and comparison stars is shown in Figure 21, and the catalogue names and coordinates for the stars are given in Table 14.

TABLE 14

THE COORDINATES AND BONNER DURCHMUSTERUNG NUMBERS OF STARS RELATED TO THE INVESTIGATION OF UZ PUPPIS

	BD	$\alpha_{1855.0}$	$\delta_{1855.0}$
UZ Puppis	-13°2170	$7^h35^m\ 2^s.6$	-13° 3'2"
Comparison Star	-12°2092	$7^h35^m\ 9^s.5$	-12°51'6"
Check Star	-13°2180	$7^h35^m44^s.0$	-13°30'1"

The extinction coefficients for the thirteen nights which proved to be usable are given in Table 16, along with their probable errors. Although a large amount of data was taken on the

TABLE 15

THE DIFFERENTIAL MAGNITUDES BETWEEN THE COMPARISON AND CHECK STARS USED DURING THE PHOTOMETRIC INVESTIGATION OF UZ PUPPIS

Date	Δmag_v	Δmag_b	Δmag_u
3/ 6- 7/71	-1.467	-1.514	-1.658
3/ 5- 6/71	-1.425	-1.456	-1.561
	-1.437	-1.484	-1.578
2/17-18/71	-1.456	-1.486	-1.565
	-1.424	-1.484	-1.611
2/ 8- 9/71	-1.502	-1.537	-1.589
1/27-28/71	-1.400	-1.464	-1.539
	-1.206*	-1.235*	-1.282*

*Poor quality comparison star readings

Fig. 21. A finding chart for UZ Puppis and the comparison star used in this investigation

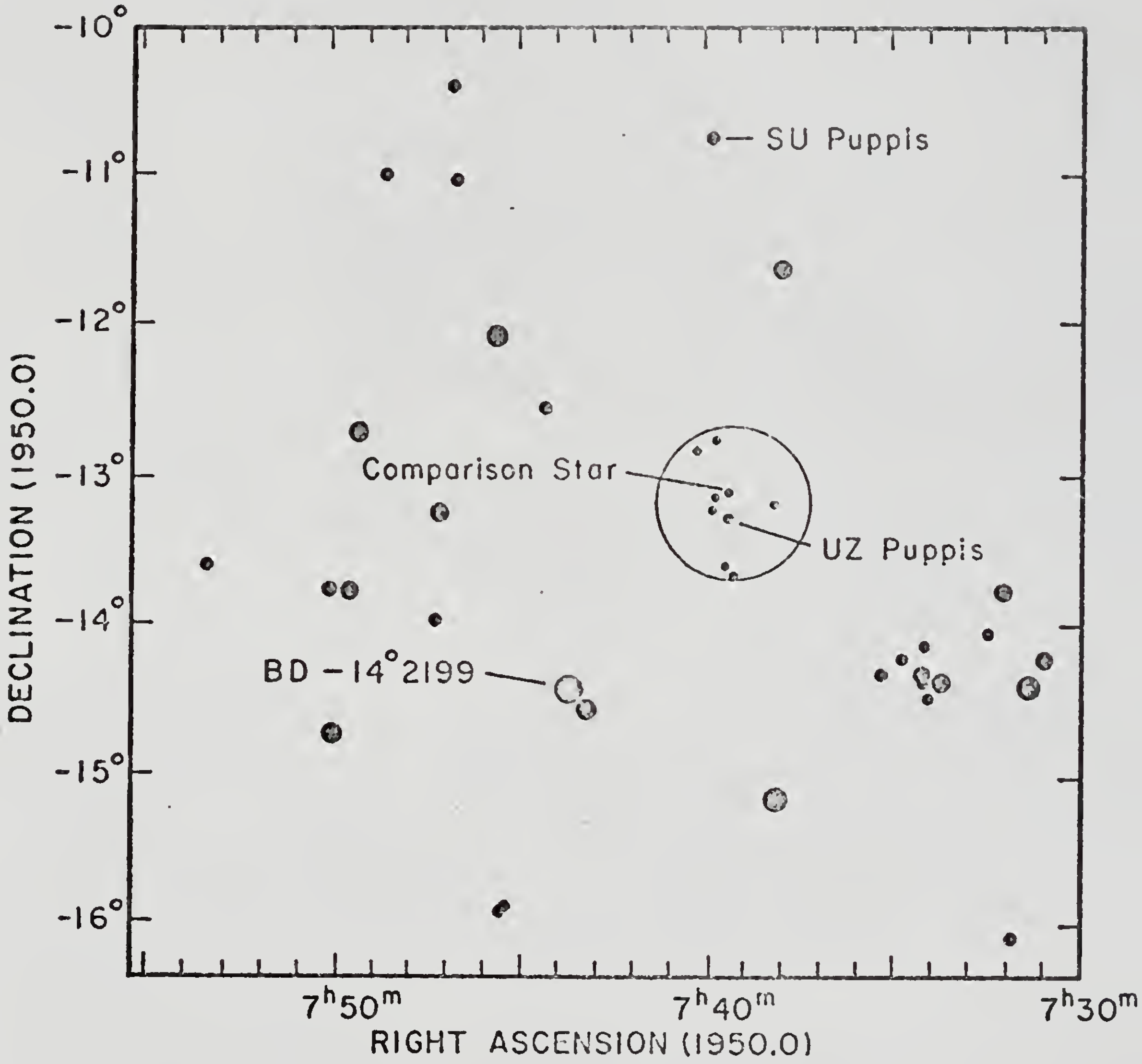
-10°
-11°
-12°
-13°
-14°
-15°
-16°
DECLINATION (1950.0)
SU Puppis
Comparison Star
UZ Puppis
BD −14°2199
7h50m
7h40m
7h30m
RIGHT ASCENSION (1950.0)

TABLE 16

FIRST ORDER EXTINCTION COEFFICIENTS AND THEIR PROBABLE ERRORS USED IN THE REDUCTION OF DATA PERTAINING TO UZ PUPPIS

Date	k_v	k_b	k_u
1/22-23/71	0.254 ±.043	0.424 ±.008	0.822 ±.033
1/27-28/71	0.171 ±.006	0.291 ±.007	0.601 ±.008
*2/ 1- 2/71	0.241 ±.113	0.325 ±.238	0.919 ±.029
2/15-16/71	0.276 ±.009	0.459 ±.008	0.768 ±.010
2/17-18/71	0.267 ±.012	0.425 ±.012	0.764 ±.016
3/ 5- 6/71	0.425 ±.012	0.650 ±.020	0.992 ±.012
*3/ 9-10/71	0.562 ±.051	0.983 ±.020	1.186 ±.053
3/17-18/71	0.250 ±.010	0.417 ±.004	0.743 ±.008
*3/ 3- 4/72	0.993 ±.889	1.151 ±.486	1.390 ±.741
*3/ 4- 5/72	(est.) 0.993	(est.) 1.151	(est.) 1.390
3/ 6- 7/72	0.225 ±.063	(est.) 0.400	0.709 ±.115
12/ 9-10/72	0.429 ±.042	0.590 ±.136	0.864 ±.063
12/11-12/72	0.258 ±.085	0.399 ±.071	0.716 ±.000

*Poor quality night

night of 3/4-5/72, it was not possible to determine the coefficients with any degree of precision; therefore, it was necessary to estimate them.

Light Elements

The present observations extended the base-line of observation of minima by a large amount, and so a period study was undertaken. On four nights enough data was obtained on both branches of the eclipse to use the Hertzsprung method for determining the time of minimum light. On two other nights enough data was taken to use the tracing paper method in which the partial data was fitted by hand to an eclipse whose mid-point was "known." This method was less precise than the Hertzsprung method and was therefore given a reduced weight in the final calculation.

Since there has never been any indication of a changing period, five rather old normal times of minimum light were also used providing a base-line of over 18,000 cycles. These had resulted from earlier least-squares solutions for the light elements and should be considerably more precise than a "time of faint light" determined from a single photographic plate. All data used in a linear least-squares solution for the light elements, along with the weights applied, is given in Table 17. The observed minus the calculated times of minimum listed in this table are plotted in Figure 22. The final elements resulting from this calculation were

$$\text{Min I} = \text{JD(hel.)}\ \underset{\pm .0002}{2440974.8707} + \underset{\pm .00000004}{0\overset{d}{.}79485183} \cdot E \quad .$$

TABLE 17

TIMES OF MINIMUM LIGHT OF UZ PUPPIS AND THE WEIGHTS USED TO CALCULATE THE LIGHT ELEMENTS

Julian Date(hel.)	Epoch	Weight	O-C(days)*
2426033.251	-18798.0	2	+0.005
27193.720	-17338.0	2	-0.010
28249.2995	-16010.0	2	+0.0061
29536.160	-14391.0	2	+0.002
29650.612	-14247.0	2	-0.005
40974.8701	0.0	3	-0.0006
.8694	0.0	3	-0.0013
.8691	0.0	3	-0.0016
40979.6383	+ 6.0	5	-0.0015
.6385	+ 6.0	5	-0.0013
.6388	+ 6.0	5	-0.0010
40998.7153	+ 30.0	5	-0.0010
.7149	+ 30.0	5	-0.0014
.7150	+ 30.0	5	-0.0013
41000.7038	+ 32.5	5	+0.0004
.7039	+ 32.5	5	+0.0005
.7053	+ 32.5	5	+0.0019
41016.6027	+ 52.5	5	+0.0023
.6022	+ 52.5	5	+0.0018
.6012	+ 52.5	5	+0.0008
41028.5243	+ 67.5	3	+0.0011
.5260	+ 67.5	3	+0.0028
.5220	+ 67.5	3	-0.0012

*Observed minus calculated time of minimum predicted from Min I = JD(hel.) 2440974.8707 + $0\overset{d}{.}79485183 \cdot E$

Fig. 22. The observed minus the calculated times of minimum light of UZ Puppis which were found in this investigation

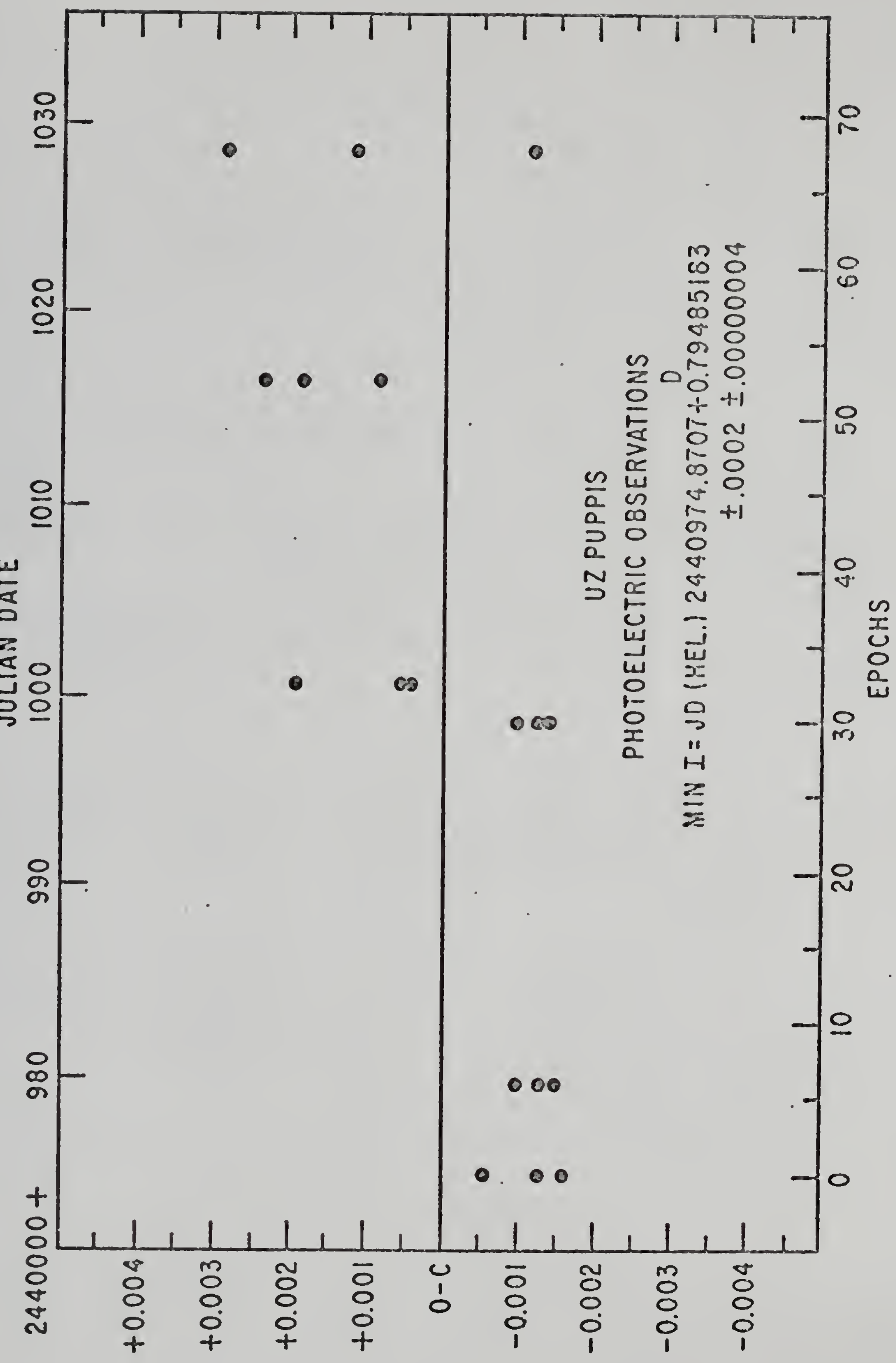
JULIAN DATE
2440000 +
980
990
1000
1010
1020
1030
O-C
+0.004
+0.003
+0.002
+0.001
-0.001
-0.002
-0.003
-0.004
UZ PUPPIS
PHOTOELECTRIC OBSERVATIONS
D
MIN I = JD (HEL.) 2440974.8707 + 0.79485163
±.0002 ±.00000004
EPOCHS
0
10
20
30
40
50
60
70

It is apparent from Figure 22 that the times of secondary minimum are displaced from a linear phase of 0.5 by about $0\overset{d}{.}003$. This could be a result of a distortion of the eclipse (the Hertzsprung routine assumes that the eclipse is geometrically symmetrical in order to find the time of mid-eclipse) or a true displacement of conjunction in phase. Since both times of primary and secondary minimum were used, the initial epoch is not adjusted to predict the center of either type of eclipse. From calculations done with primary eclipses only, it has been found that appropriate initial epoch is 2440974.8696 while that necessary to accurately predict the center of the secondary eclipse is 2440974.8718.

Color Curves

Using the light elements from the previous section, this author calculated the phase of each data point. The colors b-v and u-b were calculated and plotted as a function of phase. The results are shown in Figures 23 and 24. Although the scatter was large, this system seemed to become redder by almost 0.1 magnitude during the primary; however, since Struve (1945) found that the components were very similar in spectral type, no dramatic changes in color were expected.

Light Curves

Figures 25 through 27 show the light curves. The variations are of the β Lyrae-type, i.e., continuous variations between the eclipses with a substantial difference in their depths. The eclipses appear to be partial since there are no times of constant light.

Fig. 23. The b-v color curve for UZ Puppis

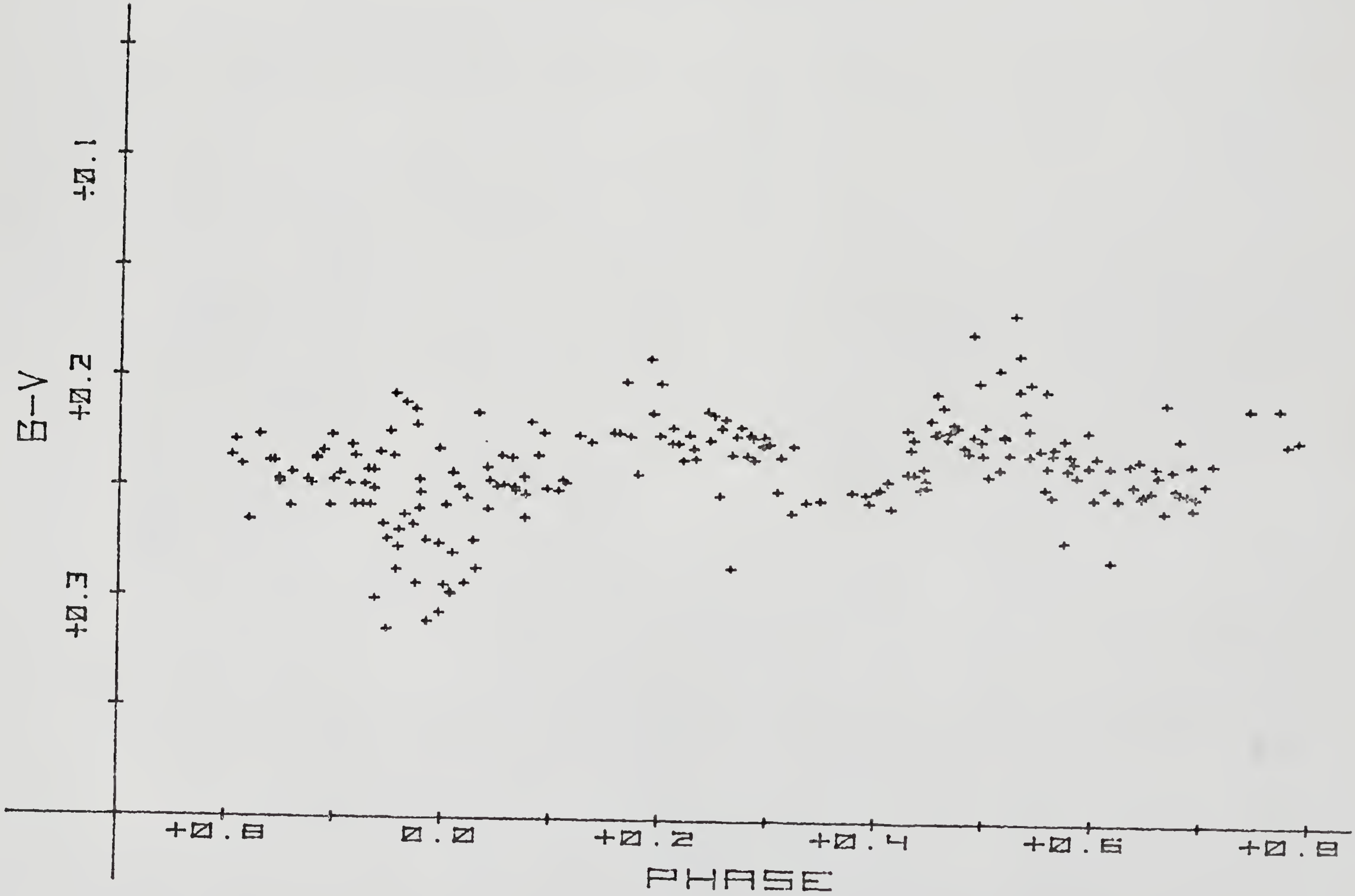
B-V
+0.1
+0.2
+0.3
+0.8
0.0
+0.2
+0.4
+0.6
+0.8
PHASE

Fig. 24. The u-b color curve for UZ Puppis

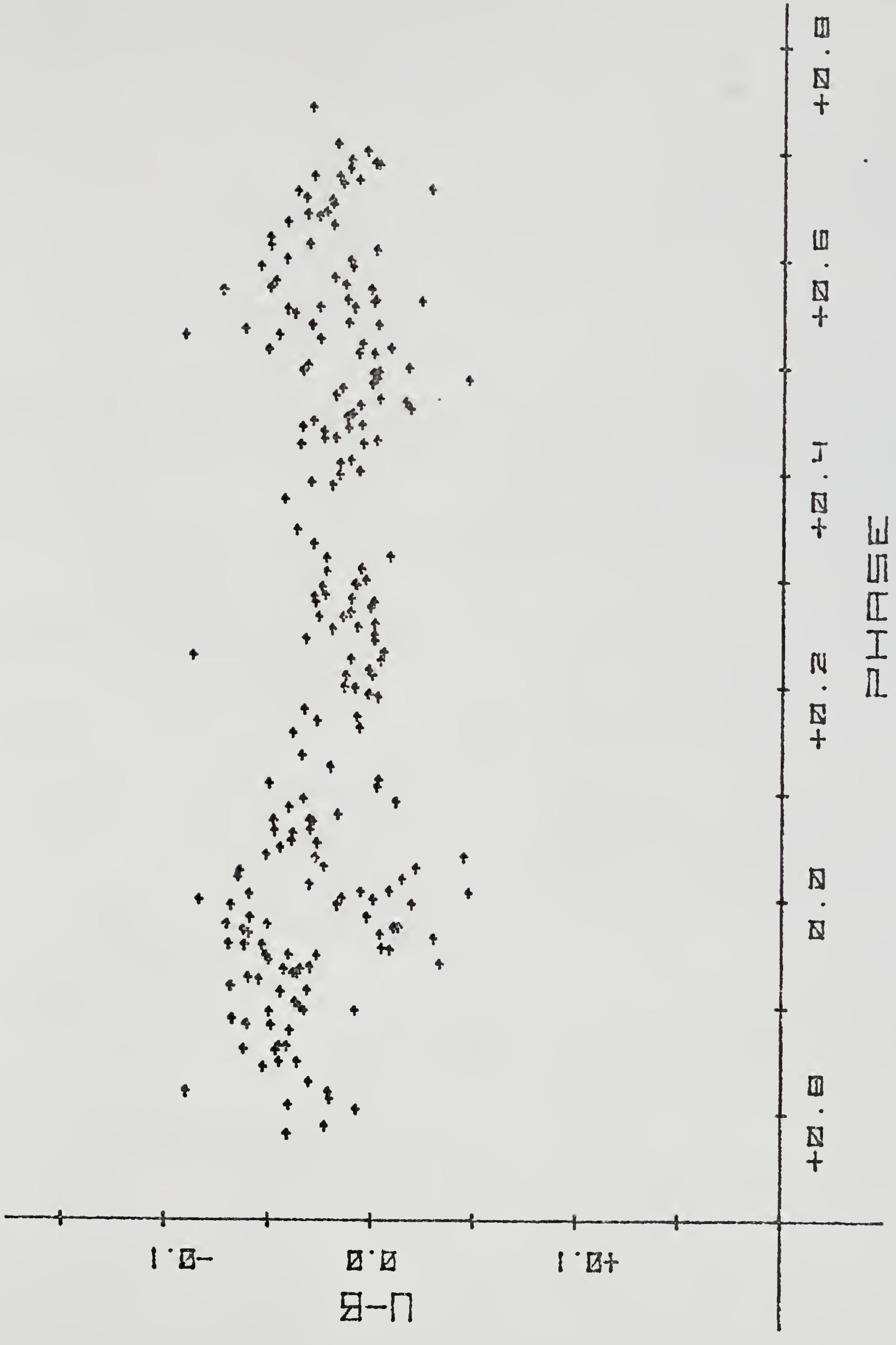
U-B
-0.1
0.0
+0.1
PHASE
+0.8
+0.6
+0.4
+0.2
0.0
+0.8

Fig. 25. The yellow light curve of UZ Puppis adjusted to 0.0 magnitude at maximum light

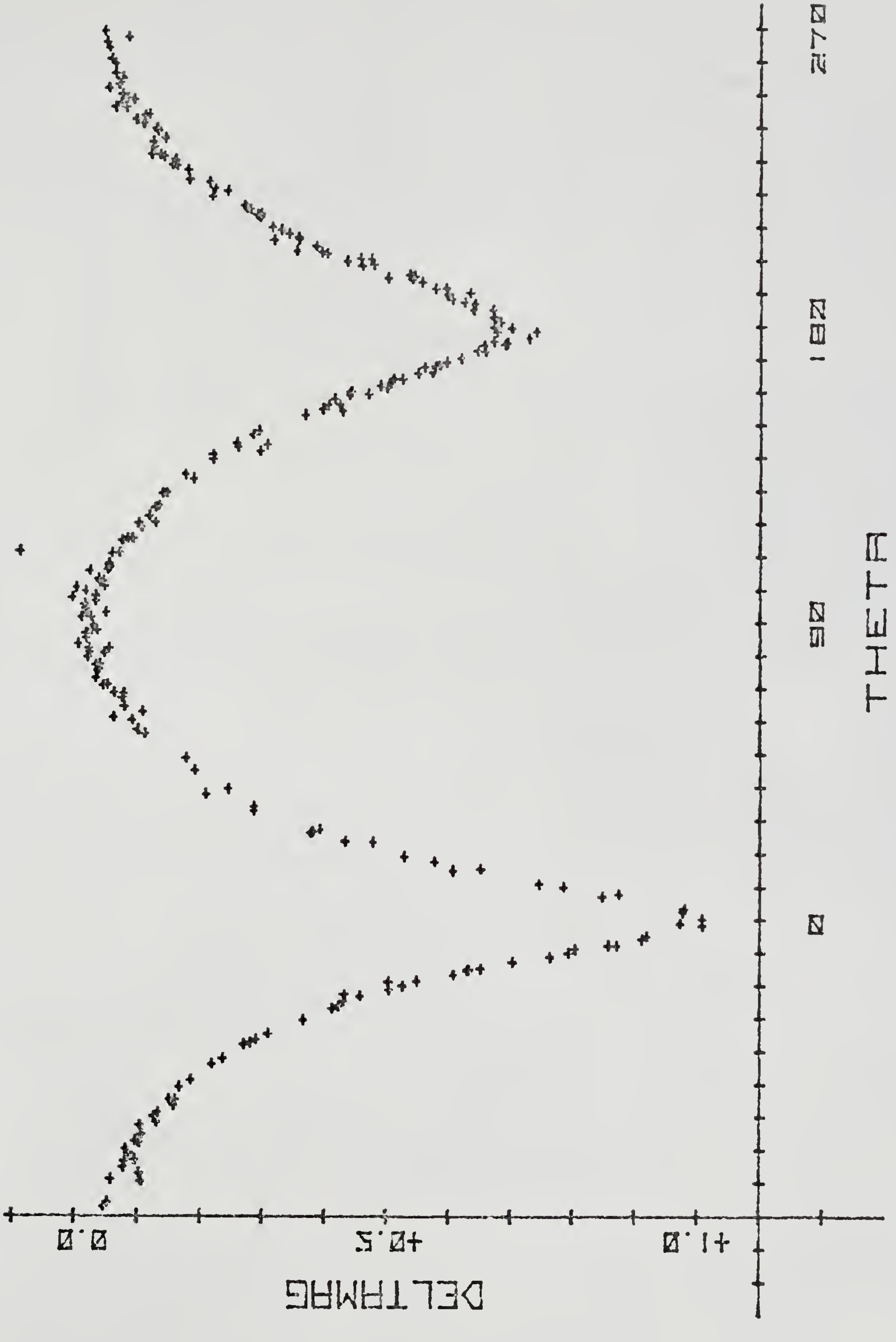
DELTAMAG
0.0
+0.5
+1.0
THETA
0
90
180
270

Fig. 26. The blue light curve of UZ Puppis adjusted to 0.0 magnitude at maximum light

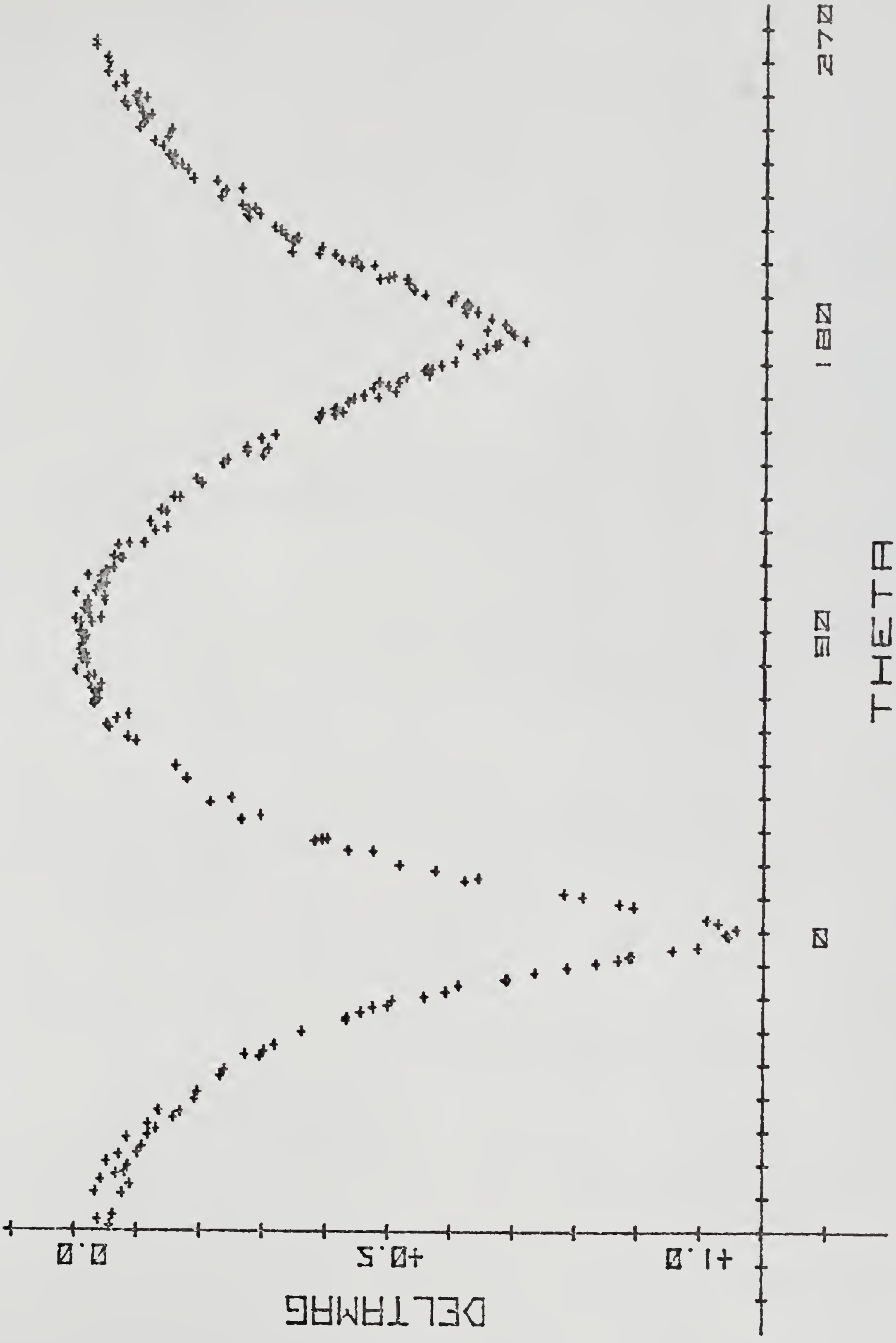
DELTAMAG
0.0
+0.5
+1.0
THETA
0
90
180
270

Fig. 27. The ultraviolet light curve of UZ Puppis adjusted to 0.0 magnitude at maximum light

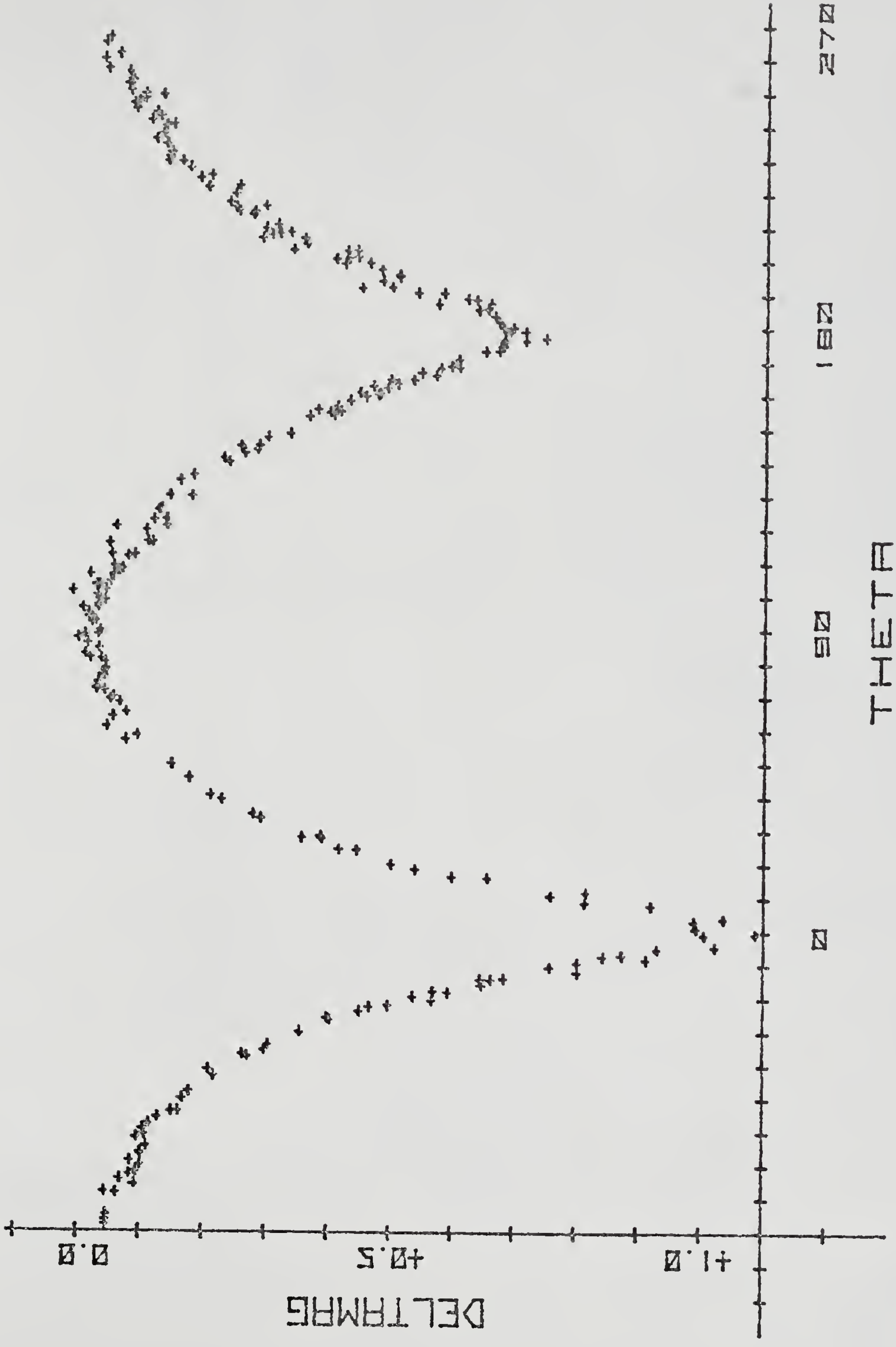
THETA
0
90
180
270
DELTAMAG
0.0
+0.5
+1.0

It is apparent from the curves that there was a pronounced periastron effect. That is, the maximum at a phase of $0^p.25$ was several hundredths of a magnitude brighter than the maximum at a phase of $0^p.75$. One possible explanation of the phenomenon is that the stars move in elliptical orbits, and when they are closest (at periastron passage), the reflection effect is larger, thus causing a net brightening of the system. O'Connell (1951) has, however, shown that this explanation is not adequate in many cases. A quantitative measurement of this effect is given in the next section.

Rectification of the Light Curves

The yellow light curve was used to find the Fourier coefficients by applying the graphical method suggested by Merrill (1970). It was apparent that the higher order cosine terms and the sine terms were significant, and therefore a least-squares calculation to find the Fourier components was performed through sine and cosine terms of the fourth order; external tangency was assumed to occur at $\theta = 43^\circ$. The results of those calculations are given in Table 18 along with the reflection coefficients calculated from the theory and the values of Z used for rectification of phase. A darkening of 0.6 on both stars was adopted.

The coefficients of the sin θ terms (B_1) were large in all cases. They describe a periastron effect of $0^m.028$ in the yellow and $0^m.036$ in the blue and ultraviolet.

The rectification was performed as discussed in the previous chapter.

TABLE 18

COEFFICIENTS USED IN THE RECTIFICATION OF THE LIGHT CURVES OF UZ PUPPIS

	v	b	u
A_0	+0.83205 ±0.00626	+0.81788 ±0.00680	+0.84407 ±0.00774
A_1	-0.00423 ±0.00604	-0.01606 ±0.00669	-0.00413 ±0.00763
A_2	-0.14116 ±0.00969	-0.17242 ±0.01054	-0.12925 ±0.01196
A_3	+0.00212* ±0.00313	-0.01361 ±0.00346	-0.00584 ±0.00395
A_4	-0.00565 ±0.00421	-0.01202 ±0.00462	-0.00163 ±0.00523
B_1	+0.01272 ±0.00104	+0.01651 ±0.00117	+0.01636 ±0.00132
B_2	+0.00003* ±0.00206	+0.00501 ±0.00227	+0.00232* ±0.00260
B_3	-0.00436 ±0.00148	+0.00038* ±0.00167	+0.00057* ±0.00191
B_4	-0.00310 ±0.00186	+0.00069* ±0.00205	+0.00020* ±0.00234
Z (0.6)	+0.24850	+0.29360	+0.22870
C_0	+0.03700	+0.03600	+0.03560
C_1	+0.00423	+0.01606	+0.00413
C_2	+0.01200	+0.01200	+0.01190

*Set equal to zero in rectification

Solutions of the Light Curves of UZ Puppis

The rectified data was fitted with the χ functions assuming a darkening coefficient of 0.6. A study of the nomographs showed that no other choice of darkening would improve the simultaneous fit to the primary and secondary eclipses.

It was apparent from the outset that it would be impossible to achieve a satisfactory fit to the data without the assumption of a third light in the system. In the blue the third light necessarily assumed constituted 37.9 percent of the total light of the system! Unfortunately, the assumption of third light is not an uncommon occurrence in the solutions of close binaries. In effect, the assumption of third light amounts to adding an additional degree of freedom to the model so that almost any shape can be fitted. In the case of UZ Puppis, however, there are some spectral peculiarities which could be interpreted in terms of an unresolved third star or some other source of light, perhaps in the binary system itself. Such an interpretation, however, would be begging the question and putting a great deal of reliance upon the rectification procedures. The "best" solutions which do not permit the existence of third light were also found and are plotted in Figures 28 through 33. The best solutions allowing third light are illustrated by solid lines. The solutions are summarized in Tables 19 and 20. The results are similar to preliminary ones given earlier by this author (Bloomer, 1972b).

In order to find the deviation of the theoretical shape from the observed data, differences between the theory and data were found over the entire light variation in each color, and these differences

Fig. 28. The theoretical solution of the yellow light curve plotted with the rectified data of the primary eclipse of UZ Puppis. The solid line represents the solution with $L_3 \neq 0$ and the dashed line the solution with $L_3 = 0$.

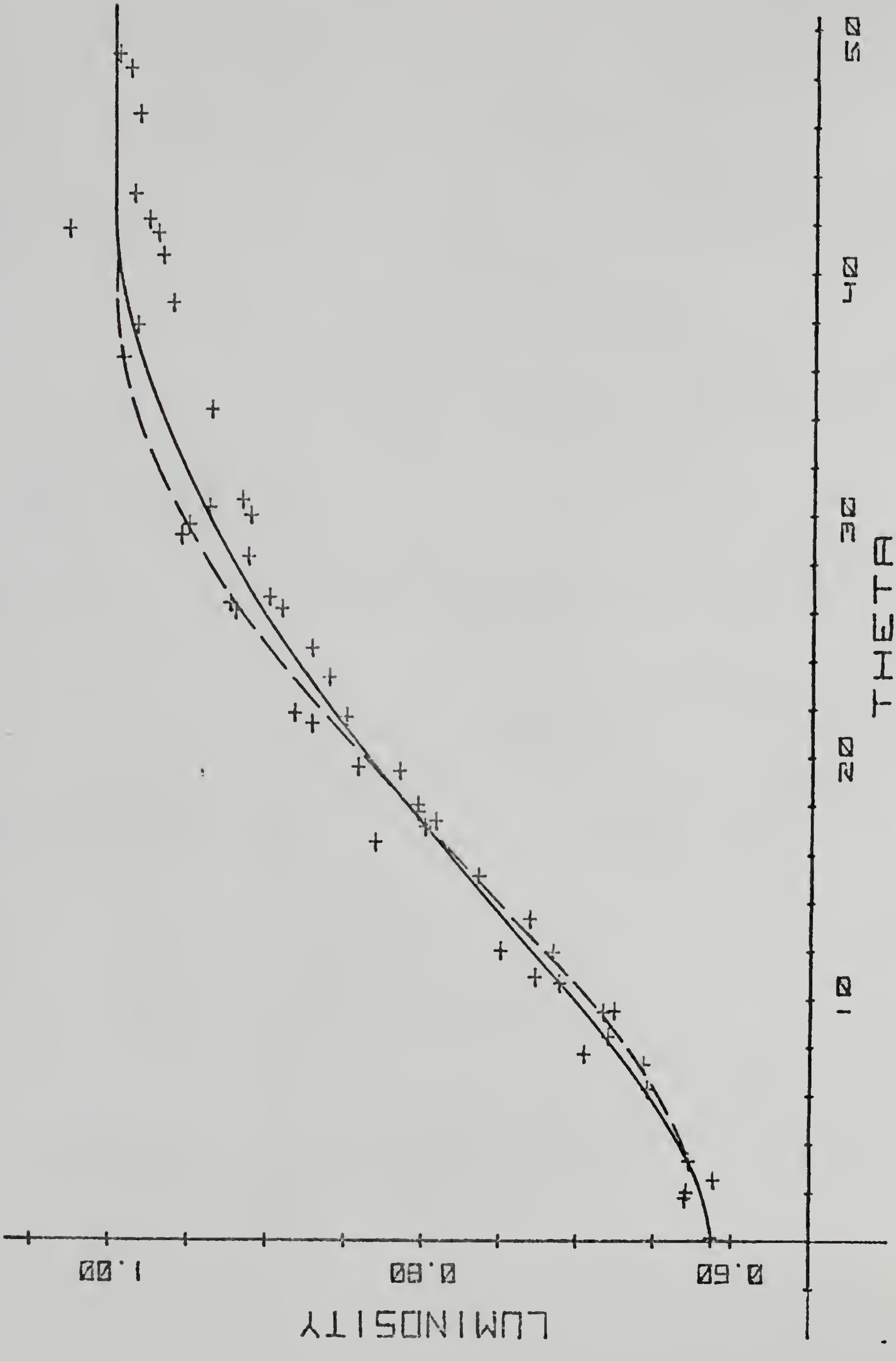
LUMINOSITY
0.60
0.80
1.00
THETA
10
20
30
40
50

Fig. 29. The theoretical solution of the yellow light curve plotted with the rectified data of the secondary eclipse of UZ Puppis. The solid line represents the solution with $L_3 \neq 0$ and the dashed line the solution with $L_3 = 0$.

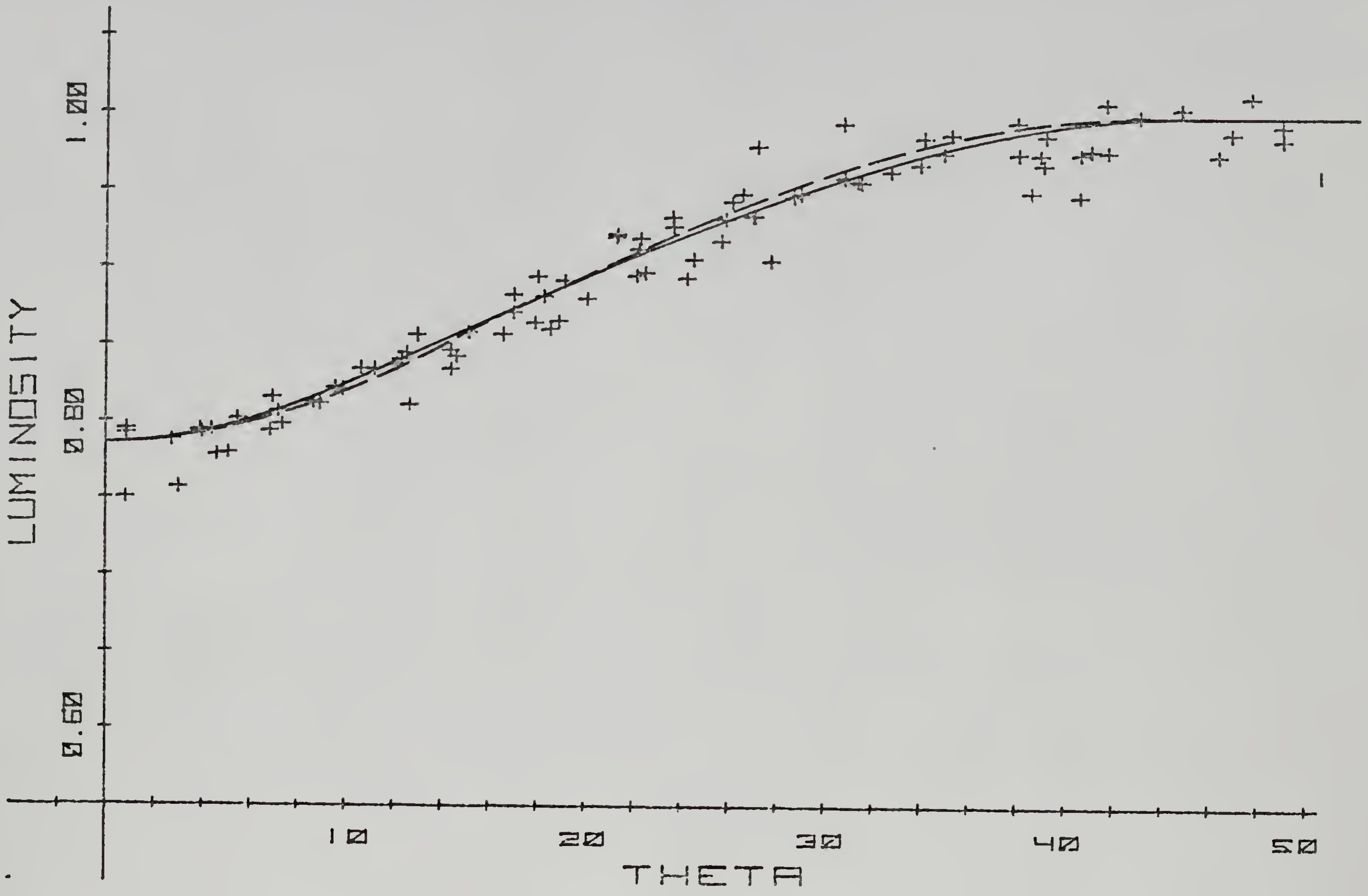
LUMINOSITY
1.00
0.80
0.60
THETA
10
20
30
40
50

Fig. 30. The theoretical solution of the blue light curve plotted with the rectified data of the primary eclipse of UZ Puppis. The solid line represents the solution with $L_3 \neq 0$ and the dashed line the solution with $L_3 = 0$.

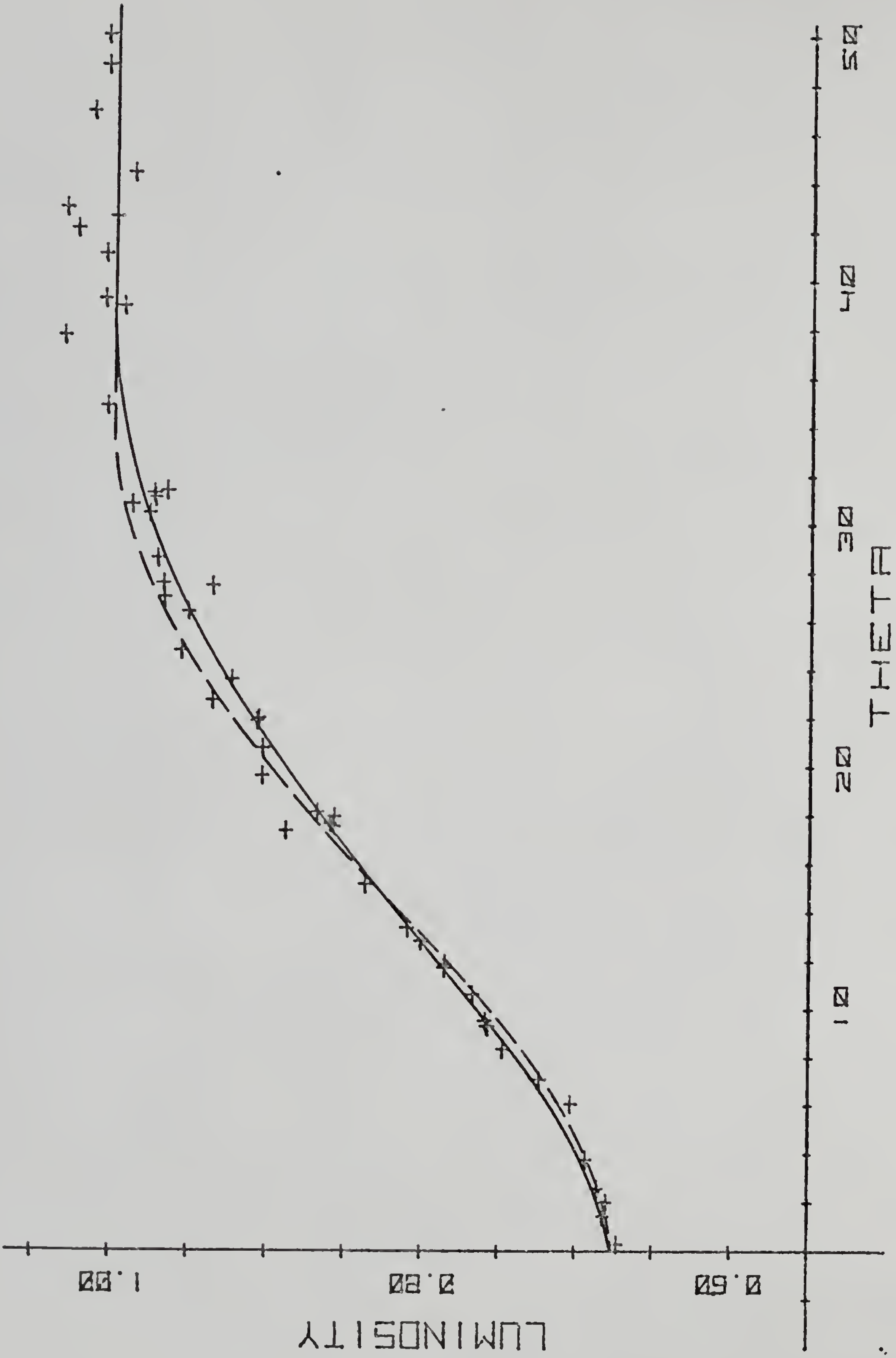
LUMINOSITY
1.00
0.80
0.60
THETA
10
20
30
40
50

Fig. 31. The theoretical solution of the blue light curve plotted with the rectified data of the secondary eclipse of UZ Puppis. The solid line represents the solution with $L_3 \neq 0$ and the dashed line the solution with $L_3 = 0$.

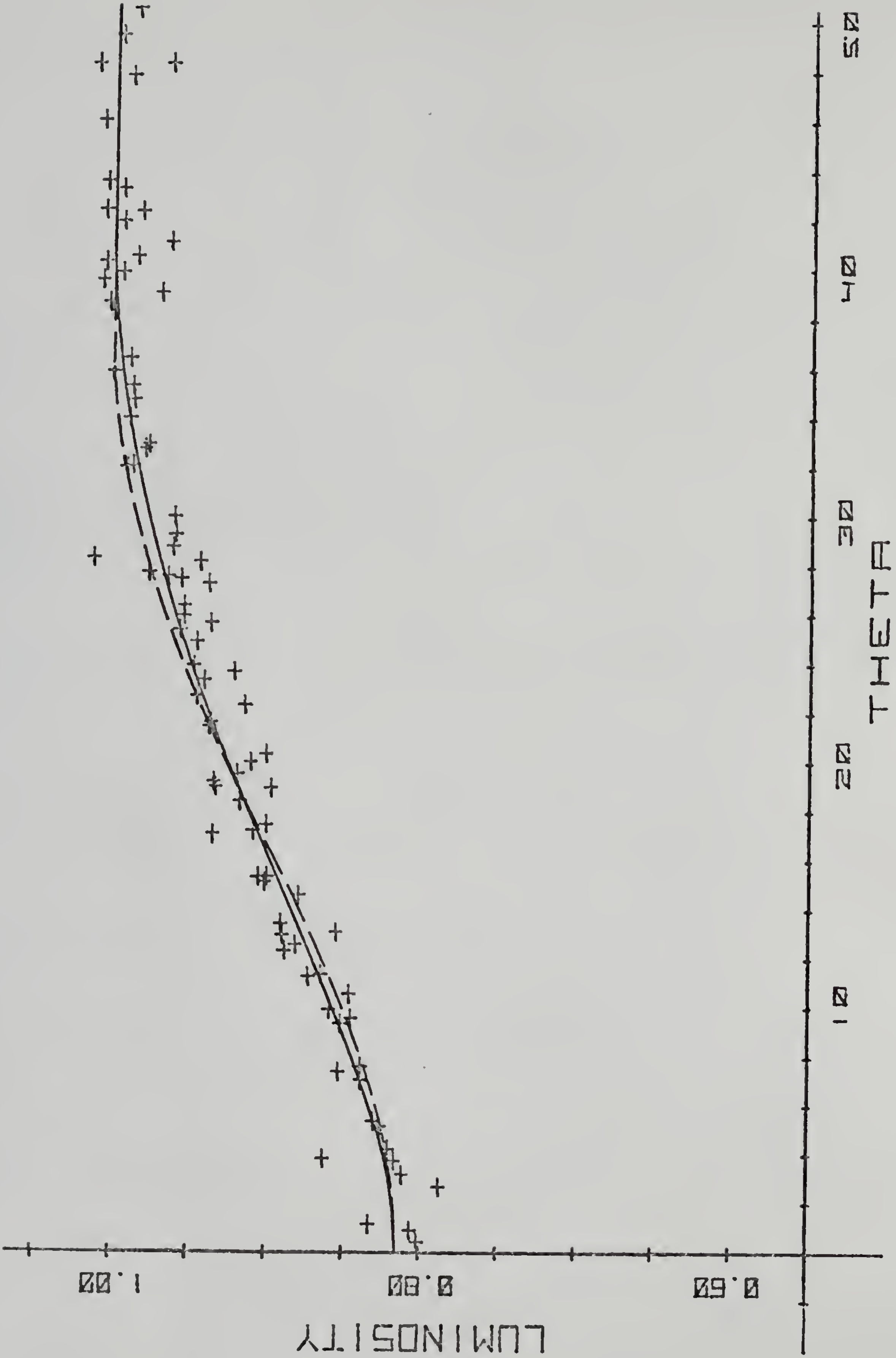
LUMINOSITY
0.60
0.80
1.00
THETA
10
20
30
40
50

Fig. 32. The theoretical solution of the ultraviolet light curve plotted with the rectified data of the primary eclipse of UZ Puppis. The solid line represents the solution with $L_3 \neq 0$ and the dashed line the solution with $L_3 = 0$.

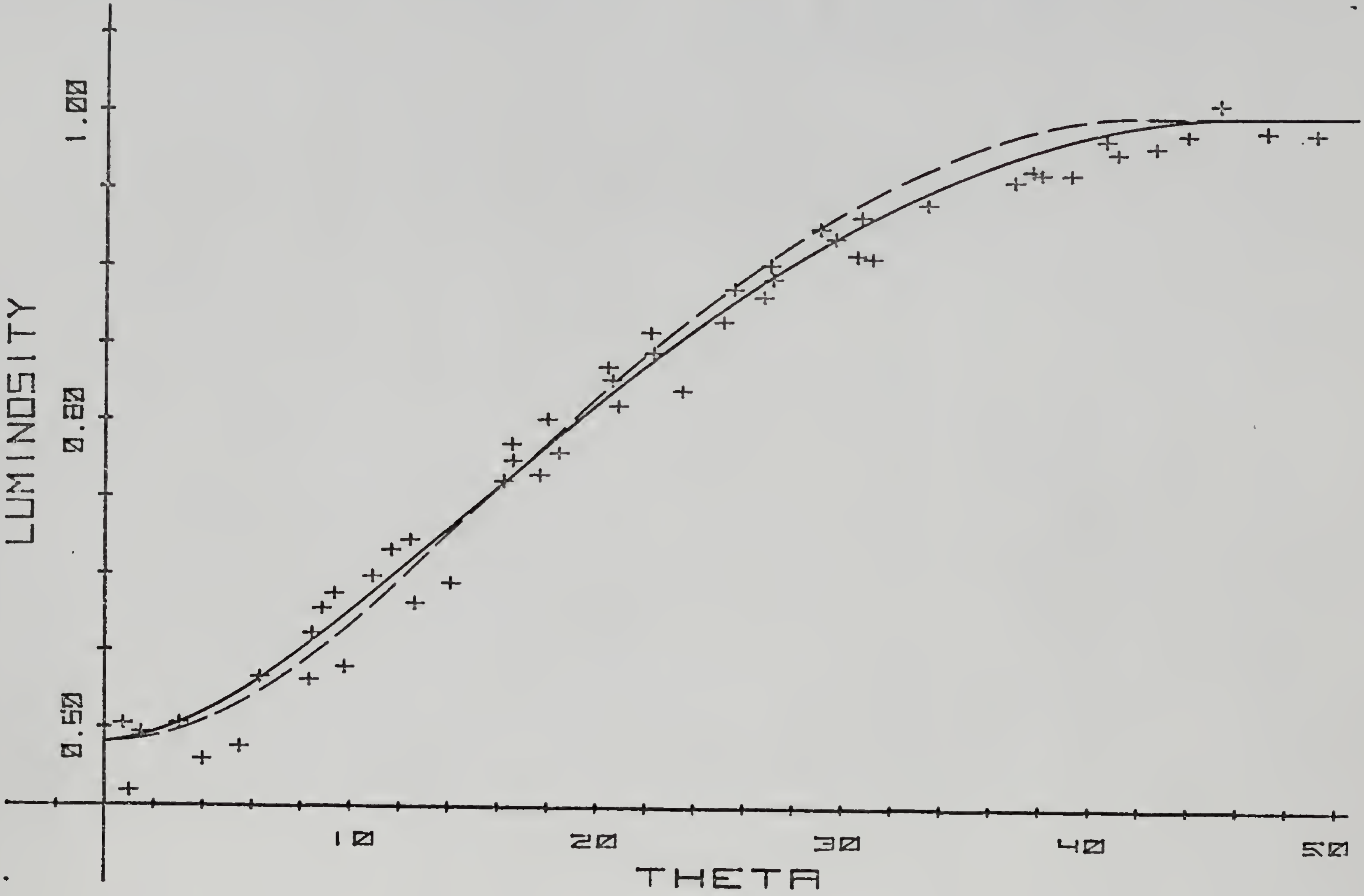
LUMINOSITY
1.00
0.80
0.50
THETA
10
20
30
40
50

Fig. 33. The theoretical solution of the ultraviolet light curve plotted with the rectified data of the secondary eclipse of UZ Puppis. The solid line represents the solution with $L_3 \neq 0$ and the dashed line the solution with $L_3 = 0$.

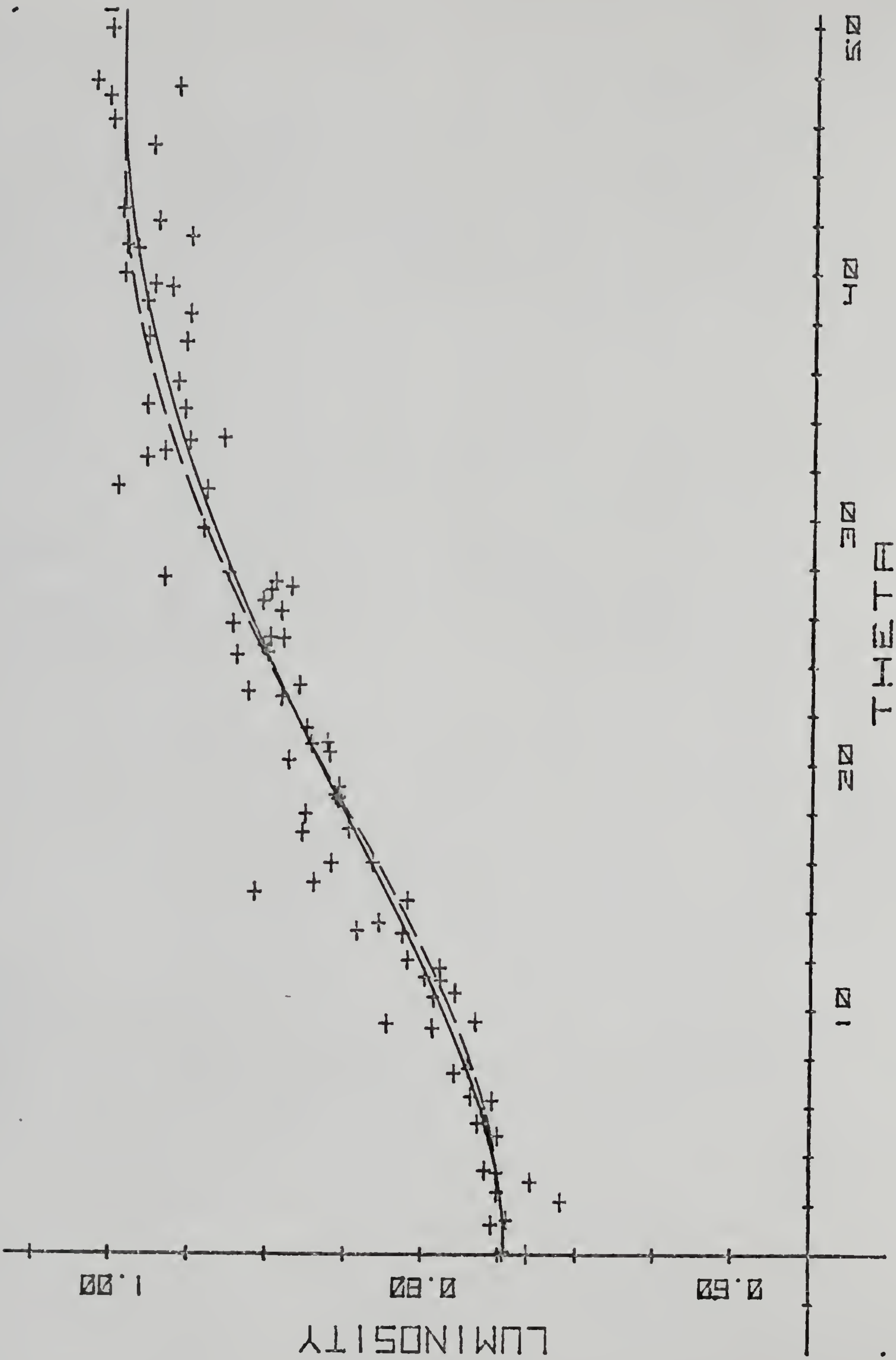
LUMINOSITY
1.00
0.80
0.60
THETA
10
20
30
40
50

TABLE 19

ELEMENTS OF THE SYSTEM UZ PUPPIS ASSUMING $L_3 \neq 0$

	v	b	u
$x_s = x_g$	0.6	0.6	0.6
k	0.86	0.86	0.84
p_o	-0.90	-0.90	-0.93
α_o^{tr}	0.954	0.954	0.970
α_o^{oc}	0.972	0.972	0.984
r_g	0.38	0.34	0.40
r_s	0.33	0.29	0.33
i	85°.1	85°.6	85°.0
j	85°.8	86°.3	85°.6
$\overline{\theta}_e$	44°.4	38°.4	46°.6
a_g	0.38	0.34	0.40
b_g	0.33	0.28	0.35
a_s	0.33	0.29	0.33
b_s	0.28	0.24	0.29
$\epsilon = \frac{a-b}{a}$	0.133	0.160	0.120
$1-\ell_o^{tr}$	0.387	0.325	0.410
$1-\ell_o^{oc}$	0.215	0.183	0.253
L_g	0.517	0.433	0.566
L_s	0.221	0.188	0.257
$\overline{J}_g/\overline{J}_s$	1.763	1.676	1.499
L_3	0.262	0.379	0.177

TABLE 20

ELEMENTS OF THE SYSTEM UZ PUPPIS
ASSUMING $L_3 = 0$

	v	b	u
$x_s = x_g$	0.6	0.6	0.6
k	0.80	0.75	0.85
p_o	-0.60	-0.50	-0.60
α_o^{tr}	0.765	0.700	0.766
α_o^{oc}	0.816	0.757	0.809
r_g	0.37	0.34	0.38
r_s	0.30	0.26	0.32
i	78°.9	80°.7	79°.3
j	80°.4	82°.2	80°.6
$\bar{\theta}_e$	40°.6	34°.3	43°.4
a_g	0.37	0.34	0.38
b_g	0.32	0.28	0.33
a_s	0.30	0.26	0.32
b_s	0.26	0.21	0.28
$\epsilon = \frac{a-b}{a}$	0.138	0.164	0.124
$1-\ell_o^{tr}$	0.387	0.325	0.410
$1-\ell_o^{oc}$	0.215	0.183	0.253
L_g	0.736	0.759	0.688
L_s	0.264	0.241	0.312
$\bar{J}_g/\bar{J}_s$	1.833	1.842	1.564

were averaged over ten-degree intervals. These calculations were performed for the solutions admitting third light as well as for those not admitting it. The results are shown in Tables 21 through 26. In addition, a statistical study of the various sections of the light curves is given in Table 34 in the Appendix. The table shows the root-mean-square deviations of the data from the theoretically predicted shape.

It was apparent from the X functions that the secondary eclipse was the occultation of the smaller star; however, the stars do not differ greatly in size. In fact, k must be close to 1.0 in order for the inclination to be so large, and yet only partial eclipses are observed. As the limit $k = 1.0$ is approached, obviously the inclination must be strictly ninety degrees in order that the eclipses may be complete.

The solutions of the blue and yellow light curves were so similar that the same k's and p_o's were finally adopted. The ultraviolet light, however, was solved totally independently, and a somewhat different solution resulted.

The consistency of the final physical parameters of the three colors lends support to the adoption of the present solutions as an acceptable photometric description of the system.

TABLE 21

AVERAGE DIFFERENCES OF THE OBSERVED DATA AND THE THEORETICAL SHAPES OVER THE YELLOW $(L_3 \neq 0)$ LIGHT CURVE OF UZ PUPPIS

Rectified Light			Un-Rectified Light	
Average θ'	Average(O-C)	n	Average θ	Average(O-C)
5°.44	+0.007	4	4°.72	+0.005
15°.36	+0.016	5	13°.41	+0.012
23°.73	+0.011	5	23°.60	+0.009
40°.04	+0.002	6	36°.15	+0.002
62°.59	+0.001	7	59°.16	+0.001
75°.08	-0.004	11	72°.92	-0.004
85°.41	-0.002	11	84°.71	-0.002
95°.69	+0.006	12	96°.55	+0.006
104°.57	0.000	11	106°.68	0.000
115°.77	-0.004	7	118°.61	-0.005
124°.29	+0.007	4	128°.18	+0.006
135°.19	-0.003	5	139°.24	-0.002
142°.63	-0.002	5	146°.49	-0.002
155°.35	-0.001	12	158°.30	-0.001
164°.83	+0.004	10	166°.76	+0.003
175°.12	-0.016	10	175°.76	-0.012
185°.39	+0.002	10	184°.68	+0.001
195°.57	-0.009	10	193°.59	-0.007
205°.31	+0.003	9	202°.30	+0.002
214°.52	-0.003	10	210°.83	-0.002
224°.75	-0.013	7	220°.70	-0.011

TABLE 21 CONTINUED

Rectified Light			Un-Rectified Light	
Average θ'	Average (O-C)	n	Average θ	Average (O-C)
235°.63	+0.009	10	231°.74	+0.008
245°.56	-0.008	8	242°.35	-0.007
254°.76	+0.006	10	252°.56	+0.006
266°.36	-0.001	5	265°.81	-0.001
275°.27	+0.001	4	276°.07	+0.001
285°.08	-0.003	8	287°.25	-0.003
295°.12	-0.001	6	298°.39	-0.001
303°.15	-0.001	4	306°.98	-0.001
315°.82	-0.019	5	319°.86	-0.016
326°.32	-0.032	4	329°.96	-0.026
335°.20	-0.003	7	338°.17	-0.002
344°.42	-0.009	8	346°.40	-0.007
354°.67	-0.007	7	355°.36	-0.005

TABLE 22

AVERAGE DIFFERENCES OF THE OBSERVED DATA AND THE THEORETICAL SHAPES OVER THE YELLOW ($L_3 = 0$) LIGHT CURVE OF UZ PUPPIS

Rectified Light			Un-Rectified Light	
Average θ'	Average (O-C)	n	Average θ	Average (O-C)
5°.44	+0.012	4	4°.72	+0.009
15°.36	+0.020	5	13°.41	+0.015
26°.73	-0.001	5	23°.60	-0.001
40°.04	-0.003	6	36°.15	-0.002
62°.59	+0.001	7	59°.16	+0.001
75°.08	-0.004	11	72°.92	-0.004
85°.41	-0.002	11	84°.71	-0.002
95°.69	+0.006	12	96°.55	+0.006
104°.57	0.000	11	106°.68	0.000
115°.77	-0.004	7	118°.61	-0.005
124°.29	+0.007	4	128°.18	+0.006
135°.19	-0.006	5	139°.24	-0.005
142°.63	-0.006	5	146°.49	-0.005
155°.35	-0.004	12	158°.30	-0.003
164°.83	+0.005	10	166°.76	+0.004
175°.12	-0.007	10	175°.76	-0.006
185°.39	+0.002	10	184°.68	+0.002
195°.57	-0.008	10	193°.59	-0.006
205°.31	-0.001	9	202°.30	-0.001
214°.53	-0.008	10	210°.83	-0.007
224°.75	-0.015	7	220°.70	-0.013

TABLE 22 CONTINUED

Rectified Light			Un-Rectified Light	
Average θ'	Average(O-C)	n	Average θ	Average(O-C)
235°.63	+0.009	10	231°.74	+0.008
245°.56	-0.008	8	242°.35	-0.007
254°.76	+0.006	10	252°.56	+0.006
266°.36	-0.001	5	265°.81	-0.001
275°.27	+0.001	4	276°.07	+0.001
285°.08	-0.003	8	287°.25	-0.003
295°.12	-0.001	6	298°.39	-0.001
303°.15	-0.001	4	306°.98	-0.001
315°.82	-0.019	5	319°.86	-0.016
326°.32	-0.044	4	329°.96	-0.035
335°.20	-0.011	7	338°.17	-0.008
344°.42	-0.006	8	346°.40	-0.005
354°.67	-0.001	7	355°.36	-0.001

TABLE 23

AVERAGE DIFFERENCES OF THE OBSERVED DATA AND THE THEORETICAL SHAPES OVER THE BLUE ($L_3 \neq 0$) LIGHT CURVE OF UZ PUPPIS

Rectified Light			Un-Rectified Light	
Average θ'	Average(O-C)	n	Average θ	Average(O-C)
4°.92	+0.001	5	4°.14	+0.001
15°.14	+0.007	4	12°.82	+0.005
24°.84	+0.002	4	21°.28	+0.001
34°.33	0.000	5	29°.88	0.000
48°.25	+0.003	4	43°.34	+0.002
65°.18	+0.002	6	61°.20	+0.002
74°.95	-0.001	9	72°.27	-0.001
85°.37	+0.001	12	84°.50	+0.001
95°.97	+0.001	10	97°.09	+0.001
104°.87	+0.001	12	107°.51	+0.001
115°.11	-0.008	6	119°.13	-0.008
123°.89	+0.003	4	128°.63	+0.003
135°.52	-0.002	6	140°.43	-0.002
142°.62	-0.006	4	147°.28	-0.005
154°.74	-0.009	13	158°.35	-0.007
165°.24	+0.010	11	167°.51	+0.007
175°.66	-0.002	8	176°.35	-0.002
185°.60	-0.001	8	184°.71	0.000
195°.52	-0.002	10	193°.15	-0.001
205°.37	-0.003	9	201°.74	-0.002
214°.17	-0.003	9	209°.72	-0.002

TABLE 23 CONTINUED

Rectified Light			Un-Rectified Light	
Average θ'	Average (O-C)	n	Average θ	Average (O-C)
224°.18	-0.008	8	219°.27	-0.007
235°.37	+0.009	8	230°.62	+0.008
245°.44	-0.002	8	241°.48	-0.002
254°.50	-0.004	10	251°.75	-0.004
264°.89	+0.013	5	263°.93	+0.013
274°.36	-0.003	5	275°.17	-0.003
285°.04	-0.001	8	287°.71	-0.001
294°.84	-0.001	6	298°.83	-0.001
302°.80	-0.001	4	307°.46	-0.001
315°.29	+0.010	5	320°.21	+0.008
325°.80	-0.001	4	330°.23	0.000
334°.89	+0.003	7	338°.49	+0.002
344°.38	0.000	8	346°.77	0.000
354°.04	-0.002	6	354°.97	-0.001

TABLE 24

AVERAGE DIFFERENCES OF THE OBSERVED DATA AND THE THEORETICAL SHAPES OVER THE BLUE (L_3= 0) LIGHT CURVE OF UZ PUPPIS

Rectified Light			Un-Rectified Light	
Average θ'	Average (O-C)	n	Average θ	Average (O-C)
4°.92	+0.005	5	4°.14	+0.003
15°.14	+0.009	4	12°.82	+0.007
24°.84	-0.012	4	21°.28	-0.009
34°.33	-0.007	5	29°.88	-0.006
48°.25	+0.003	4	43°.34	+0.002
65°.18	+0.002	6	61°.20	+0.002
74°.95	-0.001	9	72°.27	-0.001
85°.37	+0.001	12	84°.50	+0.001
95°.97	+0.001	10	97°.09	+0.001
104°.87	+0.001	12	107°.51	+0.001
115°.11	-0.008	6	119°.13	-0.008
123°.89	+0.003	4	128°.63	+0.003
135°.52	-0.002	6	140°.43	-0.002
142°.62	-0.008	4	147°.28	-0.006
154°.74	-0.016	13	158°.35	-0.012
165°.24	+0.011	11	167°.51	+0.008
175°.65	-0.001	8	176°.35	-0.001
185°.60	+0.001	8	184°.71	+0.001
195°.52	-0.001	10	193°.15	-0.001
205°.37	-0.009	9	201°.74	-0.007
214°.17	-0.008	9	209°.72	-0.006

TABLE 24 CONTINUED

Rectified Light			Un-Rectified Light	
Average θ'	Average(O-C)	n	Average θ	Average(O-C)
224°.18	-0.008	8	219°.27	-0.007
235°.37	+0.009	8	230°.62	+0.008
245°.44	-0.002	8	241°.48	-0.002
254°.50	-0.004	10	251°.75	-0.004
264°.89	+0.013	5	263°.93	+0.013
274°.36	-0.003	5	275°.17	-0.003
285°.04	-0.001	8	287°.71	-0.001
294°.84	-0.001	6	298°.83	-0.001
302°.80	-0.001	4	307°.46	-0.001
315°.29	+0.010	5	320°.21	+0.008
325°.79	-0.008	4	330°.23	-0.006
334°.89	-0.013	7	338°.49	-0.009
344°.38	+0.001	8	346°.77	0.000
354°.04	+0.003	6	354°.97	+0.002

TABLE 25

AVERAGE DIFFERENCES OF THE OBSERVED DATA AND THE THEORETICAL SHAPES OVER THE ULTRAVIOLET $(L_3 \neq 0)$ LIGHT CURVE OF UZ PUPPIS

Rectified Light			Un-Rectified Light	
Average θ'	Average (O-C)	n	Average θ	Average (O-C)
6°.26	+0.002	6	5°.51	+0.002
16°.26	-0.010	3	14°.37	-0.008
24°.32	+0.009	4	21°.66	+0.007
33°.78	-0.015	5	30°.46	-0.012
45°.63	-0.012	3	41°.93	-0.011
63°.01	+0.009	7	59°.94	+0.009
75°.20	-0.003	10	73°.27	-0.003
85°.11	-0.002	10	84°.43	-0.002
95°.33	-0.001	12	96°.05	-0.001
104°.03	+0.003	10	105°.89	+0.003
114°.18	-0.004	9	117°.06	-0.004
123°.77	-0.007	6	127°.27	-0.006
135°.40	0.000	4	139°.08	0.000
143°.02	-0.018	6	146°.52	-0.015
155°.68	-0.006	12	158°.34	-0.005
165°.36	+0.004	11	167°.07	+0.003
175°.76	-0.008	9	176°.27	-0.006
185°.11	+0.005	9	184°.71	+0.004
195°.31	+0.016	10	193°.53	+0.012
205°.51	-0.001	10	202°.75	-0.001
214°.66	+0.007	9	211°.28	+0.006

TABLE 25 CONTINUED

Rectified Light			Un-Rectified Light	
Average θ'	Average(O-C)	n	Average θ	Average(O-C)
223°.91	-0.010	7	220°.24	-0.009
234°.73	+0.011	9	231°.17	+0.010
245°.37	-0.002	9	242°.46	-0.002
254°.66	-0.005	9	252°.66	-0.005
264°.98	+0.015	5	264°.29	+0.015
274°.92	+0.007	5	275°.59	+0.007
285°.51	-0.012	7	287°.52	-0.011
294°.52	+0.004	6	297°.43	+0.004
303°.48	-0.002	5	306°.96	-0.002
316°.10	-0.005	4	319°.78	-0.004
322°.91	-0.014	3	326°.40	-0.011
334°.90	-0.003	9	337°.62	-0.003
344°.80	+0.001	7	346°.58	+0.001
354°.02	-0.008	7	354°.74	-0.006

TABLE 26

AVERAGE DIFFERENCES OF THE OBSERVED DATA AND THE THEORETICAL SHAPES OVER THE ULTRAVIOLET ($L_3 = 0$) LIGHT CURVE OF UZ PUPPIS

Rectified Light			Un-Rectified Light	
Average θ'	Average(O-C)	n	Average θ	Average(O-C)
6°.26	+0.007	6	5°.51	+0.005
16°.26	-0.006	3	14°.37	-0.005
24°.32	+0.001	4	21°.66	+0.001
33°.78	-0.025	5	30°.46	-0.021
45°.63	-0.014	3	41°.93	-0.012
63°.01	+0.009	7	59°.94	+0.009
75°.20	-0.003	10	73°.27	-0.003
85°.11	-0.002	10	84°.43	-0.002
95°.33	-0.001	12	96°.05	-0.001
104°.03	+0.003	10	105°.89	+0.003
114°.18	-0.004	9	117°.06	-0.004
123°.77	-0.007	6	127°.27	-0.006
135°.40	-0.002	4	139°.08	-0.002
145°.01	-0.022	6	146°.52	-0.018
155°.68	-0.007	12	158°.34	-0.006
165°.36	+0.005	11	167°.07	+0.004
175°.76	-0.008	9	176°.27	-0.006
185°.11	+0.005	9	184°.71	+0.004
195°.31	+0.017	10	193°.55	+0.013
205°.51	-0.002	10	202°.75	-0.001
214°.66	+0.004	9	211°.28	+0.003

TABLE 26 CONTINUED

Rectified Light			Un-Rectified Light	
Average θ'	Average(O-C)	n	Average θ	Average(O-C)
223°.91	-0.013	7	220°.24	-0.011
234°.73	+0.011	9	231°.17	+0.010
245°.37	-0.002	9	242°.46	-0.002
254°.66	-0.005	9	252°.66	-0.005
264°.98	+0.015	5	264°.29	+0.015
274°.92	+0.007	5	275°.59	+0.007
285°.51	-0.012	7	287°.52	-0.011
294°.52	+0.004	6	297°.43	+0.004
303°.48	-0.002	5	306°.96	-0.002
316°.10	-0.010	4	319°.78	-0.008
322°.91	-0.025	3	326°.40	-0.021
334°.90	-0.011	9	337°.62	-0.009
344°.80	+0.006	7	346°.58	+0.004
354°.02	-0.003	7	354°.74	-0.003

Summary of Results and Suggestions for Further Work

The eclipsing binary UZ Puppis is of the β Lyrae-type with relatively deep partial eclipses. The light curves exhibit a moderate periastron effect and a secondary eclipse which is displaced from a phase of $0^{p}.5$, defined by the center of primary eclipse, by about $0^{d}.003$. The period of the system does not seem to have changed significantly in recent decades; the period calculated from times of minimum spanning forty-one years is $0^{d}.79485183 \pm 0^{d}.00000004$ p.e.

The solutions based upon the Russell model require the assumption of a third light which contributes a very large fraction of the total light of the system. The solutions also indicate that the secondary eclipse is an occultation of a smaller star although the ratios of the radii indicate that the stars do not differ greatly in size.

If the inclination (j) equals to $85^{\circ}.9$, the average determined from this investigation, then the masses and orbital dimensions of the system based upon Struve's radial velocity data are

$$M_1 = 1.1\odot \quad ,$$

$$M_2 = 1.1\odot \quad ,$$

and

$$a_1 = a_2 = 1.6 \times 10^{6} \text{km} \quad .$$

The photometric solutions from this study are reasonably definitive, and further wide-band photometry is not warranted. However, a spectroscopic study with a large aperture telescope would be worthwhile to improve the radial velocity information and investigate the possibility of a third unresolved star.

APPENDIX

TABLE 27

AA CETI OBSERVATIONS IN YELLOW

JD HEL 2440000+	PHASE	Δmag
1261.5983	0.7792	-0.739
.6093	0.7999	-0.726
.6298	0.8381	-0.701
.6410	0.8589	-0.668
.6520	0.8795	-0.646
.6702	0.9133	-0.583
.6913	0.9526	-0.498
.7025	0.9736	-0.449
.7123	0.9919	-0.437
.7239	0.0134	-0.446
.7341	0.0326	-0.456
.7450	0.0528	-0.496
.7563	0.0740	-0.545
.7667	0.0933	-0.585
.7769	0.1123	-0.633
.7862	0.1298	-0.653
.7968	0.1496	-0.683
.8081	0.1706	-0.717
1262.5761	0.6030	-0.640
.5847	0.6190	-0.679
.5931	0.6346	-0.707
.5996	0.6467	-0.710
.6057	0.6582	-0.706
.6126	0.6710	-0.717
.6197	0.6843	-0.717
.6272	0.6983	-0.728
.6351	0.7131	-0.737
.6440	0.7295	-0.740
.6524	0.7452	-0.738
.6823	0.8010	-0.725
.6924	0.8198	-0.719
1264.5708	0.3231	-0.722
.5781	0.3369	-0.713
.5856	0.3507	-0.710
.5929	0.3644	-0.709
.6016	0.3807	-0.688
.6085	0.3936	-0.669
.6149	0.4054	-0.648
.6212	0.4173	-0.637
.6271	0.4283	-0.616
.6330	0.4391	-0.601
.6390	0.4505	-0.578
.6459	0.4632	-0.566
.6525	0.4756	-0.560
.6586	0.4869	-0.553
.6653	0.4994	-0.559
.6719	0.5118	-0.559
1264.6788	0.5247	-0.558
.6854	0.5368	-0.547
.6923	0.5497	-0.568
.6988	0.5619	-0.587
.7043	0.5721	-0.615
.7157	0.5934	-0.654
.7229	0.6069	-0.657
1268.5936	0.8260	-0.715
.6018	0.8413	-0.683
.6135	0.8631	-0.658
.6210	0.8770	-0.647
.6299	0.8936	-0.623
.6411	0.9145	-0.586
.6574	0.9450	-0.506
.6623	0.9541	-0.497
.6648	0.9587	-0.482
.6704	0.9692	-0.452
.6738	0.9755	-0.445
.6774	0.9823	-0.448
.6838	0.9941	-0.438
.6868	0.9998	-0.436
.6934	0.0121	-0.437
.6964	0.0178	-0.437
.7039	0.0317	-0.451
.7072	0.0379	-0.457
.7140	0.0505	-0.495
.7181	0.0583	-0.514
.7254	0.0718	-0.547
.7292	0.0789	-0.572
.7372	0.0938	-0.601
.7495	0.1168	-0.654
.7529	0.1230	-0.654
.7611	0.1385	-0.683
.7643	0.1444	-0.691
.7718	0.1584	-0.699
.7840	0.1811	-0.723
1281.5101	0.9161	-0.581
.5179	0.9306	-0.544
.5254	0.9448	-0.516
.5337	0.9602	-0.470
.5418	0.9752	-0.446
.5532	0.9966	-0.441
.5649	0.0183	-0.431
.5709	0.0296	-0.443
.5802	0.0469	-0.461
.5904	0.0659	-0.527
.6000	0.0838	-0.558

TABLE 27 CONTINUED

JD HEL 2440000+	PHASE	Δmag
1281.6100	0.1024	-0.605
.6166	0.1148	-0.635
.6269	0.1340	-0.651
.6388	0.1562	-0.694
.6496	0.1764	-0.707
1315.5111	0.3303	-0.710
.5185	0.3441	-0.702
.5316	0.3685	-0.679
.5447	0.3929	-0.659
.5562	0.4145	-0.627
.5587	0.4191	-0.618
.5638	0.4285	-0.609
.5723	0.4444	-0.590
.5780	0.4551	-0.562
.5806	0.4600	-0.548
.5867	0.4714	-0.543
.5890	0.4756	-0.542
.5955	0.4878	-0.545
.5985	0.4933	-0.549
.6046	0.5046	-0.545
.6069	0.5090	-0.536
.6121	0.5187	-0.549
.6145	0.5231	-0.537
.6196	0.5326	-0.558
.6222	0.5375	-0.566
.6279	0.5481	-0.566
.6309	0.5537	-0.573
.6341	0.5598	-0.583
.6393	0.5694	-0.599
.6419	0.5743	-0.609
.6468	0.5834	-0.616
.6546	0.5980	-0.641
.6628	0.6132	-0.664
1317.5121	0.0624	-0.521
.5141	0.0661	-0.531
.5191	0.0754	-0.562
.5219	0.0805	-0.565
.5290	0.0938	-0.604
.5340	0.1032	-0.621
.5377	0.1101	-0.633
.5423	0.1186	-0.642
1563.7793	0.3673	-0.678
.7976	0.4015	-0.654
.8068	0.4187	-0.642
.8165	0.4367	-0.602
.8256	0.4537	-0.544
.8430	0.4862	-0.542
.8605	0.5188	-0.540
.8814	0.5577	-0.554
1563.9023	0.5967	-0.640
1565.7743	0.0881	-0.582
.7817	0.1020	-0.621
.7880	0.1137	-0.625
.7961	0.1288	-0.663
.8039	0.1434	-0.657
.8192	0.1718	-0.697
.8310	0.1939	-0.715
.8378	0.2065	-0.711
.8405	0.2117	-0.712
.8481	0.2257	-0.714
.8510	0.2312	-0.722
.8575	0.2433	-0.724
.8613	0.2504	-0.710
.8780	0.2816	-0.754
.8858	0.2962	-0.751
.9144	0.3495	-0.690
1619.7876	0.8266	-0.701
.7941	0.8387	-0.696
.8002	0.8501	-0.650
.8140	0.8759	-0.637
.8266	0.8994	-0.607
.8325	0.9104	-0.597
.8386	0.9217	-0.557
1620.6505	0.4359	-0.601
.6568	0.4477	-0.579
.7047	0.5372	-0.554
.7098	0.5466	-0.565
.7249	0.5748	-0.607
.7319	0.5878	-0.633
.7458	0.6138	-0.670
.7609	0.6419	-0.699
.7667	0.6526	-0.711
.7724	0.6633	-0.709
.7817	0.6806	-0.719
1630.5794	0.9540	-0.475
.5835	0.9617	-0.455
.5889	0.9719	-0.444
.5946	0.9824	-0.446
.5994	0.9913	-0.445
.6041	0.0001	-0.445
.6089	0.0090	-0.442
.6132	0.0172	-0.437
.6186	0.0271	-0.449
.6241	0.0374	-0.465
.6262	0.0413	-0.474
.6307	0.0497	-0.499
.6360	0.0597	-0.517
.6428	0.0722	-0.548

TABLE 27 CONTINUED

JD HEL 2440000+	PHASE	Δmag	JD HEL 2440000+	PHASE	Δmag
1630.6455	0.0774	-0.561	1630.7546	0.2807	-0.725
.6576	0.0999	-0.634	.7606	0.2920	-0.718
.6700	0.1231	-0.640	.7660	0.3021	-0.703
.6845	0.1500	-0.677	.7711	0.3116	-0.708
.6904	0.1612	-0.694	.7773	0.3231	-0.708
.6929	0.1657	-0.705	.7847	0.3369	-0.699
.6994	0.1779	-0.700	.7913	0.3492	-0.690
.7056	0.1894	-0.724	1660.5431	0.8384	-0.704
.7185	0.2135	-0.729	.5571	0.8646	-0.648
.7244	0.2245	-0.718	.5657	0.8806	-0.634
.7363	0.2467	-0.732	.5707	0.8899	-0.617
.7425	0.2582	-0.739	.5762	0.9002	-0.593
.7490	0.2704	-0.726	.5817	0.9105	-0.598

TABLE 28

AA CETI OBSERVATIONS IN BLUE

JD HEL 2440000+	PHASE	Δmag
1261.5993	0.7812	-0.770
.6104	0.8019	-0.747
.6309	0.8401	-0.724
.6420	0.8608	-0.692
.6531	0.8815	-0.662
.6716	0.9160	-0.619
.6928	0.9555	-0.482
.7035	0.9755	-0.450
.7133	0.9937	-0.432
.7253	0.0161	-0.436
.7353	0.0348	-0.455
.7463	0.0553	-0.511
.7576	0.0763	-0.567
.7679	0.0956	-0.614
.7780	0.1144	-0.658
.7871	0.1314	-0.656
.7982	0.1521	-0.717
.8092	0.1725	-0.760
1262.5771	0.6048	-0.662
.5858	0.6211	-0.706
.5939	0.6362	-0.734
.6003	0.6480	-0.741
.6065	0.6596	-0.739
.6134	0.6724	-0.741
.6205	0.6857	-0.753
.6282	0.7001	-0.753
.6360	0.7147	-0.764
.6444	0.7304	-0.765
.6532	0.7468	-0.758
.6832	0.8026	-0.751
.6927	0.8204	-0.734
1264.5715	0.3245	-0.752
.5789	0.3383	-0.744
.5864	0.3522	-0.741
.5937	0.3658	-0.731
.6023	0.3820	-0.715
.6093	0.3950	-0.696
.6156	0.4067	-0.673
.6220	0.4187	-0.653
.6279	0.4296	-0.649
.6337	0.4404	-0.636
.6398	0.4520	-0.595
.6466	0.4646	-0.586
.6532	0.4769	-0.580
.6593	0.4883	-0.572
.6660	0.5008	-0.587
.6728	0.5135	-0.582
1264.6795	0.5260	-0.578
.6861	0.5383	-0.574
.6930	0.5511	-0.597
.6995	0.5632	-0.605
.7048	0.5732	-0.640
.7164	0.5948	-0.676
.7236	0.6081	-0.678
1268.5945	0.8277	-0.720
.6026	0.8427	-0.705
.6143	0.8646	-0.674
.6216	0.8781	-0.658
.6308	0.8954	-0.631
.6419	0.9160	-0.599
.6581	0.9463	-0.513
.6629	0.9552	-0.490
.6655	0.9601	-0.478
.6711	0.9705	-0.453
.6746	0.9771	-0.447
.6782	0.9837	-0.438
.6846	0.9958	-0.438
.6875	0.0012	-0.442
.6940	0.0133	-0.450
.6973	0.0194	-0.451
.7048	0.0333	-0.459
.7081	0.0396	-0.468
.7155	0.0534	-0.510
.7190	0.0598	-0.530
.7262	0.0732	-0.571
.7302	0.0807	-0.592
.7387	0.0967	-0.626
.7503	0.1182	-0.668
.7537	0.1245	-0.675
.7620	0.1400	-0.703
.7652	0.1461	-0.710
.7729	0.1604	-0.716
.7850	0.1829	-0.731
1281.5107	0.9173	-0.591
.5188	0.9324	-0.552
.5262	0.9462	-0.514
.5344	0.9615	-0.462
.5425	0.9766	-0.442
.5540	0.9981	-0.436
.5656	0.0197	-0.432
.5716	0.0308	-0.445
.5808	0.0480	-0.477
.5911	0.0672	-0.541
.6009	0.0854	-0.587

TABLE 28 CONTINUED

JD HEL 2440000+	PHASE	Δmag
1281.6107	0.1038	-0.613
.6174	0.1163	-0.651
.6278	0.1357	-0.664
.6396	0.1576	-0.707
.6504	0.1778	-0.720
1315.5117	0.3315	-0.738
.5192	0.3454	-0.730
.5322	0.3697	-0.696
.5453	0.3940	-0.689
.5569	0.4157	-0.642
.5593	0.4202	-0.630
.5643	0.4295	-0.626
.5728	0.4455	-0.603
.5785	0.4559	-0.571
.5812	0.4611	-0.561
.5873	0.4723	-0.561
.5896	0.4768	-0.561
.5960	0.4887	-0.566
.5991	0.4943	-0.571
.6051	0.5057	-0.566
.6074	0.5098	-0.554
.6127	0.5197	-0.563
.6150	0.5240	-0.557
.6202	0.5338	-0.572
.6228	0.5387	-0.581
.6285	0.5493	-0.589
.6319	0.5557	-0.596
.6346	0.5607	-0.603
.6399	0.5704	-0.628
.6418	0.5741	-0.628
.6476	0.5849	-0.642
.6554	0.5995	-0.671
.6636	0.6147	-0.702
1317.5126	0.0632	-0.534
.5149	0.0676	-0.546
.5198	0.0768	-0.578
.5225	0.0817	-0.591
.5294	0.0947	-0.633
.5352	0.1053	-0.652
.5382	0.1110	-0.666
.5429	0.1197	-0.679
1563.7799	0.3685	-0.713
.7985	0.4032	-0.680
.8092	0.4231	-0.649
.8175	0.4386	-0.626
.8264	0.4552	-0.568
.8440	0.4881	-0.517
.8613	0.5203	-0.565
.8824	0.5596	-0.588
1563.9031	0.5983	-0.671
1565.7752	0.0898	-0.605
.7823	0.1031	-0.647
.7890	0.1155	-0.660
.7968	0.1302	-0.688
.8047	0.1449	-0.691
.8207	0.1747	-0.717
.8317	0.1952	-0.744
.8384	0.2077	-0.739
.8413	0.2131	-0.733
.8488	0.2270	-0.735
.8519	0.2328	-0.757
.8584	0.2449	-0.747
.8626	0.2529	-0.756
.8790	0.2834	-0.781
.8867	0.2978	-0.784
.9152	0.3509	-0.712
1619.7882	0.8278	-0.738
.7951	0.8406	-0.722
.8007	0.8510	-0.673
.8146	0.8769	-0.672
.8273	0.9007	-0.637
.8332	0.9117	-0.615
.8393	0.9231	-0.607
1620.6510	0.4369	-0.620
.6575	0.4491	-0.595
.7052	0.5380	-0.572
.7101	0.5472	-0.580
.7256	0.5761	-0.633
.7328	0.5894	-0.652
.7464	0.6148	-0.689
.7616	0.6431	-0.703
.7732	0.6648	-0.735
.7823	0.6819	-0.737
1630.5799	0.9550	-0.488
.5840	0.9626	-0.466
.5895	0.9728	-0.443
.5952	0.9836	-0.438
.5998	0.9921	-0.446
.6045	0.0008	-0.442
.6093	0.0098	-0.442
.6137	0.0181	-0.443
.6192	0.0283	-0.456
.6246	0.0384	-0.471
.6266	0.0420	-0.478
.6313	0.0509	-0.507
.6367	0.0610	-0.536
.6436	0.0739	-0.570
.6462	0.0786	-0.582

TABLE 28 CONTINUED

JD HEL 2440000+	PHASE	Δmag
1630.6582	0.1010	-0.643
.6707	0.1243	-0.694
.6850	0.1510	-0.707
.6910	0.1622	-0.733
.6935	0.1669	-0.732
.6999	0.1789	-0.724
.7062	0.1905	-0.743
.7190	0.2145	-0.752
.7250	0.2256	-0.750
.7369	0.2478	-0.760
.7431	0.2594	-0.759
.7496	0.2716	-0.760
.7553	0.2821	-0.762
1630.7612	0.2932	-0.759
.7665	0.3030	-0.745
.7717	0.3127	-0.743
.7779	0.3244	-0.729
.7854	0.3382	-0.727
.7918	0.3503	-0.721
1660.5435	0.8391	-0.737
.5580	0.8662	-0.693
.5662	0.8815	-0.659
.5712	0.8907	-0.663
.5767	0.9011	-0.624
.5823	0.9115	-0.606

TABLE 29

AA CETI OBSERVATIONS IN ULTRAVIOLET

JD HEL 2440000+	PHASE	Δmag
1261.6004	0.7832	-0.706
.6116	0.8042	-0.671
.6320	0.8420	-0.641
.6431	0.8629	-0.613
.6542	0.8836	-0.596
.6727	0.9180	-0.526
.6939	0.9576	-0.388
.7045	0.9773	-0.356
.7143	0.9956	-0.349
.7263	0.0181	-0.358
.7364	0.0368	-0.376
.7476	0.0577	-0.454
.7588	0.0787	-0.516
.7691	0.0977	-0.565
.7791	0.1164	-0.600
.7887	0.1344	-0.617
.7992	0.1540	-0.669
.8102	0.1745	-0.739
1262.5781	0.6067	-0.615
.5869	0.6230	-0.671
.5948	0.6378	-0.684
.6011	0.6496	-0.683
.6072	0.6610	-0.675
.6142	0.6740	-0.686
.6213	0.6872	-0.686
.6290	0.7017	-0.696
.6368	0.7161	-0.695
.6459	0.7332	-0.704
.6541	0.7484	-0.690
.6843	0.8047	-0.690
.6943	0.8234	-0.664
1264.5724	0.3261	-0.695
.5798	0.3400	-0.672
.5872	0.3537	-0.668
.5944	0.3672	-0.656
.6031	0.3834	-0.642
.6100	0.3963	-0.630
.6162	0.4079	-0.604
.6227	0.4200	-0.586
.6286	0.4309	-0.567
.6344	0.4418	-0.561
.6407	0.4535	-0.527
.6474	0.4661	-0.515
.6540	0.4784	-0.514
.6602	0.4900	-0.510
.6668	0.5022	-0.504
.6738	0.5152	-0.499
1264.6803	0.5274	-0.491
.6868	0.5396	-0.512
.6937	0.5523	-0.532
.7001	0.5644	-0.545
.7055	0.5743	-0.572
.7172	0.5963	-0.622
.7246	0.6100	-0.646
1268.5953	0.8292	-0.653
.6034	0.8443	-0.644
.6151	0.8661	-0.608
.6222	0.8793	-0.588
.6317	0.8970	-0.567
.6426	0.9174	-0.515
.6586	0.9472	-0.443
.6635	0.9564	-0.415
.6662	0.9615	-0.403
.6720	0.9721	-0.367
.6755	0.9788	-0.361
.6790	0.9853	-0.363
.6854	0.9973	-0.349
.6885	0.0030	-0.350
.6948	0.0148	-0.365
.6982	0.0211	-0.369
.7056	0.0350	-0.391
.7090	0.0413	-0.413
.7165	0.0552	-0.442
.7197	0.0612	-0.462
.7271	0.0750	-0.501
.7312	0.0827	-0.530
.7398	0.0987	-0.577
.7511	0.1198	-0.609
.7548	0.1266	-0.614
.7626	0.1413	-0.644
.7660	0.1475	-0.659
.7738	0.1620	-0.661
.7860	0.1849	-0.678
1281.5115	0.9187	-0.516
.5195	0.9337	-0.491
.5270	0.9476	-0.441
.5352	0.9629	-0.390
.5433	0.9780	-0.363
.5549	0.9997	-0.363
.5664	0.0212	-0.355
.5722	0.0320	-0.369
.5817	0.0496	-0.413
.5919	0.0686	-0.480
.6018	0.0872	-0.540

TABLE 29 CONTINUED

JD HEL 2440000+	PHASE	Δmag	JD HEL 2440000+	PHASE	Δmag
1281.6114	0.1050	-0.574	1563.9041	0.6001	-0.593
.6181	0.1176	-0.593	1565.7761	0.0914	-0.536
.6286	0.1371	-0.610	.7830	0.1044	-0.567
.6404	0.1592	-0.656	.7899	0.1172	-0.592
.6509	0.1788	-0.674	.7978	0.1320	-0.615
1315.5124	0.3328	-0.667	.8056	0.1465	-0.610
.5199	0.3468	-0.651	.8217	0.1765	-0.660
.5330	0.3712	-0.640	.8325	0.1967	-0.664
.5460	0.3954	-0.635	.8391	0.2090	-0.671
.5575	0.4169	-0.572	.8421	0.2146	-0.695
.5598	0.4212	-0.552	.8495	0.2284	-0.682
.5649	0.4307	-0.548	.8526	0.2342	-0.694
.5734	0.4465	-0.525	.8592	0.2465	-0.677
.5791	0.4571	-0.507	.8639	0.2552	-0.692
.5820	0.4625	-0.510	.8801	0.2855	-0.690
.5878	0.4733	-0.510	.8877	0.2996	-0.719
.5902	0.4778	-0.506	.9159	0.3523	-0.641
.5967	0.4899	-0.500	1619.7890	0.8292	-0.650
.5997	0.4955	-0.502	.7957	0.8418	-0.646
.6057	0.5067	-0.491	.8010	0.8516	-0.621
.6079	0.5108	-0.490	.8152	0.8781	-0.612
.6132	0.5207	-0.498	.8280	0.9020	-0.561
.6157	0.5253	-0.484	.8339	0.9129	-0.556
.6208	0.5350	-0.507	1620.6515	0.4379	-0.547
.6235	0.5400	-0.510	.6584	0.4508	-0.516
.6291	0.5504	-0.528	.7058	0.5391	-0.497
.6327	0.5571	-0.540	.7105	0.5480	-0.519
.6353	0.5620	-0.554	.7263	0.5774	-0.554
.6406	0.5718	-0.566	.7333	0.5904	-0.586
.6425	0.5754	-0.573	.7471	0.6162	-0.630
.6483	0.5862	-0.582	.7626	0.6450	-0.641
.6561	0.6008	-0.612	.7677	0.6546	-0.671
.6645	0.6163	-0.631	.7740	0.6663	-0.670
1317.5131	0.0641	-0.458	.7830	0.6831	-0.707
.5156	0.0688	-0.469	1630.5805	0.9561	-0.393
.5205	0.0780	-0.508	.5843	0.9632	-0.377
.5231	0.0829	-0.518	.5903	0.9744	-0.367
.5299	0.0954	-0.564	.5958	0.9847	-0.352
.5358	0.1065	-0.584	.6003	0.9930	-0.350
.5388	0.1120	-0.607	.6048	0.0014	-0.351
.5435	0.1209	-0.618	.6098	0.0107	-0.342
1563.7806	0.3698	-0.630	.6142	0.0190	-0.358
.7994	0.4048	-0.588	.6198	0.0295	-0.370
.8104	0.4253	-0.550	.6252	0.0394	-0.378
.8183	0.4401	-0.552	.6269	0.0427	-0.405
.8274	0.4570	-0.527	.6319	0.0519	-0.423
.8448	0.4895	-0.464	.6378	0.0631	-0.463
.8624	0.5223	-0.482	.6443	0.0751	-0.504
.8838	0.5622	-0.519	.6468	0.0798	-0.510

TABLE 29 CONTINUED

JD HEL 2440000+	PHASE	Δmag
1630.6587	0.1020	-0.566
.6714	0.1256	-0.600
.6858	0.1524	-0.637
.6916	0.1633	-0.656
.6943	0.1683	-0.664
.7006	0.1801	-0.648
.7067	0.1915	-0.679
.7197	0.2158	-0.678
.7256	0.2268	-0.670
.7377	0.2492	-0.690
1630.7438	0.2607	-0.695
.7502	0.2725	-0.684
.7560	0.2833	-0.689
.7619	0.2945	-0.695
.7670	0.3039	-0.676
.7726	0.3144	-0.674
.7786	0.3255	-0.655
.7860	0.3394	-0.650
.7925	0.3515	-0.643

TABLE 30

STATISTICAL STUDY OF THE SOLUTIONS TO THE LIGHT VARIATIONS OF AA CETI

RMS Deviations of the Observed Data from the Theoretical Solutions over Portions of the Light Curve

	RMS Deviation	Number of Data Points
Yellow		
Primary	0.0107	54
1st Maximum	0.0181	65
Secondary	0.0165	57
2nd Maximum	0.0130	42
Blue		
Primary	0.0119	61
1st Maximum	0.0190	61
Secondary	0.0194	60
2nd Maximum	0.0152	35
Ultraviolet		
Primary	0.0108	65
1st Maximum	0.0183	55
Secondary	0.0174	60
2nd Maximum	0.0189	29

TABLE 31

UZ PUPPIS OBSERVATIONS IN YELLOW

JD HEL 2440000+	PHASE	Δmag
0974.7871	0.8948	-0.109
.8025	0.9142	-0.023
.8103	0.9240	0.024
.8196	0.9357	0.044
.8281	0.9464	0.115
.8369	0.9575	0.265
.8449	0.9675	0.378
.8522	0.9768	0.486
0979.5918	0.9396	0.116
.6019	0.9524	0.221
.6105	0.9631	0.318
.6191	0.9740	0.420
.6277	0.9848	0.535
.6364	0.9957	0.589
.6462	0.0080	0.597
.6548	0.0188	0.463
.6631	0.0293	0.361
.6719	0.0404	0.221
.6816	0.0525	0.141
.6911	0.0645	0.090
.6996	0.0752	0.004
.7153	0.0950	-0.103
.7269	0.1096	-0.145
.7397	0.1256	-0.199
.7484	0.1366	-0.213
.7649	0.1574	-0.279
.7739	0.1687	-0.299
.7829	0.1800	-0.312
.7918	0.1912	-0.313
.7997	0.2012	-0.328
.8081	0.2118	-0.353
.8167	0.2225	-0.372
.8256	0.2337	-0.386
.8347	0.2452	-0.356
.8438	0.2566	-0.381
.8526	0.2678	-0.376
.8679	0.2869	-0.346
.8772	0.2986	-0.335
0984.6328	0.2817	-0.390
.6439	0.2957	-0.367
.6556	0.3104	-0.332
.6659	0.3233	-0.308
.6764	0.3365	-0.263
.6869	0.3497	-0.263
0998.5386	0.7765	-0.286
.5440	0.7833	-0.289
.5528	0.7944	-0.295
0998.5576	0.8004	-0.304
.5658	0.8107	-0.295
.5700	0.8159	-0.284
.5783	0.8264	-0.261
.5821	0.8313	-0.265
.5898	0.8409	-0.233
.5936	0.8456	-0.231
.6023	0.8566	-0.224
.6071	0.8627	-0.205
.6177	0.8760	-0.171
.6219	0.8813	-0.153
.6314	0.8933	-0.120
.6346	0.8973	-0.100
.6388	0.9025	-0.080
.6571	0.9256	0.034
.6606	0.9300	0.042
.6640	0.9343	0.069
.6707	0.9427	0.138
.6739	0.9468	0.161
.6812	0.9559	0.244
.6818	0.9566	0.246
.6931	0.9709	0.409
.6979	0.9769	0.473
.7021	0.9822	0.528
.7114	0.9939	0.625
.7160	0.9997	0.625
.7202	0.0049	0.594
.7327	0.0207	0.490
.7374	0.0266	0.401
.7496	0.0419	0.266
.7544	0.0480	0.191
.7680	0.0651	0.045
.7737	0.0722	-0.011
.7746	0.0734	-0.007
.7889	0.0914	-0.104
.8002	0.1056	-0.181
1000.5615	0.3215	-0.316
.5732	0.3363	-0.290
.5933	0.3614	-0.252
.6033	0.3740	-0.202
.6218	0.3973	-0.093
.6261	0.4028	-0.083
.6463	0.4281	-0.021
.6503	0.4332	0.008
.6601	0.4455	0.083
.6642	0.4507	0.112
.6749	0.4642	0.186

TABLE 31 CONTINUED

JD HEL 2440000+	PHASE	Δmag
1000.6795	0.4699	0.197
.6891	0.4821	0.272
.6935	0.4876	0.304
.6944	0.4887	0.307
.7119	0.5107	0.286
.7220	0.5234	0.238
.7269	0.5296	0.211
.7402	0.5464	0.148
.7474	0.5554	0.090
.7599	0.5711	-0.004
.7654	0.5781	-0.032
.7795	0.5958	-0.095
.7850	0.6027	-0.111
.8055	0.6284	-0.209
1016.5458	0.4313	0.040
.5500	0.4366	0.035
.5588	0.4476	0.052
.5631	0.4530	0.101
.5673	0.4584	0.122
.5752	0.4683	0.173
.5946	0.4926	0.343
.5989	0.4980	0.355
.6137	0.5167	0.284
.6172	0.5211	0.254
.6211	0.5260	0.218
.6284	0.5352	0.191
.6327	0.5406	0.169
.6366	0.5455	0.156
.6439	0.5547	0.072
.6485	0.5605	0.069
.6526	0.5657	0.005
.6614	0.5767	-0.031
.6654	0.5817	-0.048
.6700	0.5875	-0.076
.6785	0.5982	-0.100
.6830	0.6039	-0.117
.6912	0.6142	-0.172
.6959	0.6201	-0.168
.7144	0.6434	-0.232
.7367	0.6715	-0.262
.7565	0.6964	-0.299
1020.5756	0.5011	0.315
.5800	0.5066	0.297
.5881	0.5169	0.252
.5920	0.5218	0.255
.5993	0.5310	0.347
.6027	0.5352	0.208
.6098	0.5442	0.113
.6222	0.5598	0.086
1020.6282	0.5673	-0.035
.6355	0.5765	-0.073
1028.5581	0.5439	0.153
.5696	0.5584	0.046
.5746	0.5646	0.014
.5856	0.5785	-0.032
.5907	0.5849	-0.060
.6016	0.5986	-0.093
.6073	0.6059	-0.121
.6174	0.6185	-0.148
.6234	0.6260	-0.177
.6349	0.6405	-0.230
.6406	0.6477	-0.250
.6530	0.6633	-0.249
.6580	0.6695	-0.260
.6691	0.6836	-0.274
.6937	0.7145	-0.317
.7212	0.7491	-0.307
1380.5453	0.3777	-0.214
.5556	0.3906	-0.170
.5586	0.3944	-0.170
.5640	0.4011	-0.130
.5665	0.4043	-0.132
.5724	0.4117	-0.105
.5747	0.4147	-0.096
.5894	0.4331	0.008
.5917	0.4361	0.016
.5963	0.4417	0.027
.5989	0.4451	0.051
.6009	0.4476	0.055
.6070	0.4552	0.118
.6095	0.4584	0.137
.6132	0.4630	0.163
.6182	0.4693	0.191
.6208	0.4726	0.209
.6234	0.4759	0.232
.6287	0.4825	0.259
.6320	0.4867	0.270
.6349	0.4903	0.286
.6409	0.4979	0.290
.6442	0.5021	0.286
.6501	0.5095	0.286
.6529	0.5130	0.322
1381.5457	0.6363	-0.212
.5526	0.6449	-0.231
.5558	0.6489	-0.257
.5616	0.6562	-0.266
.5647	0.6601	-0.268
.5772	0.6759	-0.284

TABLE 31 CONTINUED

JD HEL 2440000+	PHASE	Δmag	JD HEL 2440000+	PHASE	Δmag
1381.5799	0.6792	-0.295	1661.8022	0.2258	-0.345
.5824	0.6824	-0.281	.8052	0.2296	-0.337
.5883	0.6899	-0.328	.8122	0.2384	-0.374
.5912	0.6935	-0.320	.8154	0.2424	-0.374
.5944	0.6975	-0.310	.8297	0.2605	-0.342
.6015	0.7065	-0.338	.8324	0.2638	-0.374
.6044	0.7101	-0.311	.8402	0.2736	-0.396
1383.5522	0.1606	-0.291	.8411	0.2748	-0.358
.5606	0.1712	-0.329	.8442	0.2787	-0.374
.5773	0.1922	-0.328	.8523	0.2889	-0.353
.5822	0.1983	-0.347	.8626	0.3018	-0.337
.5919	0.2105	-0.355	.8710	0.3124	-0.481
.5960	0.2157	-0.358	.9018	0.3512	-0.258
.6042	0.2261	-0.369	.9103	0.3618	-0.245
.6073	0.2299	-0.369	1663.7220	0.6412	-0.237
.6197	0.2456	-0.365	.7289	0.6498	-0.271
.6226	0.2492	-0.362	.7606	0.6897	-0.311
.6285	0.2566	-0.366	.7693	0.7006	-0.317
.6310	0.2598	-0.372	.7760	0.7090	-0.323
.6394	0.2703	-0.359	.7831	0.7181	-0.328
.6425	0.2743	-0.357	.7901	0.7269	-0.328
.6493	0.2827	-0.344	.7932	0.7307	-0.334
.6523	0.2866	-0.352	.8010	0.7405	-0.338
.6605	0.2968	-0.339	.8042	0.7446	-0.342
.6632	0.3002	-0.336	.8120	0.7544	-0.345
.6718	0.3110	-0.320	.8153	0.7586	-0.340
.6813	0.3231	-0.300	.8307	0.7779	-0.334
.6891	0.3329	-0.286	.8390	0.7884	-0.313
.6968	0.3425	-0.273	.8430	0.7934	-0.311
1661.7624	0.1758	-0.283	.8513	0.8038	-0.309
.7718	0.1876	-0.315	.8554	0.8090	-0.288
.7807	0.1988	-0.339	.8673	0.8239	-0.287
.7853	0.2046	-0.358	.8759	0.8347	-0.259
.7947	0.2164	-0.351	.8848	0.8460	-0.240

TABLE 32

UZ PUPPIS OBSERVATIONS IN BLUE

JD HEL 2440000+	PHASE	Δmag	JD HEL 2440000+	PHASE	Δmag
0974.7877	0.8955	0.120	0998.5538	0.7956	-0.072
.8031	0.9149	0.211	.5584	0.8014	-0.067
.8108	0.9247	0.283	.5667	0.8119	-0.052
.8202	0.9365	0.350	.5711	0.8174	-0.045
.8290	0.9475	0.445	.5790	0.8274	-0.035
.8375	0.9583	0.544	.5830	0.8324	-0.023
.8455	0.9683	0.640	.5908	0.8421	0.006
.8528	0.9775	0.740	.5945	0.8468	0.017
0979.5925	0.9405	0.357	.6033	0.8579	0.039
.6026	0.9532	0.464	.6079	0.8637	0.044
.6112	0.9640	0.589	.6185	0.8770	0.081
.6198	0.9749	0.723	.6227	0.8823	0.087
.6284	0.9857	0.851	.6322	0.8942	0.144
.6371	0.9966	0.897	.6355	0.8984	0.151
.6469	0.0089	0.866	.6394	0.9033	0.168
.6555	0.0198	0.748	.6577	0.9263	0.284
.6639	0.0304	0.634	.6614	0.9310	0.307
.6726	0.0413	0.474	.6646	0.9350	0.326
.6830	0.0544	0.369	.6713	0.9435	0.409
.6924	0.0661	0.326	.6747	0.9477	0.444
.7002	0.0760	0.252	.6823	0.9573	0.542
.7160	0.0959	0.144	.6829	0.9581	0.540
.7278	0.1107	0.097	.6939	0.9719	0.687
.7404	0.1265	0.026	.6988	0.9780	0.745
.7491	0.1375	0.012	.7029	0.9832	0.811
.7657	0.1583	-0.057	.7125	0.9952	0.901
.7749	0.1699	-0.100	.7168	0.0007	0.914
.7836	0.1809	-0.069	.7211	0.0061	0.884
.7928	0.1925	-0.125	.7337	0.0220	0.725
.8005	0.2022	-0.129	.7383	0.0277	0.665
.8089	0.2128	-0.126	.7506	0.0432	0.497
.8174	0.2234	-0.136	.7557	0.0496	0.427
.8265	0.2349	-0.148	.7690	0.0664	0.286
.8357	0.2465	-0.145	.7756	0.0746	0.231
.8445	0.2576	-0.128	.7765	0.0758	0.243
.8535	0.2688	-0.141	.7900	0.0927	0.113
.8687	0.2880	-0.119	.8011	0.1068	0.063
.8779	0.2996	-0.105	1000.5622	0.3224	-0.086
0984.6224	0.2686	-0.125	.5721	0.3349	-0.027
.6336	0.2827	-0.154	.5946	0.3631	0.003
.6450	0.2970	-0.135	.6043	0.3753	0.047
.6564	0.3114	-0.079	.6226	0.3984	0.145
.6667	0.3243	-0.044	.6270	0.4039	0.154
.6771	0.3374	-0.008	.6472	0.4294	0.235
.6878	0.3509	-0.009	.6512	0.4344	0.273
0998.5395	0.7776	-0.076	.6610	0.4466	0.331
.5459	0.7856	-0.064	.6648	0.4515	0.359

TABLE 32 CONTINUED

JD HEL 2440000+	PHASE	Δmag
1000.6759	0.4654	0.413
.6802	0.4708	0.409
.6902	0.4834	0.490
.6955	0.4900	0.520
.6964	0.4912	0.526
.7130	0.5122	0.513
.7232	0.5250	0.474
.7280	0.5310	0.455
.7413	0.5477	0.355
.7485	0.5567	0.323
.7610	0.5725	0.239
.7666	0.5796	0.199
.7809	0.5975	0.121
.7860	0.6039	0.119
.8068	0.6301	0.032
1016.5465	0.4321	0.260
.5509	0.4377	0.262
.5597	0.4487	0.307
.5641	0.4543	0.323
.5682	0.4594	0.332
.5760	0.4693	0.405
.5954	0.4937	0.569
.5996	0.4990	0.550
.6143	0.5175	0.472
.6180	0.5221	0.470
.6218	0.5269	0.448
.6294	0.5364	0.389
.6334	0.5415	0.379
.6374	0.5465	0.347
.6448	0.5558	0.301
.6494	0.5616	0.294
.6535	0.5668	0.234
.6621	0.5776	0.191
.6662	0.5828	0.179
.6713	0.5891	0.163
.6795	0.5995	0.118
.6838	0.6059	0.130
.6919	0.6151	0.076
.6970	0.6215	0.109
.7376	0.6726	-0.056
.7575	0.6976	-0.045
1020.5764	0.5021	0.544
.5807	0.5075	0.535
.5890	0.5180	0.491
.5926	0.5226	0.478
.6000	0.5318	0.407
.6032	0.5359	0.387
.6106	0.5452	0.332
.6231	0.5609	0.271
1020.6289	0.5682	0.190
.6365	0.5778	0.194
.6776	0.6295	0.042
.6817	0.6346	0.059
.6887	0.6434	0.086
.6929	0.6487	0.118
.6998	0.6574	0.070
.7091	0.6692	-0.173
.7187	0.6811	-0.052
.7280	0.6929	-0.189
1028.5591	0.5451	0.377
.5707	0.5597	0.287
.5757	0.5661	0.260
.5868	0.5800	0.201
.5917	0.5862	0.172
.6027	0.6001	0.139
.6086	0.6075	0.109
.6187	0.6201	0.084
.6248	0.6278	0.069
.6361	0.6420	0.012
.6421	0.6496	0.001
.6542	0.6648	-0.010
.6591	0.6709	-0.003
.6704	0.6852	-0.052
.6949	0.7160	-0.081
.7223	0.7505	-0.096
1380.5460	0.3785	0.039
.5565	0.3917	0.081
.5590	0.3949	0.088
.5644	0.4017	0.120
.5670	0.4050	0.119
.5729	0.4123	0.142
.5752	0.4153	0.166
.5875	0.4307	0.236
.5898	0.4337	0.240
.5922	0.4366	0.259
.5970	0.4427	0.282
.5994	0.4457	0.291
.6015	0.4484	0.308
.6078	0.4562	0.347
.6101	0.4591	0.364
.6137	0.4637	0.376
.6189	0.4702	0.418
.6214	0.4733	0.433
.6239	0.4765	0.455
.6293	0.4833	0.490
.6325	0.4873	0.504
.6354	0.4910	0.463
.6416	0.4988	0.516

TABLE 32 CONTINUED

JD HEL 2440000+	PHASE	Δmag
1380.6447	0.5027	0.506
.6507	0.5102	0.543
.6538	0.5142	0.581
1381.5391	0.6279	0.041
.5466	0.6374	0.022
.5534	0.6459	-0.003
.5564	0.6498	-0.008
.5622	0.6570	-0.018
.5655	0.6611	-0.031
.5779	0.6768	-0.048
.5805	0.6800	-0.045
.5830	0.6832	-0.036
.5890	0.6907	-0.076
.5920	0.6945	-0.081
.5953	0.6987	-0.062
.6020	0.7071	-0.095
.6053	0.7113	-0.039
1383.5530	0.1616	-0.070
.5614	0.1721	-0.104
.5782	0.1933	-0.117
.5830	0.1993	-0.122
.5927	0.2115	-0.134
.6049	0.2269	-0.144
.6080	0.2308	-0.138
.6204	0.2464	-0.137
.6232	0.2499	-0.147
.6291	0.2573	-0.146
.6315	0.2604	-0.154
.6401	0.2711	-0.133
.6433	0.2752	-0.135
.6500	0.2836	-0.122
.6530	0.2875	-0.115
.6604	0.2968	-0.114
.6638	0.3010	-0.106
.6726	0.3121	-0.083
.6821	0.3241	-0.069
.6899	0.3338	0.026
.6975	0.3434	0.048
1661.7634	0.1770	-0.087
.7732	0.1894	-0.124
.7817	0.2001	-0.117
.7863	0.2058	-0.113
.7958	0.2178	-0.153
.8029	0.2267	-0.135
.8058	0.2304	-0.143
.8130	0.2394	-0.144
.8164	0.2437	-0.139
.8304	0.2613	-0.114
.8331	0.2647	-0.134
.8421	0.2760	-0.108
.8448	0.2794	-0.108
.8533	0.2902	-0.105
.8638	0.3033	-0.093
.8718	0.3134	-0.093
.8948	0.3424	-0.035
.9028	0.3524	-0.018
.9110	0.3628	0.012
1663.7228	0.6421	0.001
.7623	0.6919	-0.057
.7698	0.7013	-0.057
.7768	0.7101	-0.079
.7841	0.7193	-0.107
.7908	0.7278	-0.104
.7939	0.7316	-0.107
.8017	0.7414	-0.126
.8050	0.7456	-0.125
.8127	0.7553	-0.115
.8161	0.7595	-0.091
.8315	0.7789	-0.120
.8398	0.7894	-0.111
.8437	0.7943	-0.087
.8521	0.8049	-0.102
.8568	0.8107	-0.082
.8682	0.8250	-0.069
.8770	0.8362	-0.035
.8863	0.8479	-0.018

TABLE 33

UZ PUPPIS OBSERVATIONS IN ULTRAVIOLET

JD HEL 2440000+	PHASE	Δmag
0974.7883	0.8963	0.090
.8036	0.9156	0.182
.8115	0.9255	0.231
.8208	0.9372	0.325
.8294	0.9481	0.422
.8381	0.9590	0.476
.8462	0.9692	0.589
.8533	0.9781	0.675
0979.5933	0.9414	0.396
.6033	0.9541	0.478
.6120	0.9651	0.633
.6206	0.9758	0.745
.6291	0.9865	0.857
.6379	0.9975	0.922
.6476	0.0098	0.870
.6562	0.0206	0.753
.6647	0.0313	0.646
.6747	0.0439	0.486
.6837	0.0552	0.329
.6931	0.0670	0.273
.7009	0.0768	0.217
.7167	0.0967	0.105
.7295	0.1128	0.037
.7411	0.1274	0.002
.7500	0.1386	-0.025
.7664	0.1593	-0.100
.7755	0.1707	-0.130
.7847	0.1823	-0.099
.7934	0.1933	-0.124
.8012	0.2030	-0.145
.8097	0.2137	-0.139
.8180	0.2242	-0.133
.8273	0.2359	-0.144
.8366	0.2475	-0.145
.8453	0.2586	-0.149
.8542	0.2697	-0.170
.8695	0.2890	-0.147
.8788	0.3007	-0.111
0984.6237	0.2702	-0.145
.6345	0.2837	-0.186
.6459	0.2982	-0.158
.6575	0.3128	-0.097
.6675	0.3253	-0.065
.6780	0.3386	-0.035
.6887	0.3520	-0.048
0998.5407	0.7792	-0.112
.5469	0.7869	-0.083
0998.5549	0.7970	-0.081
.5594	0.8027	-0.073
.5676	0.8130	-0.074
.5722	0.8188	-0.065
.5799	0.8285	-0.067
.5838	0.8334	-0.070
.5915	0.8431	-0.046
.5955	0.8481	-0.024
.6042	0.8590	-0.006
.6088	0.8648	0.004
.6195	0.8783	0.043
.6237	0.8836	0.035
.6328	0.8950	0.097
.6369	0.9001	0.125
.6402	0.9043	0.131
.6583	0.9271	0.226
.6623	0.9321	0.278
.6654	0.9361	0.294
.6721	0.9444	0.366
.6755	0.9487	0.399
.6836	0.9589	0.493
.6843	0.9598	0.515
.6948	0.9730	0.634
.6997	0.9791	0.706
.7039	0.9844	0.763
.7133	0.9963	0.838
.7178	0.0019	0.826
.7222	0.0075	0.822
.7347	0.0231	0.645
.7392	0.0288	0.589
.7517	0.0446	0.429
.7567	0.0508	0.369
.7701	0.0677	0.245
.7777	0.0773	0.185
.7786	0.0785	0.215
.7908	0.0938	0.118
.8031	0.1093	0.055
1000.5632	0.3237	-0.127
.5746	0.3379	-0.116
.5955	0.3643	-0.030
.6053	0.3766	-0.014
.6236	0.3997	0.089
.6279	0.4051	0.083
.6481	0.4304	0.194
.6523	0.4357	0.207
.6621	0.4481	0.305
.6664	0.4535	0.320

TABLE 33 CONTINUED

JD HEL 2440000+	PHASE	Δmag
1000.6768	0.4665	0.376
.6811	0.4720	0.424
.6911	0.4846	0.501
.6976	0.4927	0.544
.6984	0.4937	0.511
.7139	0.5132	0.494
.7244	0.5264	0.465
.7291	0.5324	0.411
.7445	0.5518	0.309
.7494	0.5578	0.291
.7624	0.5743	0.188
.7690	0.5826	0.143
.7819	0.5988	0.100
.7868	0.6050	0.073
.8077	0.6313	0.032
1016.5474	0.4333	0.227
.5517	0.4387	0.240
.5606	0.4499	0.275
.5650	0.4554	0.297
.5690	0.4605	0.326
.5768	0.4703	0.406
.5962	0.4947	0.577
.6004	0.5000	0.543
.6149	0.5183	0.468
.6189	0.5233	0.402
.6224	0.5277	0.450
.6303	0.5376	0.327
.6343	0.5427	0.312
.6381	0.5474	0.338
.6459	0.5572	0.249
.6503	0.5628	0.271
.6543	0.5678	0.253
.6627	0.5784	0.184
.6669	0.5837	0.161
.6719	0.5900	0.140
.6804	0.6007	0.102
.6846	0.6059	0.120
.6927	0.6161	0.071
.6980	0.6228	0.078
.7163	0.6458	-0.034
.7386	0.6739	-0.028
.7583	0.6986	-0.046
1020.5771	0.5030	0.507
.5814	0.5085	0.501
.5896	0.5188	0.482
.5934	0.5235	0.487
.6007	0.5327	0.369
.6038	0.5366	0.278
.6114	0.5462	0.340
1020.6240	0.5620	0.255
.6296	0.5691	0.166
.6373	0.5788	0.115
1028.5599	0.5461	0.339
.5717	0.5610	0.235
.5774	0.5681	0.269
.5882	0.5818	0.131
.5927	0.5875	0.121
.6042	0.6018	0.077
.6099	0.6090	0.062
.6199	0.6217	0.028
.6260	0.6294	0.015
.6373	0.6435	-0.037
.6428	0.6504	-0.032
.6552	0.6661	-0.045
.6605	0.6728	-0.041
.6719	0.6871	-0.088
.6962	0.7177	-0.100
.7233	0.7517	-0.129
1380.5480	0.3810	0.007
.5570	0.3924	0.064
.5594	0.3954	0.055
.5651	0.4026	0.109
.5675	0.4056	0.113
.5734	0.4130	0.126
.5758	0.4160	0.162
.5880	0.4313	0.233
.5904	0.4344	0.243
.5926	0.4372	0.240
.5975	0.4433	0.259
.6001	0.4466	0.285
.6021	0.4491	0.309
.6084	0.4570	0.336
.6111	0.4604	0.363
.6141	0.4642	0.399
.6196	0.4711	0.437
.6219	0.4741	0.434
.6244	0.4772	0.436
.6299	0.4841	0.479
.6331	0.4881	0.508
.6361	0.4918	0.509
.6428	0.5003	0.519
.6453	0.5035	0.523
.6511	0.5108	0.531
.6553	0.5161	0.542
1381.5400	0.6291	0.124
.5473	0.6382	-0.002
.5542	0.6469	-0.034
.5571	0.6506	-0.032

TABLE 33 CONTINUED

JD HEL 2440000+	PHASE	Δmag
1381.5629	0.6578	-0.040
.5660	0.6618	-0.056
.5784	0.6774	-0.064
.5810	0.6807	-0.050
.5835	0.6838	-0.056
.5896	0.6915	-0.092
.5928	0.6955	-0.075
.5960	0.6995	-0.074
.6026	0.7078	-0.101
.6062	0.7123	-0.052
1383.5541	0.1630	-0.081
.5622	0.1732	-0.116
.5796	0.1951	-0.120
.5838	0.2003	-0.134
.5936	0.2127	-0.135
.5974	0.2174	-0.133
.6057	0.2279	-0.158
.6211	0.2473	-0.166
.6237	0.2506	-0.142
.6296	0.2580	-0.155
.6322	0.2613	-0.153
.6409	0.2722	-0.144
.6442	0.2764	-0.134
.6510	0.2849	-0.132
.6541	0.2888	-0.142
.6611	0.2976	-0.120
.6649	0.3024	-0.106
.6743	0.3142	-0.086
.6830	0.3252	-0.058
.6905	0.3346	-0.068
.6983	0.3444	-0.037
1661.7645	0.1784	-0.120
.7742	0.1906	-0.110
.7833	0.2020	-0.147
.7874	0.2072	-0.144
1661.7967	0.2189	-0.131
.8036	0.2276	-0.139
.8065	0.2313	-0.165
.8136	0.2402	-0.161
.8171	0.2446	-0.177
.8309	0.2620	-0.159
.8338	0.2656	-0.159
.8428	0.2769	-0.142
.8454	0.2802	-0.146
.8545	0.2917	-0.125
.8647	0.3045	-0.120
.8725	0.3143	-0.123
.8958	0.3436	-0.056
.9034	0.3532	-0.044
.9118	0.3637	0.004
1663.7235	0.6431	-0.015
.7631	0.6929	-0.084
.7705	0.7022	-0.098
.7775	0.7109	-0.094
.7849	0.7203	-0.134
.7916	0.7287	-0.139
.7947	0.7326	-0.116
.8026	0.7425	-0.138
.8058	0.7466	-0.131
.8135	0.7562	-0.129
.8170	0.7607	-0.128
.8323	0.7800	-0.131
.8410	0.7908	-0.106
.8443	0.7950	-0.091
.8532	0.8062	-0.090
.8579	0.8121	-0.072
.8690	0.8260	-0.079
.8781	0.8375	-0.060
.8866	0.8482	-0.014

TABLE 34

STATISTICAL STUDY OF THE SOLUTIONS TO THE LIGHT VARIATIONS OF UZ PUPPIS

RMS Deviations of the Observed Data from the Theoretical Solutions over Portions of the Light Curve

	RMS Deviation	Number of Data Points
Yellow		
Primary	0.0178	45
1st Maximum	0.0116	67
Secondary	0.0153	83
2nd Maximum	0.0121	62
Blue		
Primary	0.0100	40
1st Maximum	0.0129	74
Secondary	0.0143	69
2nd Maximum	0.0136	69
Ultraviolet		
Primary	0.0178	48
1st Maximum	0.0153	67
Secondary	0.0243	83
2nd Maximum	0.0139	59

LIST OF REFERENCES

Aitken, R. G. 1932, "New General Catalogue of Double Stars within 120° of the North Pole," Pt. 1, Publications of the Carnegie Institution of Washington, No. 417.

Batten, A. H. 1967, "Sixth Catalogue of Orbital Elements of Spectroscopic Binaries," Publications of the Dominion Astrophysical Observatory, 13, 148.

Binnendijk, L. 1960, Properties of Double Stars (Philadelphia: University of Pennsylvania Press).

Bloomer, Jr., R. H. 1971a, Information Bulletin on Variable Stars, No. 586.

Bloomer, Jr., R. H. 1971b, Information Bulletin on Variable Stars, No. 587.

Bloomer, Jr., R. H. 1972a, Information Bulletin on Variable Stars, No. 745.

Bloomer, Jr., R. H. 1972b, Quarterly Journal of the Florida Academy of Sciences, 35, 19. (abstract)

Bonner Durchmusterung; Sudlicher Teil, 1949 (Bonn: F. Dummlers).

Bookmeyer, B. B. 1968, The Astronomical Journal, 73, 26.

Boss, B. 1936, "General Catalog of 33,342 Stars for the Epoch 1950," Vol. II, Publications of the Carnegie Institution of Washington, No. 468.

Burnham, S. W. 1880, A General Catalogue of Double Stars within 121° of the North Pole, Pts. 1 and 2 (Washington, D.C.: Carnegie Institution of Washington).

Florja, N. 1932, Astronomical Circular, Tashkent, No. 1, Pt. 1.

Florja, N. 1933, Astronomical Circular, Tashkent, No. 10.

Florja, N. 1937, Publications of Sternberg Observatory, 8, Pt. 2.

Franks, W. S. 1918, Monthly Notices of the Royal Astronomical Society, 78, 82.

Gaposchkin, S. 1952, Harvard Annals, 118, Pt. 2, 13.

Gaposchkin, S. 1953, Harvard Annals, 113, Pt. 2, 132.

Goodricke, J. 1783, Philosophical Transactions of the Royal Society of London, 73, 474.

Hardie, R. H. 1962, "Photoelectric Reductions," Astronomical Techniques, edited by W. A. Hiltner (Chicago: The University of Chicago Press).

Hertzsprung, E. 1928, Bulletin of the Astronomical Institutes of the Netherlands, 4, 178.

Hoffmeister, C. 1929, Astronomische Nachricten, 236, 235.

Johnson, H. L. and Morgan, W. W. 1953, The Astrophysical Journal, 117, 313.

Knipe, G. F. G. 1965, The Astrophysical Journal, 142, 1068.

Koch, R. H., Plavec, M., and Wood, F. B. 1970, "A Catalogue of Graded Photometric Studies of Close Binaries," Publications of the University of Pennsylvania, Astronomical Series, Vol. X.

Kukarkin, B. V., Kholopov, P. N., Kukarkina, N. P., and Perova, N. B. 1972, Information Bulletin on Variable Stars, No. 717.

Lause, F. 1933, Astronomische Nachricten, 260, 293.

Locher, K. 1972, Bedeckungsveranderlichen Beobachter der Schweizerischen Astronomischen Gesellschaft, No. 1, 4.

Lucy, L. B. 1968, The Astrophysical Journal, 151, 1123.

Mergentaler, J. 1930, Acta Astronomica, Ser. C, 1, 148.

Merrill, J. E. 1950, "Tables for Solution of Light Curves of Eclipsing Binaries," Contributions from the Princeton University Observatory, No. 23.

Merrill, J. E. 1953, "Nomographs for Solution of Light Curves of Eclipsing Binaries," Contributions from the Princeton University Observatory, No. 24.

Merrill, J. E. 1970, "Rectification of Light Curves of W Ursae Majoris-Type Systems on the Russell Model," Vistas in Astronomy, Vol. 12, edited by A. Beer (New York: Pergamon Press).

O'Connell, S.J., D. J. K. 1951, Riverview College Observatory Publications, 2, 85.

Plavec, M. 1970, *Publications of the Astronomical Society of the Pacific*, *82*, No. 489, 957.

Russell, H. N. and Merrill, J. E. 1952, "The Determination of the Elements of Eclipsing Binaries," *Contributions from the Princeton University Observatory*, No. 26.

Scott, J. L. 1899, *Monthly Notices of the Royal Astronomical Society*, *59*, 428.

Scott, J. L. 1904, *Monthly Notices of the Royal Astronomical Society*, *64*, 52.

Smak, J. 1969, *Acta Astronomica*, *20*, 311.

Smith, A. G. 1972, *Quarterly Journal of the Florida Academy of Science*, *35*, Suppl. to No. 1, 18. (abstract)

Smithsonian Institute 1966, *Smithsonian Astrophysical Observatory Star Catalog*, Pt. 3 (Washington, D.C.: Smithsonian Institute).

Soloviev, A. 1943, *Astronomical Circular*, *State University of Kazan*, *19*, 4.

Starfield, S. 1971, *Monthly Notices of the Royal Astronomical Society*, *152*, 307.

Struve, O. 1945, *The Astrophysical Journal*, *102*, 1.

Wood, F. B. (ed.) 1963, *Photoelectric Astronomy for Amateurs* (New York: Macmillan Company).

Young, A. 1968, *The Observatory*, No. 965, 151.

BIOGRAPHICAL SKETCH

Raymond Howard Bloomer, Jr., the son of Mr. and Mrs. Raymond H. Bloomer, was born on May 25, 1945, in Poughkeepsie, New York. His elementary and secondary education was received in Pennsylvania and Florida, and he graduated from Dan McCarty High School in Fort Pierce, Florida, in June, 1963. In the fall of 1963 he enrolled at the Citadel, the Military College of South Carolina, where he received a Bachelor of Science degree in physics four years later. After working at the Kennedy Space Center at Cape Kennedy, Florida, in the summer of 1967, he enrolled in Graduate School at the University of Florida in Gainesville, Florida. His master's degree in physics was completed in December, 1970. He then continued his graduate studies in astronomy. His academic work was interrupted only in the summer of 1971 when he worked at the Dr. Remeis Sternwarte in Bamberg, West Germany.

Since January, 1973, he has been on active duty in the United States Air Force, and he and his wife, the former Andrea Parham Erickson, are stationed at Kirtland Air Force Base where he is employed in the Laser Division of the Air Force Weapons Laboratory.

Mr. Bloomer is a member of Sigma Xi and the American Physical Society.

I certify that I have read this study and that in my opinion it conforms to acceptable standards of scholarly presentation and is fully adequate, in scope and quality, as a dissertation for the degree of Doctor of Philosophy.

Kwan-Yu Chen

Kwan-Yu Chen, Chairman
Associate Professor of Astronomy

I certify that I have read this study and that in my opinion it conforms to acceptable standards of scholarly presentation and is fully adequate, in scope and quality, as a dissertation for the degree of Doctor of Philosophy.

A. G. Smith

Alexander G. Smith
Professor of Physics and Astronomy

I certify that I have read this study and that in my opinion it conforms to acceptable standards of scholarly presentation and is fully adequate, in scope and quality, as a dissertation for the degree of Doctor of Philosophy.

John Oliver FOR F. B. WOOD

Frank Bradshaw Wood
Professor of Astronomy

I certify that I have read this study and that in my opinion it conforms to acceptable standards of scholarly presentation and is fully adequate, in scope and quality, as a dissertation for the degree of Doctor of Philosophy.

F. Eugene Dunnam
Associate Professor of Physics

I certify that I have read this study and that in my opinion it conforms to acceptable standards of scholarly presentation and is fully adequate, in scope and quality, as a dissertation for the degree of Doctor of Philosophy.

Henri A. Van Rinsvelt
Assistant Professor of Physics

This dissertation was submitted to the Department of Physics and Astronomy in the College of Arts and Sciences and to the Graduate Council, and was accepted as partial fulfillment of the requirements for the degree of Doctor of Philosophy.

June, 1973

Dean of Graduate School

#349 v/2 [illegible] BE 117

S M2.2. 21345